IRANIAN JOURNAL OF MATHEMATICAL CHEMISTRY

University of Kashan

IJMC

http://IJMC.Kashanu.ac.ir

Iranian Journal of Mathematical Chemistry

Iranian Journal of Mathematical Chemistry (IJMC) publishes quality original research papers and survey articles in Mathematical Chemistry and related areas that are of the highest possible quality.

Research papers and review articles are selected through a normal refereeing process by a member of editorial board.

It is intended that the journal may act as an interdisciplinary forum for publishing chemically important mathematical papers. Papers published in this journal must have a clear connection to chemistry with non-trivial mathematics.

Aims and Scopes: Iranian Journal of Mathematical Chemistry is a bi publication of the University of Kashan. It contains research and expository papers as well as short communications on chemically important mathematical problems.

Preparation of Manuscripts: An abstract of 150 words or less and keywords clarifying the subject of the manuscripts are required. Authors should submit the paper electronically in word file to ijmc@kashanu.ac.ir.

The language of the journal is English. Authors who are less familiar with English language are advised to seek assistance from proficient scholars to prepare manuscripts that are grammatically and linguistically free from errors. Manuscripts should be typed with double spacing and wide margins. Papers submitted for consideration for publication have to be prepared concisely and must not exceed 30 typewritten pages, (font 12, 1.15 spacing, including tables & graphs). Diagrams and figures should be submitted as original drawings. Figures and tables are to be numbered in the sequence in which they are cited in the manuscript. Every table must have a caption that explains its content. Tables and diagrams are to be prepared in separate pages and placed at the end of the manuscript. References to the literature should be numbered in square brackets in the order in which they appear in the text. A complete list of references should be presented in numerical order at the end of the manuscript. References to journals, books, proceedings and patents must be presented in accordance with the following examples:

Journals: I. Gutman, B. Zhou and B. Furtula, The Laplacian-energy like invariant is an energy like invarint MATCH Commun. Math. Comput. Chem., 64(1) (2010), 85-96.

Patents: Primack, H.S.; Method of Stabilizing Polyvalent Metal Solutions, U.S. patent No. 4, 373, 104(1983).

Indexing/ Abstracting: The Iranian Journal of Mathematoical Chemistry is indexed/abstracted in the following:

- Islamic World Science Citation Center (ISC)
- Zentralblatt für Mathematik
- Web of Science (ISI)

EditorialBoard

Past Editors

Editor-in-Chief:

Ali Reza Ashrafi
Department of Pure Mathematics, Faculty of Mathematical Sciences, University of Kashan, Kashan87317-53153, I R IRAN
mail:ashrafi@kashanu.ac.ir

Managing Director:

Behnam Bazigaran
Department of Pure Mathematics, Faculty of Mathematical Sciences, University of Kashan, Kashan87317-53153, I R IRAN
E-mail:bazigaran@kashanu.ac.ir

Language Editor:

Seyfollah Mosazadeh
Department of Pure Mathematics, Faculty of Mathematical Sciences, University of Kashan, Kashan 87317-53153, I R IRAN
E-mail: s.mosazadeh@kashanu.ac.ir

Technical Manager:

Marzieh Pourbabaee
Department of Applied Mathematics, Faculty of Mathematical Sciences, University of Kashan, Kashan 87317-53153, I R IRAN
Email:m.pourbabaee@kashanu.ac.ir

Iranian Journal of Mathematical Chemistry

Vol. 8, No. 4 December 2017

CONTENTS **pages**

Iranian J. Math. Chem. 8 (4) December (2017) 339 − 344

Iranian Journal of Mathematical Chemistry

Journal homepage: ijmc.kashanu.ac.ir

Borderenergetic Graphs of Order 12

BORIS FURTULA• AND IVAN GUTMAN

Faculty of Science, University of Kragujevac, P. O. Box 60, 34000 Kragujevac, Serbia

ARTICLE INFO

Article History:

Received 23 May 2017
Accepted 6 June 2017
Published online 22 July 2017
Academic Editor: Tomislav Došlić

Keywords:

Graph energy
Borderenergetic graph
Spectrum (of graph)

ABSTRACT

A graph G of order n is said to be borderenergetic if its energy is equal to $2n - 2$ and if G differs from the complete graph K_n. The first such graph was discovered in 2001, but their systematic study started only in 2015. Until now, the number of borderenergetic graphs of order n was determined for $n \leq 11$. We now establish that there exist exactly 572 connected borderenergetic graphs of order 12.

1. INTRODUCTION

Let G be a simple graph of order n, possessing m edges. Let the eigenvalues of G (i.e., the eigenvalues of the adjacency matrix of G) be $\lambda_1, \lambda_2, \ldots, \lambda_n$ [1] The energy of the graph G is defined as

$$E = E(G) = \sum_{i=1}^{n} |\lambda_i| .$$

This graph-spectrum-based invariant has been extensively studied. Details of its mathematical theory can be found in the book [2] whereas details of its chemical applications in [3].

The upper bound

$$E \leq \sqrt{2mn}$$

was established by McClelland in the early 1970s [4]. In the same paper [4], an approximate formula was proposed:

•Corresponding author (Email: furtula@kg.ac.rs)
DOI: 10.22052/ijmc.2017.87093.1290

$$E \approx a\sqrt{2mn} \ , \ a \approx 0.9 \qquad (1)$$

which was eventually demonstrated to be highly accurate in the case of molecular graphs [5,6]. An additional corroboration of this formula was the analogous lower bound

$$E \geq \sqrt{\frac{16}{27}}\sqrt{2mn}$$

that holds for certain molecular graphs, in particular, for benzenoid systems [7].

According to formula (1), the energy of a graph would be a monotonically increasing function of the number *m* of edges. If this formula could be applied to all graphs, then among graphs with a fixed number *n* of vertices, the complete graph K_n would have the greatest energy, equal to $E(K_n) = 2n - 2$. Counterexamples for this naive conjecture were soon discovered [8]. Somewhat later [9], the first systematic construction of graphs with the property $E(G) > E(K_n)$ were reported.

Graphs of order *n* with the property $E(G) > 2n - 2$ were named *hyperenergetic* [10]. Numerous classes of hyperenergetic graphs have been recognized; for details see the survey [11]. The search for hyperenergetic graphs became purposeless after Nikiforov proved in 2007 [12] that for almost all *n*-vertex graphs

$$E = \left(\frac{4}{3\pi} + o(n) \right) n^{3/2}$$

implying that almost all graphs are hyperenergetic.

The question that remained open was if there exist graphs of order *n*, other than K_n, satisfying the equality

$$E(G) = 2n - 2 .$$

In 2015, such graphs were named *borderenergetic* [13]. It is understood that the complete graph is not borderenergetic.

The first borderenergetic graph was discovered by Yaoping Hou and one of the present authors already in 2001 [14], but in that time it did not attract much attention. The first systematic research of borderenergetic graphs is reported in the paper [13], which was then continued in [15-19]. By means of computer-aided checking, the following was established.

Theorem 1.

1. There are no borderenergetic graphs of order $n \leq 6$ [13].
2. There exists a unique borderenergetic graph of order 7 [13].
3. For any $n \geq 7$, there exist borderenergetic graphs of order *n* [13].
4. There are exactly 6 borderenergetic graphs of order 8 [13].

5. There are exactly 17 borderenergetic graphs of order 9 [13].
6. There are exactly 49 borderenergetic graphs of order 10 [15,18].
7. There are exactly 158 borderenergetic graphs of order 11 [18], of which 157 are connected.

We now can extend Theorem 1 by establishing:

Theorem 2. There are exactly 572 connected borderenergetic graphs of order 12.

2. NUMERICAL WORK

Determining computationally the borderenergetic graphs of order 12 is not an easy task to be done. This could be illustrated by the fact that the total number of such graphs is 164059830476. In order to reduce the number of investigated graphs, the fact that the size of the borderenergetic species must be greater than $2n-3$ is incorporated. Such intervention decreased the total number of 12-vertex connected graphs by 343198848.

The *geng* tool from the *nauty* package was employed for the generation of the dataset containing 163716631628 graphs stored in 100000 files [20]. The total size of these files is more than 2 TB. All these files are moved to the cluster having 4 nodes with 32 CPUs per node. A Python program was developed for filtering borderenergetic graphs. Using PySpark for processing large datasets, the jobs were distributed over cluster using in total 80 CPUs simultaneously. The computations took about a month or so and finally, we obtained the result that there were exactly 572 connected twelve-vertex borderenergetic graphs.

Table 1 shows the distribution of 12-vertex borderenergetic graphs by the number of edges. Their size varies from 25 to 58. It should be noted that there are no 12-vertex borderenergetic graphs with 49, 53, and 59-65 edges.

3. CONCLUSION

In this note, we reported the preliminary results on searching for and studying of connected borderenergetic graphs with twelve vertices. There are 572 such species, and these provide a class of equienergetic graphs suitable for examining the structural factors on which graph energy does depend or does not depend. In addition, the distribution of these graphs with regard to the number of edges is presented in Table 1, indicating that equienergetic graphs may significantly differ in their edge counts.

Table 1. The distribution of twelve-vertex borderenergetic graphs by the number of edges.

Number of Edges	Number of Graphs
25	2
26	5
27	1
28	8
29	7
30	42
31	20
32	62
33	58
34	50
35	44
36	43
37	37
38	27
39	25
40	24
41	20
42	26
43	12
44	14
45	14
46	7
47	4
48	7
50	2
51	1
52	4
54	1
55	2
56	1
57	1
58	1

REFERENCES

1. D. Cvetković, P. Rowlinson, S. Simić, *An Introduction to the Theory of Graph Spectra*, Cambridge Univ. Press, Cambridge, 2010.
2. X. Li, Y. Shi, I. Gutman, *Graph Energy*, Springer, New York, 2012.

3. I. Gutman, O. E. Polansky, *Mathematical Concepts in Organic Chemistry*, Springer, Berlin, 1986.
4. B. J. McClelland, Properties of the latent roots of a matrix: The estimation of π-electron energies, *J. Chem. Phys.* **54** (1971) 640−643.
5. I. Gutman, Total π-electron energy of benzenoid hydrocarbons, *Topics Curr. Chem.* **162** (1992) 29−63.
6. I. Gutman, T. Soldatović, (*n*,*m*)-Type approximations for total π-electron energy of benzenoid hydrocarbons, *MATCH Commun. Math. Comput. Chem*. **44** (2001) 169−182.
7. I. Gutman, McClelland-type lower bound for total π-electron energy, *J. Chem. Soc. Faraday Trans.* **86** (1990) 3373−3375.
8. D. Cvetković, I. Gutman, The computer system GRAPH: A useful tool in chemical graph theory, *J. Comput. Chem*. **7** (1986) 640−644.
9. H. B. Walikar, H. S. Ramane, P. R. Hampiholi, On the energy of a graph, in: R. Balakrishnan, H. M. Mulder, A. Vijayakumar (Eds.), *Graph Connections*, Allied Publishers, New Delhi, 1999, pp. 120−123.
10. I. Gutman, Hyperenergetic molecular graphs, *J. Serb. Chem. Soc*. **64** (1999) 199−205.
11. I. Gutman, Hyperenergetic and hypoenergetic graphs, in: D. Cvetković, I. Gutman (Eds.), *Selected Topics on Applications of Graph Spectra*, Math. Inst., Belgrade, 2011, pp. 113−135.
12. V. Nikiforov, Graphs and matrices with maximal energy, *J. Math. Anal. Appl*. **327** (2007) 735−738.
13. S. Gong, X. Li, G. Xu, I. Gutman, B. Furtula, Borderenergetic graphs, *MATCH Commun. Math. Comput. Chem.***74** (2015) 321−332.
14. Y. Hou, I. Gutman, Hyperenergetic line graphs, *MATCH Commun. Math. Comput. Chem*. **43** (2001) 29−39.
15. X. Li, M. Wei, S. Gong, A computer search for the borderenergetic graphs of order 10, *MATCH Commun. Math. Comput. Chem*. **74** (2015) 333−342.
16. B. Deng, X. Li, I. Gutman, More on borderenergetic graphs, *Lin. Algebra Appl.* **497** (2016) 199−208.
17. Y. Hou, Q. Tao, Borderenergetic threshold graphs, *MATCH Commun. Math. Comput. Chem.* **75** (2016) 253−262.
18. Z. Shao, F. Deng, Correcting the number of borderenergetic graphs of order 10, *MATCH Commun. Math. Comput. Chem*. **75** (2016) 263−265.
19. X. Li, M. Wei, X. Zhu, Borderenergetic graphs with small maximum or large minimum degrees, *MATCH Commun. Math. Comput. Chem*. **77** (2017) 25−36.

20. B. D. McKay, A. Piperno, Practical graph isomorphism II, *J. Symb. Comput.* **60** (2013) 94–112.

Iranian J. Math. Chem. 8 (4) December (2017) 345 − 364

Iranian Journal of Mathematical Chemistry

Journal homepage: ijmc.kashanu.ac.ir

A Numerical Study of Fractional Order Reverse Osmosis Desalination Model using Legendre Wavelet Approximation

OMAR BELHAMITI[1,•] AND BELKACEM ABSAR[2]

[1]Laboratory of Pure and Applied Mathematics, Abdelhamid Ibn Badis University, Mostaganem 27000, Algeria

[2]Laboratory of Science and Technology of the Environment and Promotion, University of Mostaganem, Mostaganem 27000, Algeria

ARTICLE INFO

Article History:

Received: 20 May, 2017
Accepted: 8 June 2017
Published online 6 July 2017
Academic Editor: Ivan Gutman

Keywords:

Reverse osmosis desalination system
Legendre wavelet method
DQL- technique
Caputo fractional derivative

ABSTRACT

The purpose of this study is to develop a new approach in modeling and simulation of a reverse osmosis desalination system by using fractional differential equations. Using the Legendre wavelet method combined with the decoupling and quasi-linearization technique, we demonstrate the validity and applicability of our model. Examples are developed to illustrate the fractional differential technique and to highlight the broad applicability and the efficiency of this method. The fractional derivative is described in the Caputo sense.

1. INTRODUCTION

In recent few decades, fractional calculus has caught much attention due to its ability to provide an accurate description of different nonlinear phenomena. Moreover, the fractional differential equations have gained considerable popularity of many researchers due to their applications in many engineering and scientific disciplines such as control theory, signal processing, information sciences, and many other physical and chemical processes and also in medical sciences, see [15−18, 20, 21, 24]. These equations are also used in the modeling

• Corresponding Author: (Email address: (omar.belhamiti@univ-mosta.dz)
DOI: 10.22052/ijmc.2017.86494.1289

of physical processes running in dynamic mode [23, 22]. In this way, this work deals with the application of fractional derivatives for the desalination phenomenon.

On the other hand, desalination of sea water appears as a strategic solution adopted by several countries to cope with drinking water availability problem. This process was intended only for industrial purposes due to the constraints of high desalination costs [1−5]. However, technological advances in the field of manufacture of membranes have reduced these costs and thus enable more countries to use this alternative as a freshwater resource. Actually, re-verse osmosis, due to its lower energy consumption and simplicity has gained much wider acceptance than the thermal alternatives. Reverse osmosis is based on a physical property called semi-permeability. Certain polymeric materials (membranes) allow water to pass more quickly than some substances such as dissolved salts. The principle is to apply a high enough pressure to overcome the osmotic pressure and reverse the flow of water.

Many mathematical models have been proposed to describe the performance of reverse osmosis unit. For more details, we cite [1−5]. But, since the memory of phenomena plays a key role in mechanics, so a possible generalization of the classic desalination model would be a system with fractional order derivative. In this line of thought, Du et al. [11] found that a physical meaning of the fractional order is an index of memory. Then, Atangana et al. [8] proved that a fractional operator can provide a better interpretation of both physical and engineering processes.

The authors in [30, 31] studied the overall performance of hollow fiber membranes by using the interplay of fiber productivity (defined as the fraction of feed recovered as permeate) and fiber selectivity or rejection. Two flow configuration modules for reverse osmosis hollow fiber membranes are considered: co-current and counter-current flow. Productivity and selectivity were plotted as functions of fiber length. It is found that at the entrance of the module, the term of productivity is equal to zero. This trend (flattening of the curve of productivity) is observed in the neighborhood of the entrance to the tube for the two cases: Co-current and Cross-current. This phenomenon is explained by the fact that the feed rate is constant and therefore the first derivative is equal to zero.

In this paper, we will focus on the use of the fractional differential operator in the sense of Caputo for modeling a seawater desalination module using the reverse osmosis process. The numerical solution of the fractional differential model (FDM) is obtained by using the Legendre wavelet method combined with the decoupling and quasi-linearization technique. For more information about this new approach, we refer the reader to [6,7,9,14]. In this approach the Block-Pulse functions (BPFs) and the operational matrix of integration are used, FDM can be transformed to lower triangular system of algebraic equations. Then the solution of this system is used to determine a new numerical solution of FDM. At the end, and since the approach is not yet tested sufficiently on FDEs, some other problems are studied.

This work is organized as follows: Section 2 gives the fundamental equations to describe the transport phenomena in reverse osmosis by using the fractional model. Section 3 introduces some necessary definitions of the Legendre wavelet method. We present a new operational fractional matrix of integration and we give the description of the proposed method. Section 4 gives the numerical investigations of the analytical findings. At the end, a conclusion follows.

2. MODELING OF REVERSE OSMOSIS DESALINATION SYSTEM

2.1. CLASSICAL MODEL OF REVERSE OSMOSIS DESALINATION SYSTEM

Sea water desalination has become an inevitable alternative for many countries to overcome the shortage of natural fresh water. Among desalination technology, reverse osmosis is the most used method. This is mainly due to its simplicity, their costs, reduced compared to thermal processes. No heating or phase separation change is necessary. The major energy required for desalting is for pressurizing the seawater feed [19]. Reverse osmosis is a method of separation and concentration in the liquid phase. This process is applied to purify water for laboratory. The process consists in passing aqueous solution under pressure through an appropriate membrane and withdrawing the membrane permeate at atmospheric pressure and ambient temperature. The product obtained is enriched in one of the mixture components. The other components are recovered in the retentate with higher concentration in the high-pressure side of the membrane. Reverse osmosis membranes are generally mounted on supports called modules. Currently, the most used modules are: hollow fiber, tubular and spiral wound modules. Tubular modules are constituted of two concentric tubes designed to separate a given feed into a higher pressure stream (retentate) and a low pressure stream (permeate) see figure 1. According to the direction of the feed flow rate, there are two types of flow pattern: the co-current and counter-current flow pattern.

Figure 1: Hollow fiber membrane.

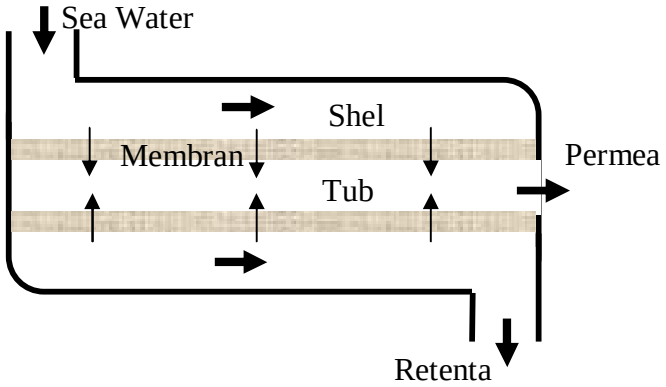

A mathematical model was developed to predict the performance of hollow fiber reverse osmosis membrane with co-current flow pattern. The mass transfer model employed in this study is the solution-diffusion model. The solvent and salt mass flux are expressed by Fick's law. This model is developed by the author [1, 2]. It consists of a set of four strongly nonlinear differential equations. This system is found, according to material balance principle:

$$\begin{cases} \frac{dQ_{sw}}{dx} = -\pi \frac{A_w}{\sigma_w} D_m \left(\Delta P - \kappa \left(\frac{\dot{Q}_{ss}}{Q_{sw}} - \frac{\dot{Q}_{fs}}{Q_{fw}} \right) \right) \\ \frac{dQ_{fw}}{dx} = \pi \frac{A_w}{\sigma_w} D_m \left(\Delta P - \kappa \left(\frac{\dot{Q}_{ss}}{Q_{sw}} - \frac{\dot{Q}_{fs}}{Q_{fw}} \right) \right) \\ \frac{d\dot{Q}_{ss}}{dx} = -\pi B_s D_m \left(\frac{\dot{Q}_{ss}}{Q_{sw}} - \frac{\dot{Q}_{fs}}{Q_{fw}} \right) \\ \frac{d\dot{Q}_{fs}}{dx} = \pi B_s D_m \left(\frac{\dot{Q}_{ss}}{Q_{sw}} - \frac{\dot{Q}_{fs}}{Q_{fw}} \right), \end{cases} \quad (1)$$

where

Q_{sw} : is the water volumetric flow rate in the shell side,

Q_{fw} : is the water volumetric flow rate in the fiber side,

$\dot{Q}_{ss}$: represents the solute mass flow rate in the shell side,

$\dot{Q}_{ss}$: is the solute mass flow rate in the fiber side,

κ is a proportionality coefficient,

A_w is the water permeability coefficient (a function of salt diffusivity through the membrane),

ΔP is the transmembrane pressure (a function of the feed, concentrate and permeate concentrations),

σ_w is the water density,

B_s is the solute permeability coefficient,

The osmotic pressure is approximately represented by a linear function of solute concentrations $\pi = \kappa C$.

2.2. REVERSE OSMOSIS DESALINATION MODEL

Lately, it has frequently been observed that the mathematical models represented by fractional order derivatives [11, 12, 13, 20] can provide better agreement between measured and simulated data than classical models based on integer order derivatives. In

classical desalination model [1, 2, 7], instead of a variation of order one, we consider, in this study, a variation of the order $1 < \alpha < 2$. Taking into account normalized variables,

$$\boldsymbol{Q}_{sw} = \frac{Q_{sw}}{Q_{sw0}}, \boldsymbol{Q}_{fw} = \frac{Q_{fw}}{Q_{sw0}}, \dot{\boldsymbol{Q}}_{ss} = \frac{\dot{Q}_{ss}}{\dot{Q}_{ss0}}, \dot{\boldsymbol{Q}}_{fs} = \frac{\dot{Q}_{fs}}{\dot{Q}_{ss0}},$$

if we replace the first order derivatives by fractional derivatives in (1), then a simple dimensional analysis shows that the left-hand sides of the equations have the dimension of $(\text{space})^{-\alpha}$. But an examination of the right-hand sides shows that they have the dimension of $(\text{space})^{-1}$, so, we need to modify the right-hand sides to adjust the dimensions [12]. Thus, we formulate the fractional model of reverse osmosis desalination using Caputo fractional derivatives of order, $1 < \alpha < 2$ [10], the model is described by the non-linear Caputo fractional differential system:

$$\begin{cases} {}_0D_x^{\alpha} Q_{sw} = -c_1 + c_2 \left(\frac{\dot{Q}_{ss}}{Q_{sw}} - \frac{\dot{Q}_{fs}}{Q_{fw}} \right) \\ {}_0D_x^{\alpha} Q_{fw} = c_1 - c_2 \left(\frac{\dot{Q}_{ss}}{Q_{sw}} - \frac{\dot{Q}_{fs}}{Q_{fw}} \right) \\ {}_0D_x^{\alpha} Q_{fw} = -c_3 \left(\frac{\dot{Q}_{ss}}{Q_{sw}} - \frac{\dot{Q}_{fs}}{Q_{fw}} \right) \\ {}_0D_x^{\alpha} Q_{fw} = c_3 \left(\frac{\dot{Q}_{ss}}{Q_{sw}} - \frac{\dot{Q}_{fs}}{Q_{fw}} \right), \end{cases} \tag{2}$$

where

$$c_1 = \left(\pi \frac{A_w}{\sigma_w} \frac{D_m}{Q_{sw0}} \Delta P \right)^{\alpha}$$
$$c_2 = \left(\pi \frac{A_w}{\sigma_w} \frac{D_m}{Q_{sw0}} \frac{\dot{Q}_{ss}}{Q_{sw0}} \right)^{\alpha}$$
$$c_3 = \left(\pi B_s \frac{D_m}{Q_{sw0}} \right)^{\alpha}.$$

Note that in the limit case $\alpha \to 1$, the system (2) reduces to the classical system (1).

3. LEGENDRE WAVELET METHOD

In this section, we present some definitions and properties of fractional calculus. Then, we introduce some preliminaries on Legendre wavelets that are used throughout this paper. This section is ended by presenting some definitions, notations and basic facts of block pulse functions, [25–27].

Let $(n-1) \leq \alpha < n, n \in \mathbb{N}^*$, a function $f \in C^n\ (a,b)$. The Caputo derivative of order $\alpha \geq 0$ is defined by

$$
\begin{aligned}
{}_0^C D_t^\alpha f(t) &= \frac{1}{\Gamma(n-\alpha)} \int_\alpha^t (t-\tau)^{n-\alpha-1} f^{(n)}(\tau)\, d\tau \\
&= I_t^{n-\alpha} \left(\frac{d^n}{dt^n} f(t) \right),
\end{aligned}
$$

where

$$
\Gamma(\alpha) := \int_0^\infty e^{-u}\, u^{\alpha-1} du, \quad Re\{\alpha\} > 0
$$

We note that the Caputo derivative of a constant function is zero. For more details on fractional calculus, we refer the reader to [10, 13].

3.1. LEGENDRE WAVELETS

On the other hand, the wavelets are a family of functions constructed from dilatations and translations of a single function called the mother wavelet. We have the following family of continuous wavelets

$$
\psi_{a,b}(t) = |a|^{-\frac{1}{2}} \psi\left(\frac{t-b}{a}\right), a, b\ \mathbb{R}, a \neq 0,
$$

where $\psi(t) \in L^2(\mathbb{R})$, a and b represent the dilation and the translation parameters respectively. If a and b have discrete values as

$$
\begin{cases} a = a_0^{-k}, a_0 > 1 \\ b = n\, b_0\, a_0^{-k}, b_0 > 1 \end{cases} \qquad n, k \in \mathbb{N},
$$

for n and m positive integers, we have the following family of discrete wavelets:

$$
\psi_{m,n}(t) = |a_0|^{\frac{m}{2}} \psi(a_0^m t - n\, b_0)
$$

where $\psi_{m,n}(t)$ forms a wavelet basis for $L^2(\mathbb{R})$. In particular, when $a_0 = 2$ and $b_0 = 1$, $\psi_{m,n}(t)$ forms an orthonormal basis. That is $\langle \psi_{m,n}, \psi_{l,k} \rangle = \delta_{m,l}\, \delta_{n,k}$ in which $\langle .,. \rangle$ denotes the inner product in $L^2([0,1])$.

In this work, the mother wavelet is the Legendre polynomials. We de ne the orthogonal Legendre polynomials of order m by the following Rodriguez recurrence formula:

$$\begin{cases} L_0(t) = 1 \\ L_1(t) = t \\ L_{m+2}(t) = \left(\frac{2\,m+3}{m+2}\right) t\, L_{m+1}(t) - \left(\frac{m+1}{m+2}\right) L_m(t), \end{cases}$$

with $m = 0,1,2,3,\ldots$ and t varies into [-1,1].

The Legendre wavelets are defined in [0; 1] by the following formula

$$\psi_{m,n}(t) = \begin{cases} \sqrt{m + 1/2}\, 2^{\frac{1}{2}}\, L_m\left(2^j t - 2n + 1\right) & \text{if } \frac{n-1}{2^{j-1}} \le t \le \frac{n}{2^{j-1}} \\ 0, & \text{otherwise,} \end{cases}$$

where $n = 1, \ldots, 2^{j-1}$ $(j \in \mathbb{N} \setminus \{0\})$, $m = 0, \ldots, n_c - 1$ $(n_c \in \mathbb{N} \setminus \{0\})$ is the order of the Legendre polynomials and *nc* is the number of collocation points. However, the dilatation parameter is $a = 2^{j/2}$ and the translation parameter is $b = (2n-1)2^{j/2}$.

The family

$$\{\psi_{m,n}(t)\}_{\substack{n=1,\ldots,2^{j-1} \\ m=0,\ldots,nc-1}}$$

forms an orthonormal basis of $L^2([0,1])$ [26]. Then, any function $f \in L^2([0,1])$ may be decomposed as

$$f(t) = \sum_{n=1}^{+\infty} \sum_{m=0}^{+\infty} C_{n,m}\, \psi_{n,m}(t), \tag{3}$$

where $C_{n,m} = \langle f, \Psi \rangle$; in which $\langle .,. \rangle$ denoted the inner product in $L^2([0,1])$.

The function in (3) can be approached by

$$f(t) = \sum_{n=1}^{2^{j-1}} \sum_{m=0}^{nc-1} C_{n,m}\, \psi_{n,m}(t) = C^T\, \Psi(t), \tag{4}$$

where C and $\Psi(t)$ are $2^{j-1}\, nc$ vectors given by

$$C = \left[C_{1,0,\ldots,} C_{1,nc-1,} C_{2,0,\ldots,} C_{2,nc-1,\ldots,} C_{2^{j-1},1,\ldots,} C_{2^{j-1},nc-1}\right]^T \tag{5}$$

$$\Psi(t) = \left[\psi_{1,0}(t), \ldots, \psi_{1,nc-1}(t), \psi_{2,0}(t), \ldots, \psi_{2,nc-1}(t), \ldots, \psi_{2^{j-1},0}(t), \ldots, \psi_{2^{j-1},nc-1}(t)\right]^T \tag{6}$$

The following property of the product of two Legendre wavelet vector functions will also be used

$$A^T \Psi(t)\, \Psi^T(t) = \Psi^T(t)\, \bar{A}, \tag{7}$$

where

$$A = \left[a_{1,0}, \dots, a_{1,nc-1}, a_{2,0}, \dots, a_{2,nc-1}, \dots, \psi_{2^{j-1},0}(t), \dots, \psi_{2^{j-1},nc-1}(t)\right]^T$$

and $\bar{A}$ is a $2^{j-1}\,nc$x$2^{j-1}\,nc$ matrix [26].

3.2. BLOCK PULSE FUNCTION

The block functions form a complete set of orthogonal functions which can be defined over [0;T] by

$$b_i(t) = \begin{cases} 1, & \text{if } \frac{i-1}{2^{j-1}nc}T \le t < \frac{i}{2^{j-1}nc}\,T \\ 0, & \text{otherwise,} \end{cases} \tag{8}$$

where, $i = 1, \dots, 2^{j-1}nc$ [27]. There are some properties for block pulse functions: the most important properties are disjointness and orthogonality.

The disjointness property follows

$$b(t)\,b^T(t)\,V = \tilde{V}\,b(t)$$

and

$$\tilde{V} = \begin{pmatrix} V_1 & \cdots & 0 \\ \vdots & \ddots & \vdots \\ 0 & \cdots & V_{2^{j-1}\,nc} \end{pmatrix},$$

where V is an $2^{j-1}nc$-vector. The block-pulse functions are orthogonal

$$\int_0^T b_i(t),\ b_i(t)\,dt = \begin{cases} \frac{T}{2^{j-1}nc}, i = j \\ 0, \text{otherwise} \end{cases}$$

where *i; j* = 1, 2,…, $2^{j-1}nc$.

3.3. OPERATIONAL FRACTIONAL MATRIX OF INTEGRATION

In the following section, we introduce new arguments for deriving the fractional Legendre wavelets operational matrix of integration.

Let $t \in [0;\ 1]$ we define the Legendre wavelets operational matrix of integration as in [6, 26],

$$\int_0^t \Psi(x)\,dx = P\ \Psi(t), \tag{9}$$

where

$$P = \frac{1}{2^{j-1}} \begin{pmatrix} L & F & \cdots & F \\ 0 & L & \ddots & \vdots \\ \vdots & \ddots & \ddots & F \\ 0 & \cdots & 0 & L \end{pmatrix},$$

is the $2^{j-1}nc$ x $2^{j-1}nc$ operational matrix of integration, and L and F are nc x nc matrices. It is not difficult to see that

$$\left({}_0I_t^0\,\Psi\right)(t) = \Psi(t),$$

$$\left({}_0I_t^1\,\Psi\right)(t) = \int_0^t \Psi(x)\,dx = P\ \Psi(t),$$

$$\left({}_0I_t^2\,\Psi\right)(t) = \int_0^t \left(\int_0^s \Psi(x)\,dx\right) ds = \int_0^t P\Psi(s)\,ds = \mathrm{P\,x\,P\,x}\,\Psi(t) = \mathrm{P}^2\ \Psi(t),$$

$$\vdots$$

$$\left({}_0I_t^n\,\Psi\right)(t) = \int_0^t \left(\int_0^s \Psi(x)\,dx \left(\int_0^\tau \Psi(x)\,dx \ldots\right) ds\right) = \mathrm{P\,x\,P\,x} \ldots \mathrm{x}\,\Psi(t) = \mathrm{P}^n\ \Psi(t),$$

On the other hand, we have

$$\left({}_0I_t^n\,\Psi\right)(t) = \frac{1}{\Gamma(n)}\int_0^t (t-\tau)^{n-1}\Psi(\tau)\,d\tau, \qquad t \in [0,1].$$

Using the convolution product, we can write

$$\left({}_0I_t^n\,\Psi\right)(t) = (\Psi\,\mathrm{x}\,\phi)(t),$$

where

$$\phi(t) = \frac{(t-\tau)^{n-1}}{\Gamma(n)},\ \text{(a causal function)}.$$

The continuous character of the function Γ(α) is used to release Γ(n) and to define the integral operator of order α>0.This operator is defined as

$${}_0I_t^\alpha\,\Psi(t) = \begin{cases} \dfrac{1}{\Gamma(\alpha)}\displaystyle\int_0^t (t-\tau)^{\alpha-1}\Psi(\tau)\,d\tau, & \alpha > 0 \\ \Psi(t), & \alpha = 0, \end{cases}$$

so

$$\left({}_0I_t^\alpha\,\Psi\right)(t) = P^\alpha\Psi(t)\,,\ \alpha > 0. \tag{10}$$

Now, to define the fractional Legendre wavelets operational matrix of integration, we give a result, in the transition matrix of the base B to the base $\Psi(t)$.

Proposition 3.3.1. For m = 0,1,…, nc-1, the relation between the Legendre wavelet vector and m-set of block-pulse functions can be written as

$$\Psi(t) = H\,B(t), \tag{11}$$

where H is the $\left(2^{j-1}nc\right)$ x $\left(2^{j-1}nc\right)$ passage matrix

$$H = \begin{pmatrix} h_{1,0} & \cdots & h_{1,nc-1} & & & & & \\ \vdots & \ddots & \vdots & \cdots & & 0 & & \\ h_{nc,0} & \cdots & h_{nc,nc-1} & & & & & \\ & \vdots & & \ddots & & \vdots & & \\ & & & & h_{1,0} & \cdots & h_{1,nc-1} & \\ & 0 & & \cdots & \vdots & \ddots & \vdots & \\ & & & & h_{nc,0} & \cdots & h_{nc,nc-1} & \end{pmatrix},$$

and

$$h_{i,m} = \sqrt{2m+1}\ \sum_{k=0}^{m-1}(-1)^{m+k}\ \frac{(m+k)!}{(m-k)!\ (k!)^2\ nc^k}\ \frac{(i)^{k+1} - (i-1)^{k+1}}{(k+1)}$$

Proof. Let

$$h_{i,m} = \int_0^1 \Psi_{n,m}(t)\ b_i(t)\ dt = \sqrt{m+\frac{1}{2}}\ 2^{j/2}\ \int_{\frac{i-1}{q}}^{\frac{i}{q}} L_m\left(2^j t - 2\,n + 1\right)\ dt.$$

On the first level n = 1, this formula becomes

$$h_{i,m} = \sqrt{m+\tfrac{1}{2}}\ 2^{j/2}\ \int_{\frac{i-1}{q}}^{\frac{i}{q}} L_m\left(2^j t - 1\right)\ dt.$$

Assuming that $2^j t - 1$, we obtain

$$h_{i,m} = \sqrt{m+1/2}\ 2^{j/2}\ \int_{\frac{2i-2}{nc}-1}^{\frac{2i}{nc}-1} L_m\,(x)\ dx$$

$$= \sqrt{m+1/2}\,2^{j/2}\ \int_{\frac{2i-2}{nc}-1}^{\frac{2i}{nc}-1} \sum_{k=0}^{m-1}(-1)^{m+k}\binom{m}{k}\binom{m+k}{m}x^k dx$$

$$= \sqrt{m+1/2}\,2^{j/2}\ \sum_{k=0}^{m-1}(-1)^{m+k}\ \frac{(m+k)!}{(m-k)!\,(k!)^2\,nc^k\,q}\ \frac{(i)^{k+1} - (i-1)^{k+1}}{(k+1)},$$

We need also the following result [27]:

Proposition 3.3.2. Let $\alpha>0$. The fractional integral of block-pulse function vector can be written as

$$(I^{\alpha} B)(t) = F^{\alpha} B(t), \tag{12}$$

where F^{α} is the $(2^{j-1}nc)$ x $(2^{j-1}nc)$ matrix given by

$$F^{\alpha} = \left(\frac{T}{2^{j-1}nc}\right)^{\alpha} \frac{1}{\Gamma(\alpha+2)} \begin{pmatrix} f_1 & f_2 & f_3 & \cdots & f_{2^{j-1}nc} \\ & f_1 & f_2 & \cdots & f_{2^{j-1}nc-1} \\ & & f_1 & \cdots & f_{2^{j-1}nc-2} \\ & 0 & & \ddots & \vdots \\ & & & & f_1 \end{pmatrix},$$

and

$$\begin{cases} f_1 = 1, \\ f_p = p^{\alpha+1} - 2(p-1)^{\alpha+1} + (p-2)^{\alpha+1}, \qquad p = 2,3,\dots,2^{j-1}nc - i + 1, \end{cases}$$

with $i = 1,2,3,\dots,2^{j-1}nc$.

Now, we prove the following result for the fractional matrix of integration:

Theorem 3.3.3. The Legendre wavelets operational matrix P of fractional integration is given by

$$P^{\alpha} = H F^{\alpha} H^{-1}. \tag{13}$$

Proof. Using (10) and (11), we can write

$$\left({}_0I_t^{\alpha} \Psi\right)(t) = (I^{\alpha} H B)(t) = H(I^{\alpha} B)(t). \tag{14}$$

Thanks to (10) and (14), yields

$$P^{\alpha}\Psi(t) = HF^{\alpha} B(t). \tag{15}$$

By (11) and (15), we get

$$P^{\alpha} HB(t) = H F^{\alpha} B(t).$$

Therefore,

$$P^{\alpha} = H F^{\alpha-1}.$$

3.4. ILLUSTRATION OF THE APPROACH

In this subsection, we will describe our approach to solve numerically the system (2). We start with the decoupling and quasi-linearization iterative technique. It is summarized as follows:

Given initial profile for each solution: $\boldsymbol{Q}_{sw}^{(0)}(x), \boldsymbol{Q}_{fw}^{(0)}(x)\ , \dot{\boldsymbol{Q}}_{ss}^{(0)}(x), \dot{\boldsymbol{Q}}_{fs}^{(0)}(x)$

$$
\begin{aligned}
{}_0D_x^{\alpha}\boldsymbol{Q}_{sw}^{(k+1)} &= -c_1 + c_2\left(\frac{\dot{\boldsymbol{Q}}_{ss}^{(k+1)}}{\boldsymbol{Q}_{sw}^{(k+1)}} - \frac{\dot{\boldsymbol{Q}}_{fs}^{(k+1)}}{\boldsymbol{Q}_{fw}^{(k+1)}}\right)\\
{}_0D_x^{\alpha}\boldsymbol{Q}_{fw}^{(k+1)} &= c_1 - c_2\left(\frac{\dot{\boldsymbol{Q}}_{ss}^{(k+1)}}{\boldsymbol{Q}_{sw}^{(k+1)}} - \frac{\dot{\boldsymbol{Q}}_{fs}^{(k+1)}}{\boldsymbol{Q}_{fw}^{(k+1)}}\right)\\
{}_0D_x^{\alpha}Q_{fw} &= -c_3\left(\frac{\dot{\boldsymbol{Q}}_{ss}^{(k+1)}}{\boldsymbol{Q}_{sw}^{(k+1)}} - \frac{\dot{\boldsymbol{Q}}_{fs}^{(k+1)}}{\boldsymbol{Q}_{fw}^{(k+1)}}\right)\\
{}_0D_x^{\alpha}Q_{fw} &= c_3\left(\frac{\dot{\boldsymbol{Q}}_{ss}^{(k+1)}}{\boldsymbol{Q}_{sw}^{(k+1)}} - \frac{\dot{\boldsymbol{Q}}_{fs}^{(k+1)}}{\boldsymbol{Q}_{fw}^{(k+1)}}\right),
\end{aligned}
$$

where $U^{(k+1)}$ and $U^{(k)}$ are the approximations of the solution at the current and the preceding iteration, respectively.

To find a solution of (2), we apply the method described above for each equation and we calculate the decoupling and quasi-linearization error by using the following formula

$$E_{DQLT}^{(k+1)} = max\left(\left\|\boldsymbol{Q}_{sw}^{(k+1)} - \boldsymbol{Q}_{sw}^{(k)}\right\|_2, \left\|\boldsymbol{Q}_{fw}^{(k+1)} - \boldsymbol{Q}_{fw}^{(k)}\right\|_2, \dots, \left\|\dot{\boldsymbol{Q}}_{ss}^{(k+1)} - \dot{\boldsymbol{Q}}_{ss}^{(k)}\right\|_2\right) \quad (16)$$

where $\|\ .\ \|_2$ represents the Euclidian norm. This procedure gives the solution of the problem when the error is less than a given small epsilon.

For $u \in C^2([0,1])$, we develop our method for the problem

$$D^{\alpha}u(t) = g(t)\,u(t) + f(t), t \in]0,1], 0 < \alpha \leq 2 \quad (17)$$

such that

$$\begin{cases} u(0) = u_0 \\ u'(0) = u_1 \end{cases} \quad (18)$$

The condition $u'(0) = u_1$ is only for $1 < \alpha \leq 2$, where $f, g \in L^2([0,1])$. We approximate the derivative $D^{\alpha}u$ and the functions g and f as in (4) as follows :

$$\begin{cases} D^{\alpha}u(t) = U^T\Psi(t) \\ g(t) = G^T\Psi(t) \\ f(t) = F^T\Psi(t) \end{cases} \quad (19)$$

Using (10), we can write

$$\begin{aligned} u(t) &= I^{\alpha}\left(D^{\alpha}\, u(t)\right) + u(0) + u'(0)t \\ &= I^{\alpha}\left(U^{T}\,\Psi(t)\right) + u_0 d^{T}\,\Psi(t) + u_1 E^{T}\,\Psi(t) \\ &= U^{T} P^{\alpha}\,\Psi(t) + u_0 d^{T}\,\Psi(t) + u_1 E^{T}\,\Psi(t)\,, \end{aligned}$$

so

$$u(t) = \left(U^{T} P^{\alpha} + u_0 d^{T} + u_1 E^{T}\right)\Psi(t) \tag{20}$$

where $d = \langle 1, \Psi(t)\rangle_{L^2([0,1])}$ and $E = \langle t, \Psi(t)\rangle_{L^2([0,1])}$. Substituting (19) and (20) into (17), we have

$$U^{T}\Psi(t) = G^{T}\Psi(t)\left(U^{T} P^{\alpha} + u_0 d^{T} + u_1 E^{T}\right)\Psi(t) + F^{T}\,\Psi(t)$$

$$\Psi^{\mathrm{T}}(t)U = G^{T}\Psi(t)\Psi^{\mathrm{T}}(t)\left(U^{T} P^{\alpha} + u_0 d^{T} + u_1 E^{T}\right)^{T} + \Psi^{\mathrm{T}}(t)F$$

$$= \Psi^{\mathrm{T}}(t)\,\tilde{G}\left(U^{T} P^{\alpha} + u_0 d^{T} + u_1 E^{T}\right)^{T} + \Psi^{\mathrm{T}}(t)F$$

Thanks to (7), we obtain the following algebraic system

$$\left(I_d - \tilde{G}(P^{\alpha})^{T}\right) U = \tilde{G}(u_0 d^{T} + u_1 E^{T})^{T} + F. \tag{21}$$

The solution of the problem (17-18) is obtained by substituting U in (20).

3.4.1. NUMERICAL TESTS

In this section, we consider an example to show the efficiency and the accuracy of the proposed approach. For $0 < \alpha \leq 1$ and $t \in [0,1]$, we consider the system :

$$\begin{cases} D^{\alpha}\, u(t) = u^{2}(t) + v(t) + \dfrac{\Gamma(\beta+1)}{\Gamma(\beta+1-\alpha)}\, t^{\beta-\alpha} - t^{2\beta} - \sqrt[\gamma]{t} \\ D^{\alpha}\, v(t) = v^{2}(t) + u(t) + \dfrac{\Gamma\left(\frac{\gamma}{2}+1\right)}{\Gamma\left(\frac{\gamma}{2}+1-\alpha\right)}\, t^{\frac{\gamma}{2}-\alpha} - t^{\gamma} - t^{\beta}, \end{cases} \tag{22}$$

such that

$$\begin{cases} u(0) = 0 \\ v(0) = 0. \end{cases} \tag{23}$$

The exact solution of (22) and (23) is given by

$$\begin{cases} u_e(t) = t^{\beta} \\ v_e(t) = \sqrt[\gamma]{t}. \end{cases}$$

We employ the Legende wavelet method combined with the decoupling and quasi-linearization technique for studying the solutions of the problem (22–23).

In the Figure 2, we see the evolution of the logarithmic error induced by the decoupling and quasi-linearization technique defined in (16). We observe a strict decrease of the error, which explains the convergence and the stability of the solution.

Figure 2: Example 2: Error induced by DQLT.

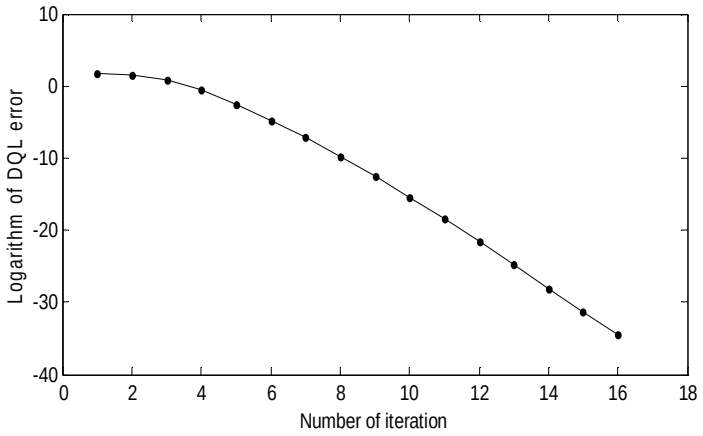

Then, as we know the exact solution, we estimate the absolute error of each solution is produced by cumulate of truncation, LWM and DQL technique by the following formula

$$E_A = \|u - u_e\|_2. \tag{24}$$

Figure 3: Example 2:The analytical and approximate solutions.

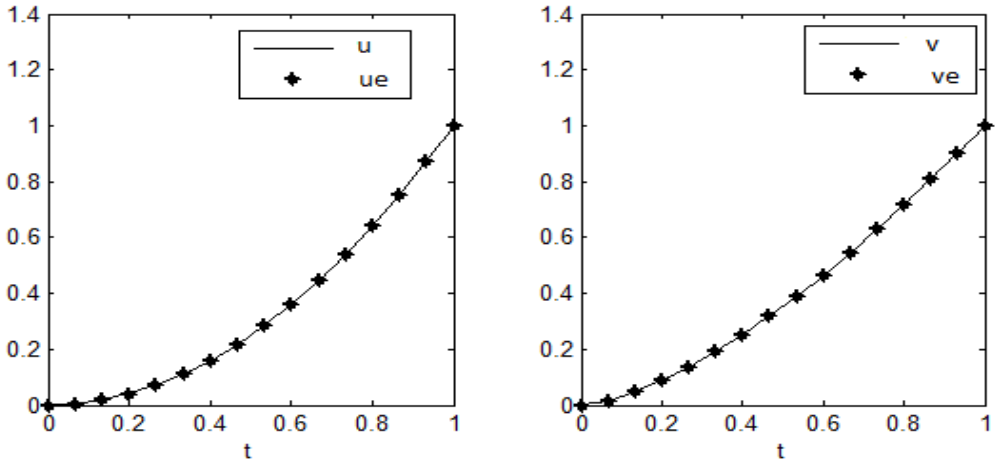

We observe a good agreement between the analytical and approximate solutions (see Figure 3). However, the obtained result shows that this approach can provide better performance.

Table 1: Example 2: The point wise errors for *u*.

t	Exact Solution	j=3 and nc=4	j=3 and nc=8	j=5 and nc=4	j=5 and nc=8
0	0	6.3318e-04	1.5723e-04	3.9868e-05	9.9852e-06
0.2	0.0400	6.4165e-04	1.6826e-04	4.0775e-05	1.0361e-05
0.4	0.1600	5.4928e-04	1.5991e-04	3.8131e-05	1.0120e-05
0.6	0.3600	4.5914e-04	1.4914e-04	3.5756e-05	9.8017e-06
0.8	0.6400	4.4651e-04	1.3749e-04	3.6947e-05	9.4494e-06
1	1.0000	4.5500e-04	1.2532e-04	3.9832e-05	9.0781e-06

Table 2: Example 2: The point wise errors for *v*.

t	Exact Solution	j=3 and nc=4	j=3 and nc=8	j=5 and nc=4	j=5 and nc=8
0	0	7.8510e-04	8.8309e-04	7.5065e-05	1.0596e-04
0.2	0.0894	8.7458e-04	1.9219e-04	7.5034e-05	2.0449e-05
0.4	0.2530	1.7925e-03	3.2299e-04	2.2016e-04	3.9049e-05
0.6	0.4648	1.0542e-03	3.4945e-04	1.1705e-04	4.2348e-05
0.8	0.7155	5.1373e-05	3.7980e-04	1.8159e-04	4.6889e-05
1	1.0000	3.7651e-05	3.8612e-04	1.7892e-04	4.7739e-05

Finally, as can be seen in Tables 1-2, only a small number of collocation points is needed to get the approximate solution, which is a full agreement with the exact solution up to 6 Digits. The obtained solutions show that this approach can effectively solve systems of fractional differential equations.

4. A SIMULATION STUDY

In this section, we propose a new numerical solution for the mathematical model described in Section 2. The proposed approach seems to be very efficient for nonlinear differential systems. Numerical test shows that one important feature of our approach is that it gives a high-quality of the solution as well as a stability and a computational speed for a small number of collocation points.

So, let us consider a small-scale reverse osmosis desalination fractional order model (2), where the co-current flow pattern is treated as shown in figure 1, associated with the conditions:

$$Q_{sw}(0) = 226.8$$
$$\dot{Q}_{ss}(0) = 2\,Q_{sw}(0)$$
$$Q_{fw}(0) = 0$$
$$\dot{Q}_{fs}(0) = 0$$

and

$$\frac{dQ_{sw}}{dx}(0) = \frac{dQ_{sw}}{dx}(0) = \frac{dQ_{sw}}{dx}(0) = \frac{dQ_{sw}}{dx}(0) = 0.$$

The membrane specifications and the operating parameters are given in the table 3 obtained from [29,28].

Table 3: The operating parameters.

Parameters	Value
The membrane diameter (D_m)	0.0576 m
Water density (σ_w)	10^3 kg/m^3
Solute permeability coefficient (B_s)	1.12×10^{-4} m/h
Water permeability constant (A_w)	4.2×10^{-13} h/m
Proportionality coefficient (κ)	$1.02 \times 10^{+12}$ m^2/h^2
Transmembrane pressure (ΔP)	$4.02 \times 10^{+13}$ kg/m/ h^2

The feed rate consisting of water and salts (solute) flows continuously and tangentially inside the membrane. Following the permselectivte property of the membrane, water diffuses faster than the solute. At the output of the module, we obtain a permeate at the tube side with a low concentration of salts, and a retentate at the shell side with a very high concentration of salts (Figure 1).

The results of simulation obtained by the proposed numerical solution method are shown in Figures 4–7. The first finding is that the behavior of the curves predicted by the model are very close to these obtained in the literature.

Figures 4–7 (A) show the variation of the solute and water flow rate in the tube and shell side along the dimensionless parameter *x*. As predicted, the variation of water and solute flow rate are close to zero at the entrance of the module. In reality, at this point of the module, water and solute flow rates are both constants and therefore, their variation is equal to zero. This behavior is demonstrated in the proposed model, which is not the case of the classical model with an integer derivative (see Figures 4–7 (B)).

Figure 4: The flow rate of the solute in tube-side.

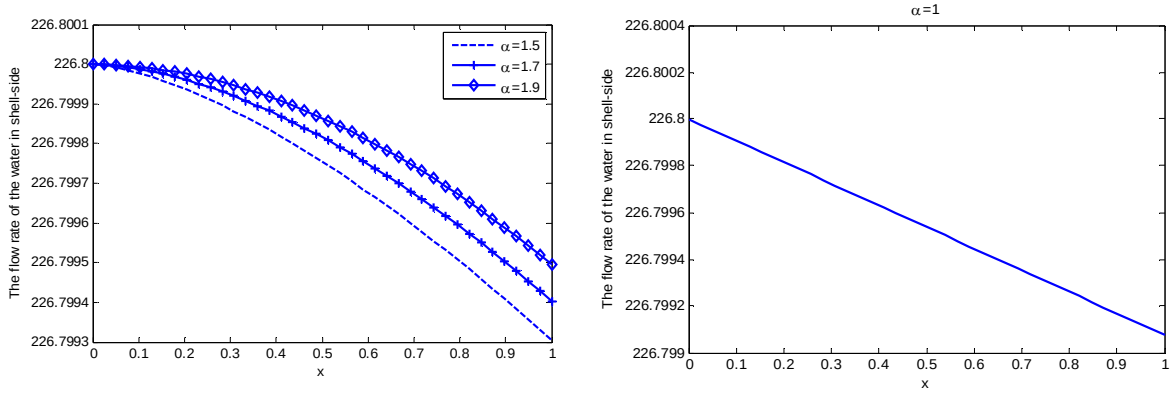

(A) (B)

Figure 5: The flow rate of the water in tube-side.

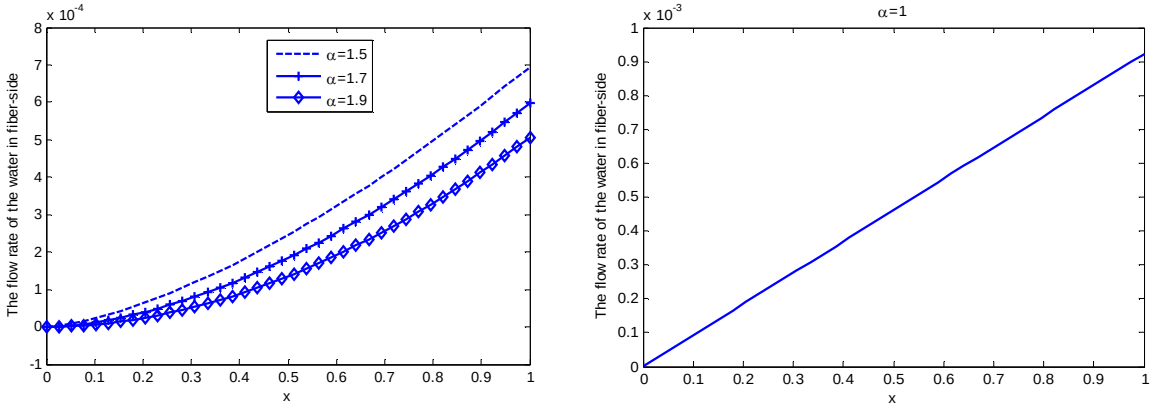

(A) (B)

Figure 6: The flow rate of the solute in shell-side.

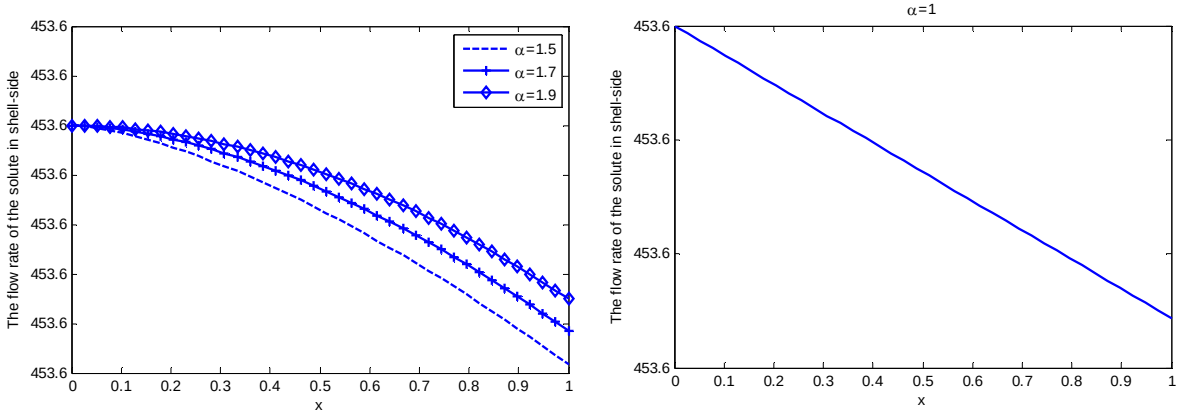

(A) (B)

Figure 7: The flow rate of the water in shell-side.

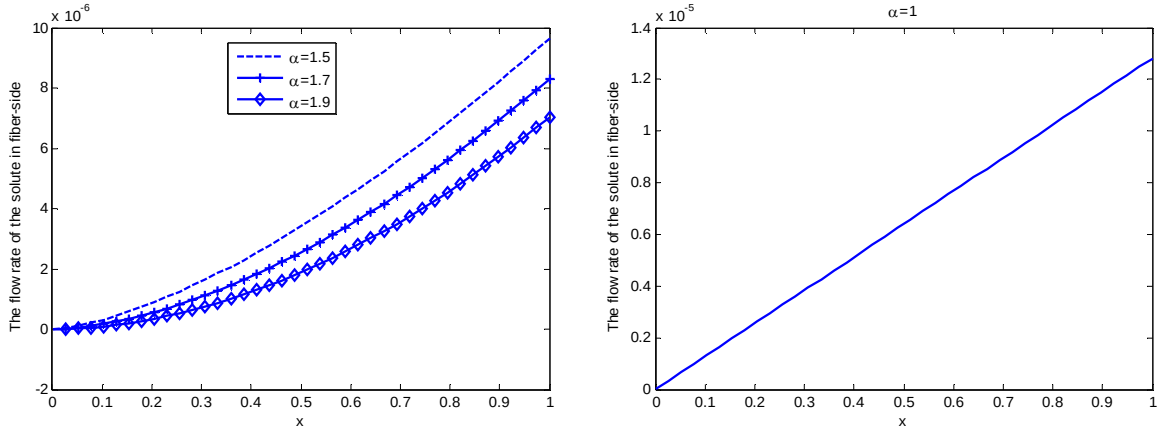

(A) (B)

Another means to verify the accuracy of the obtained results is to establish a matter balance. The following equation expresses the relative mass balance applied to the module:

$$V_1 = \frac{Q_{water}-(Q_{permeate\_water}+Q_{retentate\_water})}{Q_{feed\_water}} = 0,$$

$$V_2 = \frac{Q_{solute}-(Q_{permeate\_solute}+Q_{retentate\_solute})}{Q_{feed\_solute}} = 0.$$

The examination of the mass conservation law is a pertinent factor for the validation of our simulation. The results show the quality of the proposed model for α = 1.5, by looking V_1 for the water parameter is of the order of 2.45e-10 and V_2 for the solute parameter is less than 1.08e-12.

5. CONCLUSION

In this study, simulation of small-scale reverse osmosis desalination problem was conducted using a new fractional model. Numerical method of Legendre wavelets associated with the decoupling and quasi-linearization technique was applied to solve equations of mass transfer. Comparison of model predictions with experimental results in the literature reveals that a reasonable agreement exists between them. Simulation results reveal that fractional model can be considered as a more efficient predictor as compared with classical model. According to the model results, the calculation of the difference between the quantity of matter in the feed-side and the permeate-retentate sides shows the quality of the solutions obtained by the proposed model. It can be concluded from the obtained results that the proposed model in this work can well give the best prediction of reverse osmosis desalination phenomena.

REFERENCES

[1] A. Abbas, Model predictive control of a reverse osmosis desalination unit, *Desalin.* **194** (2006) 268–280.

[2] B. Absar and O. Belhamiti, Modeling and computer simulation of a reverse osmosis desalination plant-case study of Bousfer plant-Algeria, *Desalin. Water Treat.* **51** (2013) 5942–5953.

[3] B. Absar, S. E. M. L. Kadi and O. Belhamiti, Reverse osmosis modeling with the orthogonal collocation on finite element method, *Desalin. Water Treat.* **21** (2010) 23–32.

[4] M. G. Marcovecchio, P. A. Aguirre and N. J. Scenna, Global optimal design of reverse osmosis networks for seawater desalination: modeling and algorithm, *Desalin.* **184** (2005) 259−271.

[5] H. J. Oh, T. M. Hwang and S. Lee, A simplified simulation model of RO systems for seawater desalination, *Desalin.* **238** (2009) 128−139.

[6] N. Ablaoui-Lahmar and O. Belhamiti, Numerical study of convection-reaction-diffusion equation by the Legendre wavelet finite difference method. *Adv. Nonlinear Var. Inequal.* **19** (2016) (2) 94−112.

[7] H. Ali Merina and O. Belhamiti, Simulation Study of Nonlinear Reverse Osmosis Desalination System Using Third and Fourth Chebyshev Wavelet Methods. *MATCH Commun. Math. Comput. Chem.* **75** (2016) 629−652.

[8] A. Atangana and A. A. Secer, Note on fractional order derivatives and table of fractional derivatives of some special functions, *Abstr. Appl. Anal.* **2013** (2013) 1−8.

[9] O. Belhamiti, A new approach to solve a set of nonlinear split boundary value problems, *Commun. Nonlinear Sci. Numer. Simulat.* **17** (2012) 555−565.

[10] M. Caputo, Linear model of dissipation whose Q is almost frequency independent − II, *Geophys. J. R. Astron. Soc.* **13** (1967), 529−539.

[11] M. Du, Z. Wang and H. Hu, Measuring memory with the order of fractional derivative, *Sci. Rep*. **3** (2013) 1−3.

[12] K. Diethelm, A fractional calculus based model for the simulation of an outbreak of dengue fever, *Nonlinear Dyn.* **71** (2013) 613−619.

[13] F. Gorenflo and F. Mainardi, Fractional Calculus: Integral and Differential Equations of Fractional Order, in Fractals and Fractional Calculus in Continuum Mechanics, Series CISM Courses and Lecture Notes, Springer Verlag, Wien, **378** (1997), 223−276.

[14] M. Hamou Maamar and O. Belhamiti, New (0,2) Jacobi multi-wavelets adaptive method for numerical simulation of gas separations using hollow fiber membranes, *Commun. Appl. Nonlinear Anal.* **22** (2015) 3, 61−81.

[15] H. A. Jalab and R. W. Ibrahim, Texture enhancement for medical images based on fractional differential masks, *Discrete Dyn. Nat. Soc.* **2013**, Article ID 618536, (2013), 10 pages.

[16] H. A. Jalab and R. W. Ibrahim, Texture enhancement based on the Savitzky-Golay fractional, differential operator, *Math. Probl. Eng.* **2013**, Article ID 149289, (2013), 8 pages.

[17] A. A. Kilbas and S. A. Marzan, Nonlinear differential equation with the caputo fraction derivative in the space of continuously differentiable functions, *Differ. Equ.* **41** (2005) 84−89.

[18] J. Klafter, S. C. Lim and R. Metzler, *Fractional Dynamics. Recent Advances*, World Scientific, Singapore, (2011).

[19] A. D. Khawajia, I. K. Kutubkhanaha and J. M. Wieb, Advances in seawater desalination technologies. *Desalin.* **221** (2008) 47−69.

[20] K. Hakiki and O. Belhamiti, A dynamical study of fractional order obesity model by a combined Legendre wavelet method, submited, (2016).

[21] V. Lakshmikantham and A. S. Vatsala, Basic theory of fractional differential equations, *Nonlinear Anal.* (2008), 2677−2682.

[22] Y. Q. Liu and J. H. Ma, Exact solutions of a generalized multi-fractional nonlinear diffusion equation in radical symmetry, *Commun. Theor. Phys.* **52** (2009) 857−861.

[23] J. Lu and G. A. Chen, Note on the fractional-order Chen system, *Chaos, Solitons and Fractals* **27** (2006) 685−688.

[24] C. Qing−li, H. Guo and Z. A. Xiu−qiong, Fractional differential approach to low contrast image enhancement, *Int. J. Knowledge Lang. Proces.* **3** (2012) 20−29.

[25] M. Rehman and R. A. Khan, The Legendre wavelet method for solving fractional differential equations, *Commun. Nonlinear Sci. Numer. Simulat.* **16** (2011) 4163−4173.

[26] M. Razzaghi and S. Yousefi, Legendre wavelets direct method for variational problems, *Math. Comput. Simul.* **53** (2000) 185−192.

[27] C. H. Wang, On the generalization of Block Pulse Operational matrices for fractional and operational calculus, *J. Frankin Inst.* **315** (1983) 91−102.

[28] C. S. Slater, Development of a simulation model predicting performance of reverse osmosis batch systems, *Separa. Sci. Techno.* **27** (1992) 1361−1388.

[29] C. S. Slater, J. M. Zielinski, R. G. Wendel and C. G. Uchrin, Modeling of small scale reverse osmosis systems, *Desalin.* **52** (1985) 267−284.

[30] V. M. Starov, J. Smart and D. R. Lloyd, Performance optimization of hollow fiber reverse osmosis membranes, Part I. Development of theory, *J. Membrane Sci.* **103** (1995) 257−270.

[31] J. Smart, V. M. Starov and D.R. Lloyd, Performance optimization of hollow fiber reverse osmosis membranes. Part II. Comparative study of flow configurations, *J. Membrane Sci.* **119** (1996) 117−128.

Iranian J. Math. Chem. 8 (4) December (2017) 365 − 375

Iranian Journal of Mathematical Chemistry

Journal homepage: ijmc.kashanu.ac.ir

Solving Time–fractional Chemical Engineering Equations by Modified Variational Iteration Method as Fixed Point Iteration Method

A. HAGHBIN[•,1] AND H. JAFARI[2]

[1]Department of Mathematics, Gorgan branch, Islamic Azad University, Gorgan, Iran

[2]Department of Mathematics, University of Mazandaran, P. O. Box 47416−95447, Babolsar, Iran

ARTICLE INFO

Article History:

Received 18 May 2015
Accepted 27 October 2015
Published online 8 May 2017
Academic Editor: Ivan Gutman

Keywords:

Fractional differential equations
Variational iteration method
Fixed point theory
Chemical reactor

ABSTRACT

The variational iteration method (VIM) was extended to find approximate solutions of fractional chemical engineering equations. The Lagrange multipliers of the VIM were not identified explicitly. In this paper we improve the VIM by using concept of fixed point iteration method. Then this method was implemented for solving system of the time fractional chemical engineering equations. The obtained approximate solutions are compared with the numerical results in the literature to show the applicability, efficiency and accuracy of the method.

1. INTRODUCTION

Fractional calculus is a power tool for finding solution of non-linear problems. So, it has a tremendous use in basic sciences and engineering, see e.g. [1−8].

The VIM is one of the powerful methods within the exact and approximate analyticalsolutions for solving nonlinear equations. The method was first initiated by [9], and it was successfully used by various researchers to investigate the linear andnonlinear problems [9, 10]. We mention that Jafari et.al. applied the variational iterationmethod to the modified Camassa-Holm and Degasperis−Procesi equations andfractional Davey−Stewartson equations, [10, 11]. Momani and Odibat [12] has implementedthe variational iteration method to solve nonlinear fractional differentialequations. It was shown by several authors (see e.g. Wazwaz [13]) that this method ismore powerful than existing techniques such as the Adomian decomposition method [14, 15], perturbation

•Corresponding Author (Email address:ahmadbin@yahoo.com)
DOI: 10.22052/ijmc.2017.29095.1109

method, etc. Besides, the VIM gives rapidly convergent successiveapproximations of the exact solution if such a solution exists. Another importantadvantage is related to the fact that the VIM is capable of greatly reducing the sizeof calculation while still maintaining high accuracy of the numerical solution.

In [16, 17], it was shown that the VIM for obtaining approximate solutions of initialvalue problems is a version of the well-established fixed point iteration methods.In this paper, we are interested into approximate solutions of time fractionalchemical engineering problems as follow:

$$\begin{aligned} D_*^{\alpha 1} x_1(t) &= f_1(t, x_1, ..., x_n) \\ D_*^{\alpha 2} x_2(t) &= f_2(t, x_1, ..., x_n) \\ &\vdots \\ D_*^{\alpha n} x_n(t) &= f_n(t, x_1, ..., x_n) \end{aligned} \tag{1}$$

where $D_*^{\alpha i}$ is the Caputo derivative of x_i of order a_i and $0 < a_i \leq 1$, subject to the initial conditions

$$x_1(0) = c_0, x_2(0) = c_2, ..., x_n(0) = c_n. \tag{2}$$

The general response expressions contain a parameter α describing the order of the fractional derivative that can be varied to obtain various responses. The solutions corresponding to ordinary chemical problems, performing the same dynamics, are also determined as a special case of our general solutions. The organization of this paper is as follows: In Section 2, some basic definitions and properties of the fractional calculus are given. In section 3, we introduce variational iteration method and deform it to fixed point iteration method. In Section 4, the mentioned method in Section 3 is used to seek an approximate solution of chemical Eq. (1) with the given initial conditions (2). Also, the accuracy and efficiency of the scheme is investigated with three numerical illustrations in that section. Finally, Section 5 consists of some brief conclusions.

2. PRELIMINARY

In this section, we give some definitions and properties of the fractional calculus.

Definition 2.1. A real function $f(t); t > 0,$ is said to be in the space $C_\mu, \mu \in R,$ if there exists a real number $p(>\mu)$, such that $f(t) = t^p f_1(t),$ where $f_1(t) \in C(0, \infty),$ and it is said to be in the space $C_\mu^n,$ if and only if $f^{(n)} \in C_\mu, n \in N.$

Definition 2.2. The Riemann–Liouville fractional integral operator (J^{α}), of order $\alpha > 0$, of a function $f \in C_{\mu}, \mu \geq -1,$ is defined as

$$J^{\alpha} f(t) = \frac{1}{\Gamma(\alpha)} \int_0^t (t-s)^{\alpha-1} f(s) ds, \quad \alpha > 0,$$
$$J^{\alpha} f(t) = f(t), \quad \alpha = 0.$$

The main properties of the operator (J^{α}) can be found in [18, 19], we mention only the following: For $f \in C_{\mu}, \mu \geq -1, \alpha, \beta \geq 0$ and $\gamma > -1$:

1. $J^{\alpha} J^{\beta} f(t) = J^{\alpha+\beta} f(t)$
2. $J^{\alpha} J^{\beta} f(t) = J^{\beta} J^{\alpha} f(t)$
3. $J^{\alpha} t^{\gamma} = \frac{\Gamma(\gamma+1)}{\Gamma(\alpha+\gamma+1)} t^{\alpha+\gamma}$

The Riemann–Liouville derivative has certain disadvantages when trying to model real-world phenomena with fractional differential equations. Therefore, we shall introduce a modified fractional differential operator D^{α} proposed by Caputo in his work on the theory of viscoelasticity [20].

Definition 2.3. The fractional derivative of $f(t)$ in the Caputo sense is defined as

$$D^{\alpha} f(t) = J^{n-\alpha} D^n f(t) = \frac{1}{\Gamma(n-\alpha)} \int_0^t (t-s)^{n-\alpha-1} f^{(n)}(s) ds$$

Also, we need here two of it's basic properties.

Lemma 2.1. If $n-1 < \alpha \leq n, n \in N$ and $f \in C_{\mu}^n, \mu \geq -1$ then $(D^{\alpha} J^{\alpha}) f(t) = f(t)$ and $(J^{\alpha} D^{\alpha}) f(t) = f(t) - \sum_{k=0}^{n-1} f^{(k)}(0^+) \frac{t^k}{k!}, t > 0.$

3. THE VIM AND FIXED POINT ITERATION METHOD

To illustrate the basic concepts of the VIM we consider the following general nonlinear system:

$$L_i(u_i(t)) + N(u_1(t),...,u_m(t)) = g_i(t);\ i = 1,2,...,m, \tag{3}$$

where L_i is the linear operator and N_i is the nonlinear operator, and $g_i(t)$ is the inhomogeneous term. In the VIM correction function for Eq. (3) can be written as [9]:

$$u_{i,n+1}(t) = u_{i,n}(t) + \int_0^t \lambda_i(t-\tau)(L_i(u_{i,n}(\tau)) + N_i(\tilde{u}_1(\tau),...,\tilde{u}_m(\tau)) - g_i(\tau))d\tau;\ i = 1,2,...,m. \tag{4}$$

It is obvious that the successive approximation $u_{i,n}; n \geq 0$ can be established by determining λ_i, a general Lagrange multiplier, which can be identified optimally via the variational theory [21]. The function $\tilde{u}_{i,n}$ is a restricted variation, which means $\delta\tilde{u}_{i,n} = 0$. Therefore, we first determine the Lagrange multiplier λ_i that will be identified via integration by parts. The successive approximations $u_{i,n}(t), n > 0$ of the solution $u_i(t)$ will be readily obtained upon using the obtained Lagrange multiplier and by using any selective function $u_{i,0}$ as zeroth approximation which satisfy in given initial condition. Consequently, the exact solution may be procured by using,

$$u_i(t) = \lim_{n\to\infty} u_{i,n}(t) \tag{5}$$

Obviously, identification of the Lagrange multipliers is crucial to derive a variational iteration formula. Now, if we change our attitude and consider the VIM as special case of fixed point iteration [16, 17] we can find a simple and straight manner to determine Lagrange multipliers. In this order from (3) if L^{-1} exist then we have:

$$u_i(t) = \phi_i(t) + L_i^{-1}[g_i(t) - N_i(u_1(t),...,u_m(t))];\ i = 1,2,...,m, \tag{6}$$

where $\phi_i(t)$ is $Ker(L_i)$ which determined by initial condition. In fact, we get Lagrange multipliers automatically while calculating inverse of operator L_i. Applying simple fixed point iteration method on (6) we get

$$u_{i,n+1}(t) = \phi_i(t) + L_i^{-1}[g_i(t) - N_i(u_{1,n}(t),...,u_{m,n}(t))];\ i = 1,2,...,m. \tag{7}$$

Here recursive formula (7) are constructed for two special case of linear fractional differential equation as follow

$$\begin{cases} if\ \ L(u) = D^{\alpha}u\ \ then\ \ L^{-1}(f) = \int_0^t \dfrac{(t-\tau)^{\alpha-1}}{\Gamma(\alpha)} f(\tau)\,d\tau\ \ \ and \\ u_{n+1}(t) = \phi(t) + \int_0^t \dfrac{(t-\tau)^{\alpha-1}}{\Gamma(\alpha)}(g(\tau) - N(u_n(\tau)))\,d\tau, \end{cases} \tag{8}$$

$$\begin{cases} \text{if } \; L(u) = D^{\alpha}u + \omega u \;\; \text{then } \; L^{-1}(f) = \int_0^t (t-\tau)^{\alpha-1} E_{\alpha,\alpha}(-\omega(t-\tau)^{\alpha}) f(\tau)\, d\tau \text{ and} \\ u_{n+1}(t) = \phi(t) + \int_0^t (t-\tau)^{\alpha-1} E_{\alpha,\alpha}(-\omega(t-\tau)^{\alpha})[g(\tau) - N(u_n(\tau))]d\tau. \end{cases} \tag{9}$$

4. TEST PROBLEMS

In this section, we present three examples to illustrate the applicability of new method to solve linear and nonlinear chemical fractional differential equations.

Example 4.1. *Chemical Reactor.* A reaction $A \to B$ takes place in two reactors in series. The reactors are well mixed but are not at steady state. The unsteady-state mass balance for each stirred tank reactor are given in the form of system of fractional differential equations are

$$\begin{aligned} D^{\alpha}u(t) &= \frac{1}{\tau}(CA_0 - u) - \beta u \\ D^{\alpha}v(t) &= \frac{-1}{\tau}v - \beta u \\ D^{\alpha}w(t) &= \frac{1}{\tau}(u - w) - \beta w \\ D^{\alpha}y(t) &= \frac{1}{\tau}(v - y) - \beta y \end{aligned} \tag{10}$$

where CA_0 is the concentration of A at the inlet of first reactor. $CA_1(=u)$ is the concentration of A at the outlet of the first reactor (and inlet of the second). $CA_2(=w)$ is the concentration of A at the outlet of the second reactor. $CB_1(=v)$ is the concentration of B at the outlet of the first reactor (and inlet of the second). $CB_2(=y)$ is the concentration of B in the second reactor. τ is the residence time for each reactor, and β is the rate constant for reaction of A to produce B. Consider CA_0 is equal to 10, $\beta = 0.1$ and $\tau = 5$. Initial conditions

$$CA_1(0) = u(0) = 0, CA_2(0) = w(0) = 0, CB_1(0) = v(0) = 0, CB_2(0) = y(0) = 0 \tag{11}$$

By setting L_1, L_2, L_3 *and* L_4 for this system

$$
\begin{aligned}
L_1(u(t)) &= D^{\alpha}u(t) + \frac{3}{10}u(t) \\
L_2(v(t)) &= D^{\alpha}v(t) + \frac{1}{5}v(t) \\
L_3(w(t)) &= D^{\alpha}w(t) + \frac{3}{10}w(t) \\
L_4(y(t)) &= D^{\alpha}y(t) + \frac{3}{10}y(t)
\end{aligned}
\tag{12}
$$

and using (9), the transform of Eq. (10) with initial conditions (11) leads to the following recurrence relations:

$$u_{n+1}(t) = \int_0^t (t-\tau)^{\alpha-1} E_{\alpha,\alpha}(-\frac{3}{10}(t-\tau)^{\alpha})(2)\, d\tau \tag{13}$$

$$v_{n+1}(t) = \int_0^t (t-\tau)^{\alpha-1} E_{\alpha,\alpha}(-\frac{1}{5}(t-\tau)^{\alpha})[\frac{1}{10}u_n(\tau)]d\tau \tag{14}$$

$$w_{n+1}(t) = \int_0^t (t-\tau)^{\alpha-1} E_{\alpha,\alpha}(-\frac{3}{10}(t-\tau)^{\alpha})[\frac{1}{5}u_n(\tau)]d\tau \tag{15}$$

$$y_{n+1}(t) = \int_0^t (t-\tau)^{\alpha-1} E_{\alpha,\alpha}(-\frac{3}{10}(t-\tau)^{\alpha})[\frac{1}{5}v_n(\tau)]d\tau \tag{16}$$

We start with initial approximations $u_0(t) = 0, v_0(t) = 0, w_0(t) = 0, y_0(t) = 0,$ which satisfy in Eqs. (11). In right hand said of Eq.(13) there isn't u_n so its exact solution will obtain at first iteration . In the second iteration we get exact solutions of $v(t)$ and $w(t)$ by using the exact solution of $u(t) = u_1(t)$ in right hand said of Eqs. (14) and (15). Finally, in the third iteration all exact solutions can be obtain as follow

$$
\begin{aligned}
u(t) &= \frac{20}{3}(1 - E_{\alpha}(\frac{-20}{3}t^{\alpha})) \\
v(t) &= \frac{10}{3}(1 - 3E_{\alpha}(\frac{-1}{5}t^{\alpha}) + 2E_{\alpha}(\frac{-3}{10}t^{\alpha})) \\
w(t) &= \frac{40}{9}(1 - \sum_{m=0}^{\infty}\frac{(1-m)(-3/10)^m}{\Gamma(m\alpha+1)}t^{m\alpha}) \\
y(t) &= \frac{20}{9}(1 - 9E_{\alpha}(\frac{-1}{5}t^{\alpha}) + \sum_{m=0}^{\infty}\frac{(8-2m)(-3/10)^m}{\Gamma(m\alpha+1)}t^{m\alpha})
\end{aligned}
$$

Example 4.2. *Concentration of Reactants.* The concentrations of three reactants are in the form of a system of nonlinear FDEs as

$$\begin{aligned} D^{\alpha}u(t) &= -k_1 u + k_2 v\, w \\ D^{\alpha}v(t) &= -k_3 u - k_4 v\, w - k_5 v^2 \\ D^{\alpha}w(t) &= k_6 v^2 \end{aligned} \tag{17}$$

where k_1, k_2, k_3, k_4, k_5 and k_6 are constant parameters (k_1 = 0.04, k_2 = 0.01, k_3 = 400, k_4 = 100, k_5 = 30000, k_6 = 30). The initial conditions are given by

$$u(0) = 1, \quad v(0) = 0, \quad w(0) = 0. \tag{18}$$

By setting $L = D^{\alpha}$ as a linear operator for every equation in (17) and using (8), we get the recursive formula for concentration equations as follow

$$\begin{aligned} u_{n+1}(t) &= -\int_0^t \lambda(t-\tau)(-k_1 u_n(\tau) + k_2 v_n(\tau)\, w_n(\tau))\, d\tau \\ v_{n+1}(t) &= -\int_0^t \lambda(t-\tau)(-k_3 u_n(\tau) + k_4 v_n(\tau)\, w_n(\tau) + k_5 v_n{}^2(\tau))\, d\tau \\ w_{n+1}(t) &= \int_0^t \lambda(t-\tau)(k_6 v_n{}^2(\tau))\, d\tau \end{aligned} \tag{19}$$

where

$$\lambda(t,\tau) = \frac{(t-\tau)^{\alpha-1}}{\Gamma(\alpha)}$$

By starting with an initial approximation $u_0(t) = 1, v_0(t) = 0$ and $w_0(t) = 0$ given by Eq. (18) and using the above iteration formulae (19) we can directly obtain the other components. The first four components of the series are given by

$$\begin{aligned} u(t) &= 1 - \frac{t^{\alpha}}{25\Gamma(1+\alpha)} + \frac{t^{2\alpha}}{625\Gamma(1+2\alpha)} - \frac{t^{3\alpha}}{15625\Gamma(1+3\alpha)} \\ v(t) &= -\frac{400t^{\alpha}}{\Gamma(1+\alpha)} + \frac{16t^{2\alpha}}{\Gamma(1+2\alpha)} - \frac{4800000000t^{3\alpha}}{\Gamma(1+\alpha)^2\Gamma(1+3\alpha)} \\ w(t) &= \frac{4800000t^{3\alpha}}{\Gamma(1+\alpha)^2\Gamma(1+3\alpha)} \end{aligned} \tag{20}$$

For $\alpha = 1$ we have

$$\begin{aligned} u(t) &= 1 - 0.04t + 0.0008t^2 - 0.000106667t^3 \\ v(t) &= 400t - 8t^2 - 1.6\times 10^9 t^3 \\ w(t) &= 1600000t^3 \end{aligned}$$

which is the same of solution in [22].

Example 4.3. Chemical Reaction there is the system of nonlinear FDE equation which representing a nonlinear reaction,

$$\begin{aligned} D^{\alpha}u(t) &= -u \\ D^{\alpha}v(t) &= u - v^2 \quad (21) \\ D^{\alpha}w(t) &= v^2 \end{aligned}$$

with the initial conditions are given by

$$u(0) = 1,\ v(0) = 1,\ w(0) = 0. \quad (22)$$

By setting $L = D^{\alpha}$ as a linear operator for every equation in (21) and using (8), the recursive formula for reaction equation (21) is

$$\begin{aligned} u_{n+1}(t) &= 1 - \int_0^t \lambda(t-\tau)u_n(\tau)d\tau \\ v_{n+1}(t) &= -\int_0^t \lambda(t-\tau)(-u_n(\tau)v_n{}^2(\tau))\,d\tau \quad (23) \\ w_{n+1}(t) &= \int_0^t \lambda(t-\tau)v_n{}^2(\tau)\,d\tau \end{aligned}$$

where

$$\lambda(t,\tau) = \frac{(t-\tau)^{\alpha-1}}{\Gamma(\alpha)}.$$

By using recurrence relation (23) and initial approximation $u_0(t) = 1, v_0(t) = 0$ and $w_0(t) = 0$ given by Eq. (22) three Iteration terms of solutions are obtained as follow:

$$\begin{cases} u_1(t) = 1 - \dfrac{t^{\alpha}}{\Gamma(1+\alpha)}, \\ v_1(t) = \dfrac{t^{\alpha}}{\Gamma(1+\alpha)}, \\ w_1(t) = 0, \end{cases} \quad (24)$$

$$\begin{cases} u_2(t) = 1 - \dfrac{t^{\alpha}}{\Gamma(1+\alpha)} + \dfrac{t^{2\alpha}}{\Gamma(1+2\alpha)}, \\ v_2(t) = \dfrac{t^{\alpha}}{\Gamma(1+\alpha)} - \dfrac{t^{2\alpha}}{\Gamma(1+2\alpha)} - \dfrac{t^{3\alpha}\Gamma(1+2\alpha)}{\Gamma(1+\alpha)^2\Gamma(1+3\alpha)}, \\ w_2(t) = \dfrac{t^{3\alpha}\Gamma(1+2\alpha)}{\Gamma(1+\alpha)^2\Gamma(1+3\alpha)}, \end{cases} \quad (25)$$

$$\begin{cases} u_3(t) = 1 - \dfrac{t^{\alpha}}{\Gamma(1+\alpha)} + \dfrac{t^{2\alpha}}{\Gamma(1+2\alpha)} - \dfrac{t^{3\alpha}}{\Gamma(1+3\alpha)}, \\ v_3(t) = \dfrac{t^{\alpha}}{\Gamma(1+\alpha)} - \dfrac{t^{2\alpha}}{\Gamma(1+2\alpha)} - \left(\dfrac{1}{\Gamma(1+3\alpha)} - \dfrac{\Gamma(1+2\alpha)}{\Gamma(1+\alpha)^2\Gamma(1+3\alpha)}\right)t^{3\alpha}, \\ w_3(t) = \dfrac{t^{3\alpha}\Gamma(1+2\alpha)}{\Gamma(1+\alpha)^2\Gamma(1+3\alpha)}. \end{cases} \tag{26}$$

In the third iteration the first four components of the series solution are expressed and we have the following approximate solution

$$u(t) = 1 - \frac{t^{\alpha}}{\Gamma(1+\alpha)} + \frac{t^{2\alpha}}{\Gamma(1+2\alpha)} - \frac{t^{3\alpha}}{\Gamma(1+3\alpha)},$$

$$v(t) = \frac{t^{\alpha}}{\Gamma(1+\alpha)} - \frac{t^{2\alpha}}{\Gamma(1+2\alpha)} - \left(\frac{1}{\Gamma(1+3\alpha)} - \frac{\Gamma(1+2\alpha)}{\Gamma(1+\alpha)^2\Gamma(1+3\alpha)}\right)t^{3\alpha},$$

$$w(t) = \frac{\Gamma(1+2\alpha)t^{3\alpha}}{\Gamma(1+\alpha)^2\Gamma(1+3\alpha)},$$

which is the same of solution in [23].

5. CONCLUSION

For illustration purposes, we considered three examples. Results obtained using the scheme presented here agree well with the numerical results presented elsewhere. Results also show that the numerical scheme is very effective and convenient for solving nonlinear partial differential equations of fractional order. The numerical computations associated with the three examples discussed above were performed by using the Computer Algebra System Mathematica.

ACKNOWLEDGEMENT: The corresponding author would like to express his appreciation to the research vice president of Islamic Azad University, Gorgan branch due to financial support.

REFERENCES

1. D. Baleanu, K. Diethelm, E. Scalas, J. J. Trujillo, *Fractional Calculus Models and Numerical Methods, Series on Complexity, Nonlinearity and Chaos,* World Scientific, 2012.

2. A. A. Kilbas, H. M. Srivastava, J. J. Trujillo, *Theory and applications of fractional differential Equations*, North-Holland Mathematics Studies, 204. Elsevier Science B.V., Amsterdam, 2006.

3. V. Kiryakova, *Generalized Fractional Calculus and Applications*, Longman and John Wiley, Harlow−New York, 1994.

4. F. Mainardi, An historical perspective on fractional calculus in linear viscoelasticity, *Frac. Calc. Appl. Anal*. **15**(4) (2012), 712−718.

5. A. B. Malinowska, D. F. M. Torres, Fractional calculus of variations for a combined Caputo derivative, *Frac. Calc. Appl. Anal.* **14** (4) (2011), 523−538.

6. K. B. Oldham, J. Spanier, *The Fractional Calculus*, Academic Press, New York and London, 1974.

7. I. Podlubny, *Fractional Differential Equations*, Academic Press, San Diego, 1999.

8. S. G. Samko, A. A. Kilbas, O. I. Marichev, *Fractional Integrals and Derivatives*: *Theory and Applications*, Gordon and Breach, Yverdon, 1993.

9. J. H. He, Variational iteration method some recent result and new interpretations, *J. Comput. Appl. Math.* **207** (2007) 3−17.

10. H. Jafari, M. Zabihi, E. Salehpor, Application of variational iteration method for modified Camassa−Holm and Degasperis−Procesi equations, *Numer. Meth. Part. D. E.* **26** (5) (2010) 1033−1039.

11. H. Jafari, A. Kadem, D. Baleanu, T. Yilmaz, Solutions of the fractional Davey−Stewartson equations with variational iteration method, *Rom. Rep. Phys.* **64** (2) (2012) 337−346.

12. S. Momani, Z. Odibat, Numerical comparison of methods for solving linear differential equations of fractional order, *Chaos Soliton. Fract.* **31** (2007) 1248−1255.

13. A. M. Wazwaz, A comparison between the variational iteration method and Adomian decomposition method, *J. Comput. Appl. Math.* **207** (2007) 129−136.

14. V. Daftardar−Gejji, H. Jafari, Adomian decomposition: A tool for solving a system of fractional differential equations, *J. Math. Anal. Appl.* **2** (2005) 508−518.

15. S. Momani, N. Shawagfeh, Decomposition method for solving fractional Riccati differential equations, *Appl. Math. Comput.* **182** (2006) 1083–1092.

16. H. Jafari, A comparison between the variational iteration method and the successive approximations method, *App. Math. Letters* **32** (2014) 1–5.

17. A. S. Khuri, A. Sayfy, Variational iteration method: Green's functions and fixed point iterations perspective, *Appl. Math. Letters* **32** (2014) 28–34.

18. K. S. Miller, B. Ross, *An Introduction to the Fractional Calculus and Fractional Differential Equations*, John Wiley and Sons, New York, 1993.

19. K. B. Oldham, J. Spanier, *The Fractional Calculus*, Academic Press, New York, 1974.

20. M. Caputo, Linear models of dissipation whose Q is almost frequency independent. Part II, *J. Roy. Astr. Soc.* (1967) 529–539.

21. M. Inokuti, H. Sekine, T. Mura, General use of the Lagrange multiplier in nonlinear mathematical physics, in: S. Nemat-Nasser (Ed.), *Variational Method in Mechanics of Solids*, Pergamon Press, Oxford, 1978, pp. 156–162.

22. D. D. Ganji, M. Nourollahi, E. Mohseni, Application of He's method to nonlinear chemistry problems, *Comp. Math. Appl.* **54** (2007) 1122–1132.

23. N. Alam Khan, A. Ara, A. Mahmood, Approximate solution of time-fractional chemical engineering equations: A comparative study, Int. J. Chem. Reactor Eng. **8** (2010) Article A19.

Iranian J. Math. Chem. 8 (4) December (2017) 377 − 390

Iranian Journal of Mathematical Chemistry

Journal homepage: ijmc.kashanu.ac.ir

The Ratio and Product of the Multiplicative Zagreb Indices

RAMIN KAZEMI•

Department of Statistics, Imam Khomeini International University, Qazvin, Iran

ARTICLE INFO

Article History:

Received 9 May 2016
Accepted 7 June 2016
Published online 20 April 2017
Academic Editor: Sandi Klavžar

Keywords:

molecular graph with tree structure
multiplicative Zagreb index
moment
Doob's supermartingale inequality

ABSTRACT

The first multiplicative Zagreb index $\Pi_1(G)$ is equal to the product of squares of the degree of the vertices and the second multiplicative Zagreb index $\Pi_2(G)$ is equal to the product of the products of the degree of pairs of adjacent vertices of the underlying molecular graphs G. Also, the multiplicative sum Zagreb index $\Pi_3(G)$ is equal to the product of the sums of the degree of pairs of adjacent vertices of G. In this paper, weintroduce a new version of the multiplicative sum Zagreb index and study the moments of the ratio and product of all indices in a randomly chosen molecular graph with tree structure of order n. Also, a supermartingale is introduced by Doob's supermartingale inequality.

1. INTRODUCTION

Molecular graphs can distinguish between structural isomers, compounds which have the same molecular formula but non-isomorphic graphs- such as isopentane and neopentane. On the other hand, the molecular graph normally does not contain any information about the three-dimensional arrangement of the bonds, and therefore cannot distinguish between conformational isomers (such as cis and trans 2-butene) or stereoisomers (such as D- and L-glyceraldehyde).

In some important cases (topological index calculation etc.) the following classical definition is sufficient: molecular graph is connected undirected graph one-to-one corresponded to structural formula of chemical compound so that vertices of the graph

•Corresponding author (Email: r.kazemi@sci.ikiu.ac.ir)
DOI: 10.22052/ijmc.2017.53731.1198

correspond to atoms of the molecule and edges of the graph correspond to chemical bonds between these atoms.

In the fields of chemical graph theory, molecular topology, and mathematical chemistry, a topological index also known as a connectivity index is a type of a molecular descriptor that is calculated based on the molecular graph of a chemical compound. Topological indices are numerical parameters of a graph which characterize its topology and are usually graph invariant. Topological indices are used for example in the development of quantitative structure-activity relationships (QSARs) in which the biological activity or other properties of molecules are correlated with their chemical structure. The simplest topological indices do not recognize double bonds and atom types (C, N, O etc.) and ignore hydrogen atoms ("hydrogen suppressed") and defined for connected undirected molecular graphs only. More sophisticated topological indices also take into account the hybridization state of each of the atoms contained in the molecule. Hundreds of indices were introduced. The Hosoya index is the first topological index recognized in chemical graph theory, and it is often referred to as the topological index. Other examples include the Wiener index, Randi c′ 's molecular connectivity index, Balaban's J index, and the TAU descriptors [12].

Let G be a molecular graph. Two vertices of G, connected by an edge, are said to be adjacent. The number of vertices of G, adjacent to a given vertex v, is the degree of this vertex, and will be denoted by $d(v)$. Gutman [5] introduced the following general form for topological indices:

$$TI_s = TI_s(G) = \sum_{uv \in E(T)} F(d(u), d(v)),$$

where the summation goes over all pairs of adjacent nodes u, v of molecular graph G, and where $F = F(x, y)$ is an appropriately chosen function. In particular, $F(x,y) = (xy)^{-1/2}$ for Randić index, $F(x, y) = x + y$ for the first Zagreb index, $F(x, y) = xy$ for the second Zagreb index, $F(x, y) = |x - y|$ for the third Zagreb index, $F(x, y) = (xy)^{\lambda}$ $(\lambda \in \mathbb{R})$ for the second variable Zagreb index, $F(x,y) = ((x+y-2)(xy)^{-1})^{1/2}$ for the ABC index, $F(x, y) = (xy(x + y - 2)^{-1})^3$, for the augmented Zagreb index, $F(x, y) = 2\sqrt{xy}(x + y)^{-1}$ for the geometric-arithmetic index, $F(x, y) = 2(x + y)^{-1}$ for the harmonic index and $F(x,y) = (x+y)^{-1/2}$ for the sum-connectivity index.

Todeschini *et al.* [15,16] proposed that multiplicative variants of molecular structure descriptors be considered. Thus we have the following general form for topological indices:

$$TI_p = TI_p(G) = \prod_{uv \in E(T)} F(d(u), d(v)).$$

When this idea is applied to Zagreb indices, one arrives at their multiplicative versions $\Pi_1(G)$ and $\Pi_2(G)$, defined as $\Pi_1(G) = \prod_{v \in V(G)} (d(v))^2$ and $\Pi_2(G) = \prod_{uv \in E(G)} d(u)d(v)$ [3, 4]. Réti and Gutman [14] provided lower and upper bounds for Π_1 and Π_2 of a connected graph in terms of the number of vertices, number of edges, and the ordinary, additive Zagreb indices M_1 and M_2. Let T_n be the set of trees with n vertices. Gutman [6] determined the elements of T_n, extremal w.r.t. Π_1 and Π_2. Iranmanesh *et al.* [7] computed these indices for link and splice of graphs. In continuation, with use these graphs, they computed the first and the second multiplicative Zagreb indices for a class of dendrimers. Liu and Zhang [13] introduced several sharp upper bounds for Π_1-index in terms of graph parameters including the order, size, radius, Wiener index and eccentric distance sum, and upper bounds for Π_2-index in terms of graph parameters including the order, size, the first Zagreb index, the first Zagreb coindex and degree distance. Xu and Hua [18] obtained a unified approach to characterize extremal (maximal and minimal) trees, unicyclic graphs and bicyclic graphs with respect to multiplicative Zagreb indices, respectively. Recently, Wang and Wei studied these indices in *k*-trees [17].

Another multiplicative version of the first Zagreb index is defined as $\Pi_3(G) = \prod_{uv \in E(G)} (d(u) + d(v))$ and is named as the multiplicative sum Zagreb index. Eliasi *et al.* [2] proved that among all connected graphs with a given number of vertices, the path has minimal Π_3. They also determined the trees with the second-minimal Π_3. Kazemi [11] studied Π_1, Π_2 and Π_3 in random molecular graphs with tree structure. He gave the lower and upper bounds related to the moments of these indices.

We introduce the modified multiplicative sum Zagreb index, defined as

$$\Pi_4(G) = \prod_{uv \in E(G)} (d(u) + d(v))^{d(u)d(v)},$$

and study it in random molecular graphs with tree structure. An illustrative example is provided in Figure 1.

2. EVOLUTION PROCESS

The structures of many molecules such as dendrimers and acyclic molecules are tree like. We present the following evolution process for random trees of order n, which turns out to be appropriate when studying the multiplicative Zagreb indices of molecular graphs with tree structure [10].

Every order-n tree can be obtained uniquely by attaching nth node to one of the $n-1$ nodes in a tree of order $n-1$. It is of particular interest in applications to assume the random tree model and to speak about a random tree with n nodes, which means that all

trees of order n are considered to appear equally likely. Equivalently one may describe random trees via the following tree evolution process, which generates random trees of arbitrary order n. At step 1 the process starts with a node. At step i the ith node is attached to any previous node v of the already grown tree T of order $i-1$ with probability $p_i(v) = 1/(i-1)$. For applicability of our own results and specially connection with the chemical relevance, see [9].

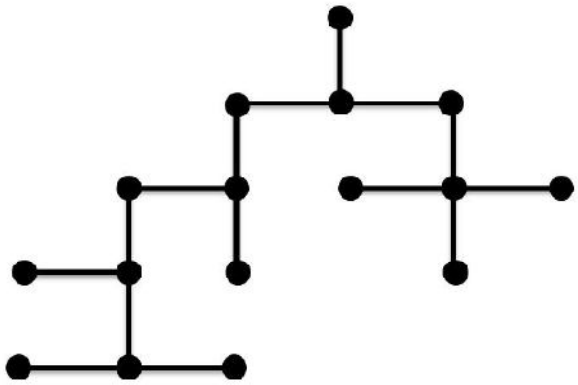

Figure 1. A molecular graph with $\Pi_1 = 6718464$, $\Pi_2 = 8707129344$, $\Pi_3 = 14400000000$ and $\Pi_4 = 4\times10^{51}$.

Let $d(v,n)$ denote the degree of node v in our structure of order n. It is obvious that $1 \le d(v,n) \le n-1$. We define B_n to be the sigma-field generated by the first n stages of the random molecular graphs with tree structure. Let T_n be the set of trees with order n. Then by definition of the multiplicative Zagreb indices for $k \ge 1$ and $i = 1,2,3$ [11],

$$\frac{\Pi_i(T_n)^k}{\Pi_i(T_{n-1})^k} = f_{\Pi_i}(d(U,n-1))^k, \quad (1)$$

where U is independent of B_{n-1}. Let $\{y_1,...,y_k\}$ be the neighborhood of the vertex U. Also

$$f_{\Pi_i}(d(U,n-1)) = \begin{cases} \left(\dfrac{d(U,n-1)+1}{d(U,n-1)}\right)^2, & for\ i=1 \\ \left(\dfrac{d(U,n-1)+1}{d(U,n-1)}\right)^{d(U,n-1)} \times (d(U,n-1)+1), & for\ i=2 \\ \displaystyle\prod_{k=1}^{d(U,n-1)} \frac{d(U,n-1)+d(y_k,n-1)+1}{d(U,n-1)+d(y_k,n-1)}, & for\ i=3. \end{cases}$$

It is obvious that

$$a_{\Pi_i} := \min\ f_{\Pi_i}(d(U,n-1))^k = \begin{cases} \left(\dfrac{n-2}{n-3}\right)^{2k}, & \text{for } i=1 \\ 4^k, & \text{for } i=2 \\ \left(3\dfrac{n-1}{n-2}\right)^k, & \text{for } i=3 \end{cases}$$

and

$$d_{\Pi_i} := \max\ f_{\Pi_i}(d(U,n-1))^k = \begin{cases} 4^k, & \text{for } i=1 \\ \left(\dfrac{n-2}{n-3}\right)^{k(n-3)}(n-2)^k, & \text{for } i=2 \\ \left(\dfrac{n-1}{n-2}\right)^{k(n-3)}(n-1)^k, & \text{for } i=3. \end{cases}$$

Theorem 1 [11] *Let* $\mathbf{E}(\Pi_i(T_n)^k)\,(k\geq 1, i=1,2,3)$ *be the* k *th moment of* $\Pi_i(T_n)$ *of a molecular graph* T_n *with tree structure of order* n. *Then for* $n\geq 5$,

$$(n-2)^{2k} \leq \mathbf{E}(\Pi_1(T_n)^k) \leq 4^{k(n-2)} \quad (a.e.),$$

$$4^{k(n-2)} \leq \mathbf{E}(\Pi_2(T_n)^k) \leq (n-2)^{(n-2)k}, \quad (a.e.),$$

$$\left(\frac{2}{9}3^n(n-1)\right)^k \leq \mathbf{E}(\Pi_3(T_n)^k) \leq 2^k(n-1)^{k(n-2)}, \quad (a.e.).$$

3. MAINRESULTS

3.1 RATIO OF THE MULTIPLICATIVE ZAGREB INDICES

In this section, we obtain lower and upper bounds for the moments of the ratio of the multiplicative Zagreb indices (Π_1, Π_2 and Π_3).

Theorem 2 *Suppose*

$$\Pi_{i,j,k}(T_n) = \mathbf{E}\left(\frac{\Pi_i(T_n)}{\Pi_j(T_n)}\right)^k, \quad i\neq j,\ i,j=1,2,3.$$

Then

$$\Pi_{1,2,k}(T_n) \geq \left(\frac{n-2}{(n-3)^2}\right)^{k(n-2)}, \Pi_{1,3,k}(T_n) \geq \frac{1}{2^k}\left(\frac{n-2}{(n-3)(n-1)^{\frac{1}{2}}}\right)^{2k(n-2)},$$

$$\Pi_{2,1,k}(T_n) \geq 1,\ \Pi_{2,3,k}(T_n) \geq \frac{1}{2^k}\left(\frac{4}{n-1}\right)^{k(n-2)},$$

$$\Pi_{3,1,k}(T_n) \geq 2^k\left(\frac{3}{4}\frac{n-1}{n-2}\right)^{k(n-2)},\ \Pi_{3,2,k}(T_n) \geq 2^k\left(\frac{3(n-1)}{(n-2)^2}\right)^{k(n-2)}.$$

Proof. It is obvious that for $i = 1,2,3,\ \Pi_i(T_n)^k > \Pi_i(T_{n-1})^k$. Then

$$\begin{aligned}
\Pi_{i,j,k}(T_n) &= \mathbf{E}\left(\mathbf{E}\left(\frac{\Pi_i(T_n)^k}{\Pi_j(T_n)^k}\,|\,\mathsf{B}_{n-1}\right)\right) \\
&> \mathbf{E}\left(\mathbf{E}\left(\frac{\Pi_i(T_{n-1})^k}{\Pi_j(T_n)^k}\,|\,\mathsf{B}_{n-1}\right)\right) \\
&= \mathbf{E}\left(\Pi_i(T_{n-1})^k\,\mathbf{E}\left(\frac{1}{\Pi_j(T_n)^k}\,|\,\mathsf{B}_{n-1}\right)\right) \\
&\geq \mathbf{E}\left(a_{\Pi_i}\Pi_i(T_{n-2})^k\,\mathbf{E}\left(\frac{1}{\Pi_j(T_n)^k}\,|\,\mathsf{B}_{n-1}\right)\right) \\
&\geq \cdots \geq \mathbf{E}\left(a_{\Pi_i}^{n-2}\Pi_i(T_2)^k\,\mathbf{E}\left(\frac{1}{\Pi_j(T_n)^k}\,|\,\mathsf{B}_{n-1}\right)\right) \\
&= a_{\Pi_i}^{n-2}b_{\Pi_i}^k\,\mathbf{E}\left(\mathbf{E}\left(\frac{1}{\Pi_j(T_n)^k}\,|\,\mathsf{B}_{n-1}\right)\right),\quad b_{\Pi_i} = \Pi_i(T_2) \\
&= a_{\Pi_i}^{n-2}b_{\Pi_i}^k\,\mathbf{E}\left(\frac{1}{\Pi_j(T_n)^k}\right),
\end{aligned}$$

where $b_{\Pi_1} = b_{\Pi_2} = 1,\ b_{\Pi_3} = 2$. By Jensen's inequality [1],

$$\Pi_{i,j,k}(T_n) \geq a_{\Pi_i}^{n-2}b_{\Pi_i}^k\,\frac{1}{\mathbf{E}(\Pi_j(T_n)^k)},$$

and proof is completed by Theorem 1.

Corollary 1 *Suppose* $m \neq n\,(m,n \in \mathsf{N})$ *and*

$$\Pi_{i,j,k}(T_m,T_n) = \mathbf{E}\left(\frac{\Pi_i(T_n)}{\Pi_j(T_m)}\right)^k,\quad i,j = 1,2,3.$$

Then

$$\Pi_{1,1,k}(T_m,T_n) \geq \left(\frac{n-2}{n-3}\right)^{2k(n-2)} 4^{-k(m-2)},\ \Pi_{2,2,k}(T_m,T_n) \geq \frac{4^{k(n-2)}}{(m-2)^{k(m-2)}},$$

$$\Pi_{3,3,k}(T_m,T_n) \geq \left(\frac{3(n-1)}{n-2}\right)^{k(n-2)} (m-1)^{-k(m-2)},$$

$$\Pi_{1,2,k}(T_m,T_n) \geq \left(\frac{n-2}{n-3}\right)^{2k(n-2)} (m-2)^{-k(m-2)},$$

$$\Pi_{1,3,k}(T_m,T_n) \geq \frac{1}{2^k}\left(\frac{n-2}{n-3}\right)^{2k(n-2)} (m-1)^{-k(m-2)},$$

$$\Pi_{2,1,k}(T_m,T_n) \geq 4^{n-m},\ \Pi_{2,3,k}(T_m,T_n) \geq \frac{4^{k(n-2)}}{2^k (m-1)^{k(m-2)}},$$

$$\Pi_{3,1,k}(T_m,T_n) \geq 2^k\left(3\frac{n-1}{n-2}\right)^{k(n-2)} 4^{-k(m-2)},$$

$$\Pi_{3,2,k}(T_m,T_n) \geq 2^k\left(\frac{3(n-1)}{(n-2)^2}\right)^{k(n-2)} (m-2)^{-k(m-2)}.$$

With this approach, we can obtain the sharp lower bounds for different values of k.

Theorem 3 *Suppose*

$$\Pi_{i,j,k}(T_n) = \mathbf{E}\left(\frac{\Pi_i(T_n)}{\Pi_j(T_n)}\right)^k, \quad i \neq j,\ i,j = 1,2,3.$$

Then

$$\Pi_{1,2,k}(T_n) \leq 4^{k(n-2)},\ \Pi_{1,3,k}(T_n) \leq \left(\frac{1}{2}\right)^k 4^{k(n-2)},$$

$$\Pi_{2,1,k}(T_n) \leq \left(\frac{n-2}{n-3}\right)^{k(n-3)(n-2)} (n-2)^{k(n-2)},$$

$$\Pi_{2,3,k}(T_n) \leq \left(\frac{1}{2}\right)^k \left(\frac{n-2}{n-3}\right)^{k(n-3)(n-2)} (n-2)^{k(n-2)},$$

$$\Pi_{3,1,k}(T_n) \leq 2^k\left(\frac{n-1}{n-2}\right)^{k(n-3)(n-2)} (n-1)^{k(n-2)},$$

$$\Pi_{3,2,k}(T_n) \leq 2^k\left(\frac{n-1}{n-2}\right)^{k(n-3)(n-2)} (n-1)^{k(n-2)}.$$

Proof. We have [11]:

$$\mathbf{E}(\Pi_1(T_n)^k \mid \mathsf{B}_{n-1}) \leq d_{\Pi_1}\Pi_1(T_{n-1})^k, \qquad (a.e.),$$

$$\mathbf{E}(\Pi_2(T_n)^k \mid \mathsf{B}_{n-1}) \leq d_{\Pi_2}\Pi_2(T_{n-1})^k, \qquad (a.e.),$$

$$\mathbf{E}(\Pi_3(T_n)^k \mid \mathsf{B}_{n-1}) \leq d_{\Pi_3}\Pi_3(T_{n-1})^k, \qquad (a.e.). \quad (2)$$

Thus

$$\begin{aligned}
\Pi_{i,j,k}(T_n) &= \mathbf{E}\left(\mathbf{E}\left(\frac{\Pi_i(T_n)^k}{\Pi_j(T_n)^k} \,|\, \mathsf{B}_{n-1} \right) \right) \\
&\le \mathbf{E}\left(\mathbf{E}\left(\frac{\Pi_i(T_n)^k}{\Pi_j(T_{n-1})^k} \,|\, \mathsf{B}_{n-1} \right) \right) \\
&= \mathbf{E}\left(\frac{1}{\Pi_j(T_{n-1})^k} \mathbf{E}(\Pi_i(T_n)^k \,|\, \mathsf{B}_{n-1}) \right) \\
&\le d_{\Pi_i} \mathbf{E}\left(\frac{\Pi_i(T_{n-1})^k}{\Pi_j(T_{n-1})^k} \right) \\
&\le d_{\Pi_i} \mathbf{E}\left(\frac{\Pi_i(T_{n-1})^k}{\Pi_j(T_{n-2})^k} \right) \\
&= d_{\Pi_i} \mathbf{E}\left(\mathbf{E}\left(\frac{\Pi_i(T_{n-1})^k}{\Pi_j(T_{n-2})^k} \,|\, \mathsf{B}_{n-2} \right) \right) \\
&= d_{\Pi_i} \mathbf{E}\left(\frac{1}{\Pi_j(T_{n-2})^k} \mathbf{E}(\Pi_i(T_{n-1})^k \,|\, \mathsf{B}_{n-2}) \right) \\
&\le d_{\Pi_i}^2 \mathbf{E}\left(\frac{\Pi_i(T_{n-2})^k}{\Pi_j(T_{n-2})^k} \right) \\
&\le \cdots \le d_{\Pi_i}^{n-2} \mathbf{E}\left(\frac{\Pi_i(T_2)^k}{\Pi_j(T_2)^k} \right) \\
&= d_{\Pi_i}^{n-2} \Pi_{i,j,k}(T_2),
\end{aligned}$$

where

$\Pi_{1,3,k}(T_2) = \Pi_{2,3,k}(T_2) = (1/2)^k$,

$\Pi_{3,1,k}(T_2) = \Pi_{3,2,k}(T_2) = 2^k$,

$\Pi_{2,1,k}(T_2) = \Pi_{1,2,k}(T_2) = 1$.

Now, the proof is completed by inequalities (2).

We can introduce the upper bounds similar to Corollary 1.

Corollary 2 *Let* $i, j, k, l = 1,2,3,\ n, p \ge 5$ *and*

$$\Pi_{i,j,k,l}(T_n, T_p) = \mathbf{E}\left(\frac{\Pi_i(T_n)}{\Pi_j(T_n)} \frac{\Pi_k(T_p)}{\Pi_l(T_p)} \right).$$

Let $r, s \in [1, \infty]$ with $1/r + 1/s = 1$. By Holder's inequality,

$$\Pi_{i,j,k,l}(T_n, T_p) \le \Pi_{i,j,r}(T_n)^{\frac{1}{r}} \Pi_{k,l,s}(T_p)^{\frac{1}{s}}.$$

For example,

$$\Pi_{1,2,3,2}(T_5, T_6) \le \Pi_{1,2,r}(T_5)^{\frac{1}{r}} \Pi_{3,2,s}(T_6)^{\frac{1}{s}} \le \frac{5^{16}}{4^9}.$$

3.2 MODIFIED MULTIPLICATIVE SUM ZAGREB INDEX

For a path P_n,

$$\Pi_4(P_n) = 256(n-3)+18,\ n \ge 3$$

and for a star S_n,

$$\Pi_4(S_n) = n^{n-1}(n-1),\ \ n \ge 2$$

Lemma 1 *Let*

$$f(x, y_1, ..., y_x) = (x+2)^{x+1} \prod_{i=1}^{x} \frac{(x+y_i+1)^{(x+1)y_i}}{(x+y_i)^{xy_i}},\ x, y_i = 1,2,3,...,n-3.$$

Then

$$f(1,1,...,1) \le f(x, y_1, ..., y_x) \le f(n-3, n-3, ..., n-3).$$

Proof. It is enough to note that the function $f(x, y_1, ..., y_x)$ is increasing in each y_i and x. Let vertex U is uniformly distributed on the vertex set $\{v_1, v_2, ..., v_{n-1}\}$. Then by definition of the modified multiplicative sum Zagreb index,

$$\Pi_4(T_n) = \Pi_4(T_{n-1})(d(U, n-1)+2)^{d(U,n-1)+1} \times \prod_{i=1}^{d(U,n-1)} \frac{(d(U,n-1)+d(y_i,n-1)+1)^{(d(U,n-1)+1)d(y_i,n-1)}}{(d(U,n-1)+d(y_i,n-1))^{d(U,n-1)d(y_i,n-1)}}, \quad (3)$$

where U is independent of B_{n-1} and node y_i is the neighborhood of the vertex U.

Theorem 4 *Let* $\mathbf{E}(\Pi_4(T_n)^k)\ (k \ge 1)$ *be the* k *th moment of* $\Pi_4(T_n)$ *of a molecular graph* T_n *with tree structure of order* n. *Then for* $\mathsf{T}_n \setminus \{P_n, S_n\}$,

$$2^k \left(\frac{81}{2}\right)^{k(n-2)} \le \mathbf{E}(\Pi_4(T_n)^k) \le 81^k \prod_{j=3}^{n-1} j^{k(j-1)} \left(\frac{(2j-3)^{j-1}}{(2j-4)^{j-2}}\right)^{k(j-2)^2}, \quad (a.e.). (4)$$

Proof. It is obvious that $\Pi_4(T_{n-1})$ is B_{n-1}-measurable and the n th vertex is attached to any previous vertex v of the already grown structure T_{n-1} with probability 1/(n−1) [8,10]. From Lemma 1 and Equation (3),

$$\mathbf{E}(\Pi_4(T_n)^k \mid \mathsf{B}_{n-1}) = \mathbf{E}(\Pi_4(T_n)^k \mid d(v_j, n-1),\ j = 1, ..., n-1)$$

$$\geq \frac{\Pi_4(T_{n-1})^k}{n-1}\sum_{j=1}^{n-1}\prod_{i=1}^{d(v_j,n-1)}(d(v_j,n-1)+2)^{k(d(v_j,n-1)+1)}\frac{(d(v_j,n-1)+2)^{k(d(v_j,n-1)+1)}}{(d(v_j,n-1)+1)^{kd(v_j,n-1)}}$$

$$\geq \Pi_4(T_{n-1})^k\left(\frac{81}{2}\right)^k, \quad (a.e.)$$

$$\geq \cdots \geq 2^k\left(\frac{81}{2}\right)^{k(n-2)},$$

since $\Pi_4(T_2)=2$. We can obtain the upper bound from Lemma 1 and $\Pi_4(T_3)=81$.

Theorem 5 *Assume* $\Pi_{4,i,k}=\left(\frac{\Pi_4(T_{i+1})}{\Pi_4(T_{i-1})}\right)^k$, *for* $i\geq 5$ *and* $k\geq 1$. *Then almost everywhere,*

$$\left(\frac{81}{2}\right)^{2k}\leq \mathbf{E}(\Pi_{4,i,k})\leq (i-1)^{k(i-2)}\left(\frac{(2i-5)^{i-2}}{(2i-6)^{i-3}}\right)^{k(i-3)^2}(j-1)^{k(j-2)}\left(\frac{(2j-5)^{j-2}}{(2j-6)^{j-3}}\right)^{k(j-3)^2}.$$

Proof. Suppose $Y_{4,i,k}=\left(\frac{\Pi_4(T_i)}{\Pi_4(T_{i-1})}\right)^k$ for $i\geq 5$. Then $\mathbf{E}(\Pi_{4,i,k})=\mathbf{E}(Y_{4,i,k}Y_{4,i+1,k})$. Now, from Theorem 4 and the law of the iterated expectation,

$$\mathbf{E}(\Pi_{4,i,k})=\mathbf{E}(\mathbf{E}(Y_{4,i,k}Y_{4,i+1,k}\,|\,\mathsf{B}_i))$$
$$=\mathbf{E}(Y_{4,i,k}\mathbf{E}(Y_{4,i+1,k}\,|\,\mathsf{B}_i)), \quad (a.e.)$$
$$\geq\left(\frac{81}{2}\right)^k\mathbf{E}(Y_{4,i,k})$$
$$=\left(\frac{81}{2}\right)^k\mathbf{E}(\mathbf{E}(Y_{4,i,k}\,|\,\mathsf{B}_{i-1}))$$
$$\geq\left(\frac{81}{2}\right)^{2k}.$$

With this approach, we can obtain the upper bound.

Corollary 3 *We have*

$$\Pi_{1,4,k}(T_n)\geq\frac{\left(\frac{n-2}{n-3}\right)^{2k(n-2)}}{81^k\prod_{j=3}^{n-1}j^{k(j-1)}\left(\frac{(2j-3)^{j-1}}{(2j-4)^{j-2}}\right)^{k(j-2)^2}},$$

$$\Pi_{2,4,k}(T_n) \geq \frac{4^{k(n-2)}}{81^k \prod_{j=3}^{n-1} j^{k(j-1)} \left(\frac{(2j-3)^{j-1}}{(2j-4)^{j-2}} \right)^{k(j-2)^2}},$$

$$\Pi_{3,4,k}(T_n) \geq \frac{2^k \left(\frac{3(n-1)}{n-2} \right)^{k(n-2)}}{81^k \prod_{j=3}^{n-1} j^{k(j-1)} \left(\frac{(2j-3)^{j-1}}{(2j-4)^{j-2}} \right)^{k(j-2)^2}},$$

$$\Pi_{4,1,k}(T_n) \geq \frac{2^k \left(\frac{81}{2} \right)^{k(n-2)}}{4^{k(n-2)}}, \ \Pi_{4,2,k}(T_n) \geq \frac{2^k \left(\frac{81}{2} \right)^{k(n-2)}}{(n-2)^{k(n-2)}},$$

$$\Pi_{4,3,k}(T_n) \geq \frac{\left(\frac{81}{2} \right)^{k(n-2)}}{(n-1)^{k(n-2)}}, \ \Pi_{1,4,k}(T_n) \leq \frac{4^{k(n-2)}}{2^k},$$

$$\Pi_{2,4,k}(T_n) \leq \frac{1}{2^k} \left(\frac{n-2}{n-3} \right)^{k(n-2)(n-3)} (n-2)^{k(n-2)},$$

$$\Pi_{3,4,k}(T_n) \leq \left(\frac{n-1}{n-2} \right)^{k(n-3)(n-2)} (n-1)^{k(n-2)},$$

$$\Pi_{4,1,k}(T_n) \leq 2^k (n-1)^{k(n-2)^2} \left(\frac{(2n-5)^{n-2}}{(2n-6)^{n-3}} \right)^{k(n-3)^2(n-2)},$$

$$\Pi_{4,2,k}(T_n) \leq 2^k (n-1)^{k(n-2)^2} \left(\frac{(2n-5)^{n-2}}{(2n-6)^{n-3}} \right)^{k(n-3)^2(n-2)},$$

$$\Pi_{4,3,k}(T_n) \leq (n-1)^{k(n-2)^2} \left(\frac{(2n-5)^{n-2}}{(2n-6)^{n-3}} \right)^{k(n-3)^2(n-2)}.$$

since

$$a_{\Pi_4} = \left(\frac{81}{2} \right)^k, \ b_{\Pi_4} = 2, \ d_{\Pi_4} = (n-1)^{k(n-2)} \left(\frac{(2n-5)^{n-2}}{(2n-6)^{n-3}} \right)^{k(n-3)^2}.$$

Also, $\Pi_{1,4,k}(T_2) = \Pi_{2,4,k}(T_2) = (1/2)^k$, $\Pi_{4,1,k}(T_2) = \Pi_{4,2,k}(T_2) = 2^k$, $\Pi_{3,4,k}(T_2) = \Pi_{4,3,k}(T_2) = 1$.

Theorem 6 *Let* T *be a finite stopping time for* $\left\{ \frac{\Pi_1(T_n)^k}{\mathbf{E}(\Pi_4(T_n)^k)}, \mathsf{B}_n \right\}_{n \geq 5}$. *Then*

$$\mathbf{E}\left(\frac{\Pi_1(T_{\mathsf{T}})^k}{\mathbf{E}(\Pi_4(T_{\mathsf{T}})^k)} \right) \leq 1.$$

Also, for $\lambda \geq 0$,

$$P\left(\sup_{n\geq 5} \frac{\Pi_1(T_n)^k}{\mathbf{E}(\Pi_4(T_n)^k)} \geq \lambda \right) \leq \frac{1}{\lambda}.$$

Proof. We have

$$\mathbf{E}\left(\frac{\Pi_1(T_n)^k}{\mathbf{E}(\Pi_4(T_n)^k)} \mid \mathsf{B}_{n-1} \right) = \frac{\mathbf{E}(\Pi_1(T_n)^k \mid \mathsf{B}_{n-1})}{\mathbf{E}(\Pi_4(T_n)^k)}$$

$$\leq \frac{4^k \Pi_1(T_{n-1})^k}{\left(\frac{81}{2}\right)^k \mathbf{E}(\Pi_4(T_{n-1})^k)}, \quad (a.e.)$$

$$\leq \frac{\Pi_1(T_{n-1})^k}{\mathbf{E}(\Pi_4(T_{n-1})^k)}, \quad (a.e.).$$

Then $\left\{ \frac{\Pi_1(T_n)^k}{\mathbf{E}(\Pi_4(T_n)^k)}, \mathsf{B}_n \right\}_{n\geq 5}$ is a supermartingale. Also, $\frac{\Pi_1(T_n)^k}{\mathbf{E}(\Pi_4(T_n)^k)} > 0$. Proof is completed by Doob's supermartingale inequality [1].

Theorem 7 *Suppose* $5 \leq m < n$. *For* $i = 1,2,3,4$ *and* $k_1, k_2 \geq 1$,

$$\frac{\mathbf{E}(\Pi_i(T_n)^{k_1} \Pi_j(T_m)^{k_2})}{\mathbf{E}(\Pi_i(T_m)^{k_1} \Pi_j(T_m)^{k_2})} \geq a_{\Pi_i},$$

where $a_{\Pi_i} = \min f_{\Pi_i}(d(U, n-1))^{k_1}$.

Proof. If $m < n$, then $\Pi_i(T_m) \leq \Pi_i(T_{n-1})$ and $\mathsf{B}_m \subseteq \mathsf{B}_{n-1}$. Then

$$\begin{aligned}
\mathbf{E}(\Pi_i(T_n)^{k_1} \Pi_j(T_m)^{k_2}) &= \mathbf{E}(\mathbf{E}(\Pi_i(T_n)^{k_1} \Pi_j(T_m)^{k_2} \mid \mathsf{B}_m)) \\
&= \mathbf{E}(\Pi_j(T_m)^{k_2} \mathbf{E}(\Pi_i(T_n)^{k_1} \mid \mathsf{B}_m)) \\
&= \mathbf{E}(\Pi_j(T_m)^{k_2} \mathbf{E}(\mathbf{E}(\Pi_i(T_n)^{k_1} \mid \mathsf{B}_{n-1}) \mid \mathsf{B}_m)) \\
&\geq \mathbf{E}(\Pi_j(T_m)^{k_2} \mathbf{E}(a_{\Pi_i} \Pi_i(T_{n-1})^{k_1} \mid \mathsf{B}_m)) \\
&\geq a_{\Pi_i} \mathbf{E}(\Pi_i(T_m)^{k_1} \Pi_j(T_m)^{k_2}),
\end{aligned}$$

since by [1, Theorem 5.5.10],

$$\mathbf{E}(\mathbf{E}(\Pi_i(T_n) \mid \mathsf{B}_m) \mid \mathsf{B}_{n-1}) = \mathbf{E}(\Pi_i(T_n) \mid \mathsf{B}_m) = \mathbf{E}(\mathbf{E}(\Pi_i(T_n) \mid \mathsf{B}_{n-1}) \mid \mathsf{B}_m) \quad (a.e.).$$

For example,

$$\mathbf{E}(\Pi_4(T_n)\Pi_4(T_m)) \geq 2\left(\frac{81}{2}\right)^{m-1}.$$

Suppose $5 \le m < n$ and $r, s \in [1, \infty]$ with $1/r + 1/s = 1$. Then for $i = 1,2,3,4$ and $k_1, k_2 \ge 1$,

$$\mathbf{E}(\Pi_i(T_n)^{k_1} \Pi_j(T_m)^{k_2}) \le (\mathbf{E}(\Pi_i(T_n)^{k_1 r}))^{\frac{1}{r}} (\mathbf{E}(\Pi_j(T_m)^{k_2 s}))^{\frac{1}{s}}, \quad (a.e.)$$

This bound is an immediate consequence of Holder's inequality. Let $\Pi_m(T_n) = \sum_{i=1}^{m} \Pi_i(T_n), 1 \le m \le 4$. Then for $r > 1$,

$$\mathbf{E}(\Pi_m(T_n))^r \le m^{r-1} \sum_{i=1}^{m} \mathbf{E}(\Pi_i(T_n))^r.$$

For example, $\mathbf{E}((\Pi_1(T_n) + \Pi_3(T_m))^2) \le 2(4^{2(n-2)} + (m-2)^{2(m-2)})$.

REFERENCES

1. R. B. Ash, C. A. Doléans-Dade, Probability and Measure Theory, Second Edition, Academic Press, 2000.
2. M. Eliasi, A. Iranmanesh, and I. Gutman, Multiplicative versions of first Zagreb index, *MATCH Commun. Math. Comput. Chem.* **68** (2012) 217−230.
3. M. Ghorbani, M. Songhori, Computing Multiplicative Zagreb Indices with respect to Chromatic and Clique Numbers, *Iranian J. Math. Chem.* **5** (1) (2012) 11−18.
4. M. Ghorbani, N. Azami, Note on multiple Zagreb indices, *Iranian J. Math. Chem.* **3** (2) (2012) 137−143.
5. I. Gutman, Degree-based topological indices, *Croat. Chem. Acta* **86** (4) (2013) 351−361.
6. I. Gutman, Multiplicative Zagreb indices of trees, *Bull. Internat. Math. Virt. Inst.* **1** (2011) 13−19.
7. A. Iranmanesh, M. A. Hosseinzadeh, and I. Gutman, On multiplicative Zagreb indices of graphs, *Iranian J. Math. Chem.***3**(2) (2012), 145−154.
8. R. Kazemi, Probabilistic analysis of the first Zagreb index, *Trans. Comb.* **2** (2) (2013) 35−40.
9. R. Kazemi, The eccentric connectivity index of bucket recursive trees, *Iranian J. Math. Chem.* **5** (2) (2014) 77−83.
10. R. Kazemi, The second Zagreb index of molecular graphs with tree structure, *MATCH Commun. Math. Comput. Chem.* **72** (2014) 753−760.
11. R. Kazemi, Note on the multiplicative Zagreb indices, *Discrete Appl. Math.* **198** (1) (2016) 147−154.
12. R. Kazemi, A. Fallah, Analysis on some degree-based topological indices, *J. of Sci. Math. Issue* **25** (98.2) (2016) 15−24.
13. J. Liu, Q. Zhang, Sharp upper bounds for multiplicative Zagreb indices, *MATCH Commun. Math. Comput. Chem.* **68** (2012), 231−240.

14. T. Réti, I. Gutman, Relations between ordinary and multiplicative Zagreb indices, *Bull. Internat. Math. Virt. Inst.* **2** (2012) 133−140.
15. R. Todeschini, D. Ballabio, and V. Consonni, Novel molecular descriptors based on functions of new vertex degrees, in: I. Gutman, B. Furtula (Eds.), Novel Molecular Structure Descriptors Theory and Applications I, Univ. Kragujevac, Kragujevac, (2010) 72−100.
16. R. Todeschini, V. Consonni, New local vertex invariants and molecular descriptors based on functions of the vertex degrees, *MATCH Commun. Math. Comput. Chem*. **64** (2010) 359−372.
17. S. Wang, B. Wei, Multiplicative Zagreb indices of k-trees, *Discrete Appl. Math.* **180** (2015) 168−175.
18. K. Xu, H. Hua, A unified approach to extremal multiplicative Zagreb indices for trees, unicyclic and bicyclic graphs, *MATCH Commun. Math. Comput. Chem*. **68** (2012) 241−256.

Iranian J. Math. Chem. 8 (4) December (2017) 391 − 401

Iranian Journal of Mathematical Chemistry

Journal homepage: ijmc.kashanu.ac.ir

Extremal Trees with Respect to Some Versions of Zagreb Indices Via Majorization

M. ELIASI• AND A. GHALAVAND

Department of Mathematics; Khansar Faculty of Mathematics & Computer Science, Khansar, Iran

ARTICLE INFO

Article History:

Received 11 January 2016
Accepted 17 February 2016
Published online 21 July 2017
Academic Editor: Ivan Gutman

Keywords:

Majorization
General first Zagreb index
Multiplicative Zagreb index

ABSTRACT

The objective of this article is to apply majorization theory to identifythe classes of trees with extremal (minimal or maximal) values of some topological indicesamong all trees of order $n \geq 12$.

1. INTRODUCTION

Throughout this article, only finite, undirected and simple graphs without loops and multiple edges are considered. Let G be such a graph and $V(G)$ and $E(G)$ be its vertex and edge set, respectively. The degree of a vertex v in G is the number of edges assigned to it, denoted by $d_G(v)$. The number of vertices of degree i will be denoted by n_i or $n_i(G)$. Evidently, $\sum_{i=1}^{\Delta(G)} n_i = |V(G)|$, where $\Delta(G)$ is the maximum degree of G. Assume that $V(G) = \{v_1, ..., v_n\}$ and $d_k \geq d_{k+1}$, for $k = 1, \dots, n-1$, where $d_k := d_G(v_k)$. Then $D(G) = (d_1, d_2, \dots, d_n)$ is called the degree sequence of G. If the emphasis is on G, sometimes $d_k(D(G))$ is applied instead of d_k.

For an edge uv of $E(G)$, the $G - uv$ defines the subgraph of G obtained by deleting uv. In a similar manner, for any two nonadjacent vertices x and y of G, $G + xy$ is a graph obtained from G by adding the edge xy. A pendant vertex is a vertex with degree one and a tree is a connected acyclic graph. A star of order n, denoted by S_n, is the tree with $n-1$ pendant vertices and the path P_n is the tree of order n with exactly two pendant vertices. The symbol $\tau(n)$ represents the class of trees with n vertices.

•Corresponding Author (Email address:eliasi@math.iut.ac.ir)
DOI:10.22052/ijmc.2017.46693.1161

A topological index is a number related to a graph, which is invariant under each graph isomorphism. Topological indices play a significant role in mathematical chemistry, especially in the QSPR/QSAR assessments (See [6, 15]).

The first Zagreb index, introduced by Gutman and Trinajstić [14], is an important topological index in mathematical chemistry. This index is used by various researchers in QSPR/ QSAR studies [1, 20, 22]. In addition, the first Zagreb index has been subjected to a great number of mathematical studies [2, 3, 5, 12, 13]. The first Zagreb index of a graph G is defined as $M_1(G) = \sum_{v\in V(G)} d_G(v)^2 = \sum_{uv\in E(G)}[d_G(u) + d_G(v)]$. Recently, for an arbitrary real number α, except from 0 and 1, Li and Zheng [16] introduced the first general Zagreb index M_1^α of G as follows $M_1^\alpha(G) = \sum_{v\in V(G)} d_G(v)^\alpha$. Li and Zhao [17] characterized all trees with the first three smallest and largest values of the first general Zagreb index, where α is an integer or a fraction $1/k$ for a nonzero integer k. Todeschini et al. [22, 23] proposed the multiplicative versions of additive topological indices, applied to the first Zagreb index as $\pi_1(G) = \prod_{v\in V(G)} d_G(v)^2$, $\pi_1^*(G) = \prod_{v\in V(G)}[d_G(u) + d_G(v)]$ and $\pi_2(G) = \prod_{uv\in E(G)}[d_G(u)d_G(v)]$. The symbols π_1 and π_2 are referred to as the multiplicative Zagreb indices.

In [11], Gutman showed thatamong all trees with $n \geq 5$ vertices, the extremal (minimal and maximal) trees regarding the multiplicative Zagreb indices are the path P_n and star S_n. Eliasi [7] identified thirteen trees with the first through ninth greatest multiplicative Zagreb index among all trees of order n. In the same line, Eliasi and Ghalavand [10] introduced a graph transformation, which decreases π_2. By applying this operation, they identified the eight classes of trees with the first through eighth smallest π_2 among all trees of order $n \geq 12$. Also the effects on the first general Zagreb index were observed when some operations including edge moving, edge separating and edge switching were applied to the graphs [18]. Moreover, by using majorization theory, the authors [18] obtained the largest or smallest first general Zagreb indices among some classes of connected graphs. Some more outstanding mathematical studies on multiplicative Zagreb indices are [4, 8, 9, 19, 21, 24].

This paper is an attempt to investigate into the first general Zagreb index and the multiplicative Zagreb indices of trees via applying a new graph operation plus majorization theory, in particular, Schur-Convex function theory. Furthermore, some hands-on techniques and concluding remarks which complement the previous studies concerning aforementioned topological indices are introduced.

2. PRELIMINARY RESULTS

Let $x = (x_1, x_2, \dots, x_n)$ and $y = (y_1, y_2, \dots, y_n)$ be two non-increasing sequences of real numbers. If they meet the conditions $\sum_{i=1}^{k} x_i \leq \sum_{i=1}^{k} y_i$, for $1 \leq k \leq n-1$ and

$\sum_{i=1}^{k} x_i = \sum_{i=1}^{k} y_i$, then it is deduced that x is ***majorized*** by y, thus $x \preccurlyeq y$. Furthermore, $x \prec y$ means that $x \preccurlyeq y$ and $x \neq y$. A real-valued function φ defined on a set $\Omega \subseteq R^n$ is said to be Schur-convex on Ω if $x \preccurlyeq y$ implises $\varphi(x) \leq \varphi(y)$. It is called strictly Schur-convex on Ω if the inequality is stric. The following theorems are supposed to be utilized in the next sections.

Theorem 1. Let G and G' be two connected graphs with degree sequences $D(G)$ and $D(G')$, respectively. If $D(G) \preccurlyeq D(G')$, then (**I**) $\pi_1(G) \geq \pi_1(G')$. This equality holds if an only if $D(G) = D(G')$. (**II**) $\pi_2(G) \leq \pi_2(G')$, where equality holds if an only if $D(G) = D(G')$ (See [7]).

Theorem 2. Let G be a connected graph with degree sequence $D(G)$ and G' be a connected graph with degree sequence $D(G')$. (**I**) If $D(G) \preccurlyeq D(G')$, $\alpha < 0$ or $\alpha > 1$, then $M_\alpha(G) \leq M_\alpha(G')$; equality holds if and only if $D(G) = D(G')$. (**II**) If $D(G) \preccurlyeq D(G')$, $0 < \alpha < 1$, then $M_\alpha(G) \geq M_\alpha(G')$; equality holds if and only if $D(G) = D(G')$ (See [18]).

For positive integers $x_1, x_2, \ldots, x_m$ and $y_1, y_2, \ldots, y_m$, let

$$T({x_1}^{(y_1)}, {x_2}^{(y_2)}, \ldots, {x_m}^{(y_m)})$$

be the class of trees with x_i vertices of the degree y_i, $i = 1,\ldots,m$. This class may be empty. It is easy to see that if $G \in T({x_1}^{(y_1)}, {x_2}^{(y_2)}, \ldots, {x_m}^{(y_m)})$, then $\pi_1(G) = \prod_{i=1}^{m} {y_i}^{2x_i}$, $\pi_2(G) = \prod_{i=1}^{m} {y_i}^{x_i y_i}$ and $M_\alpha(G) = \sum_{i=1}^{m} x_i {y_i}^{\alpha}$.

Lemma 1. There is a tree of order n (>2) in $T({x_1}^{(y_1)}, {x_2}^{(y_2)}, \ldots, {x_m}^{(y_m)})$ if and only if $\sum_{i=1}^{m} x_i y_i = 2n - 2$.

Proof. It is well-known that if $a_1, a_2, \ldots, a_n$ are positive integers with n> 2, then there exists a tree with degree sequence of $a_1, a_2, \ldots, a_n$ if and only if $\sum_{i=1}^{n} a_i = 2n - 2$. Hence there exists a tree $T \in T({x_1}^{(y_1)}, {x_2}^{(y_2)}, \ldots, {x_m}^{(y_m)})$ if and only if $\sum_{i=1}^{m} x_i y_i = 2n - 2$, as desired.

Remark 1. Let $n \geq 12$. According to Lemma 1, the class of trees in Table 1 are nonempty.

Lemma 2. Let T be a tree with n vertices. Then $n_1(T) = 2 + \sum_{i=3}^{\Delta(T)} n_i(i-2)$ and $n_2(T) = n - 2 - \sum_{i=3}^{\Delta(T)} n_i(i-1)$.

Proof. The above equations are obtained using $n_1 + n_2 + \sum_{i=3}^{\Delta(T)} n_i = n$ and $n_1 + 2n_2 + \sum_{i=3}^{\Delta(T)} i n_i = 2(n-1)$.

3. A GRAPH TRANSFORMATION

A graph transformation that decreases the degree sequences of trees regarding the majorization is illustrated in this section.

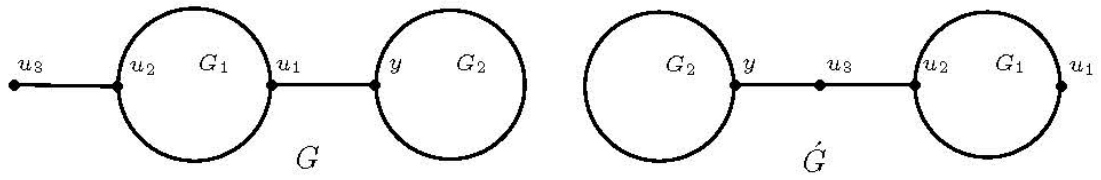

Figure 1. The Trees G_1, G_2, G and G' in Lemma 3.

Lemma 3. Let G_1 be a tree and $u_1, u_2, u_3 \in V(G_1)$, where $d_{G_1}(u_1) \geq 2$, $d_{G_1}(u_2) \geq 2$, $d_{G_1}(u_3) = 1$, and $u_2u_3 \in E(G_1)$. In addition, assume that G_2 is another tree and y is a vertex in G_2. As illustrated in Figure 1, let G be the graph obtained from G_1 and G_2 by attaching vertices y, u_1 and $G'=G-yu_1+yu_3$. Then $D(G') \prec D(G)$.

Proof. Suppose that $d_{G_1}(u_1) = x$ and $D(G)=(d_1, d_2,\ldots,d_i,d_{i+1}=x+1,d_{i+2},\ldots,d_m,1,\ldots,1)$. Since $D(G')=(d_1, d_2,\ldots,d_i,d_{i+1}=x,d_{i+2},\ldots,d_m,2,1,\ldots,1)$,

(I) For each k ($1 \leq k \leq i$), $\sum_{j=1}^{k} d_j(D(G)) = \sum_{j=1}^{k} d_j(D(G'))$.

(II) For each k ($i+1 \leq k \leq m$), $\sum_{j=1}^{k} d_j(D(G)) < \sum_{j=1}^{k} d_j(D(G'))$.

(III) For each k ($m+1 \leq k \leq n$), $\sum_{j=1}^{k} d_j(D(G)) = \sum_{j=1}^{k} d_j(D(G'))$.

Thus $D(G') \prec D(G)$.

For a positive number $n \geq 12$, let $F(n) = \{T \in \tau(n) \mid \Delta(T) = 4\}$.

Theorem 3. Suppose that T' is a tree with $n \geq 12$ vertices such that $\Delta(T') = 3$ and that $n_3(T') \geq 6$. If $T \in T(5^{(3)}, (n-12)^{(2)}, 7^{(1)})$, then $D(T) \prec D(T')$.

Proof. We prove the theorem by induction on $n_3(T')$. If $n_3(T') = 6$, then by using Lemma 3 on a vertex of degree 3 in T' we obtain a tree, like T, with 5 vertices of degree 3. Since $\Delta(T) = 3$, Lemma 2 shows that $n_1(T) = 7$ and $n_2(T) = n - 12$; therefore, $T \in$

$T(5^{(3)}, (n-12)^{(2)}, 7^{(1)})$ and by Lemma 3, $D(T) \prec D(T')$. Now assume that $n_3(T') > 6$. Again, by using Lemma 3, we reduce the number of vertices of degree 3. Now we apply the induction hypothesis to $n_3(T')$ and obtain the result.

Theorem 4. Suppose that $T' \in F(n)$ and $T \in T(1^{(4)}, 2^{(3)}, (n-9)^{(2)}, 6^{(1)})$. If $n_4(T') = 1$ and $n_3(T') \geq 3$, then $D(T) \prec D(T')$.

Proof. The proof is by inductionon on $n_3(T')$. If $n_3(T') = 3$, then by applying Lemma 3 on a vertex of degree 3 in T', we obtain a tree, say T, with two vertices of degree 3. Since $\Delta(T) = 4$ and $n_4(T) = 1$, Lemma 2 indicates that $n_1(T) = 6$ and $n_2(T) = n - 9$. Therefore, $T \in T(1^{(4)}, 2^{(3)}, (n-9)^{(2)}, 6^{(1)})$ and $D(T) \prec D(T')$ is obtained by Lemma 3. Now assume that $n_3(T') > 3$. Afterward, by using Lemma 3, we decrease the number of vertices of degree 3, and thus the proof can be verified by induction hypothesis.

Theorem 5. Suppose that $T' \in F(n)$ and $T \in T(2^{(4)}, (n-8)^{(2)}, 6^{(1)})$. If $n_4(T') \geq 2$ and $T' \notin T(2^{(4)}, (n-8)^{(2)}, 6^{(1)})$, then $D(T) \prec D(T')$.

Proof. By repeating application of Lemma 3 on vertices of degree 4 in T', a tree T_t with $n_4(T_t) = 2$ in terms of adequate number of times (t–times) can be gained. By repeating application of Lemma 3 on vertices of degree 3 in T_t, adequate number of times (s–times), a tree T_s with $n_4(T_s) = 2$ and $n_3(T_s) = 0$ can again be obtained. Now, by Lemma 2, we conclude that $n_1(T_s) = 6$ and $n_2(T_s) = n - 8$. Consequently, $T_s \in T(2^{(4)}, (n-8)^{(2)}, 6^{(1)})$ and Lemma 3 gives $D(T) = D(T_s) \prec D(T')$.

Theorem 6. Suppose that T' is a tree with n ($\geq$12) vertices and $\Delta(T') \geq 5$. If $T' \notin T(1^{(5)}, (n-6)^{(2)}, 5^{(1)})$ and $T \in T(1^{(5)}, (n-6)^{(2)}, 5^{(1)})$, then $D(T) \prec D(T')$.

Proof. Suppose $v_1 \in V(T')$ and $d_{T'}(v_1) = \Delta(T')$. Let $U = \{v \in V(T') \mid v \neq v_1, d_{T'}(v) \geq 3\}$. Again, using Lemma 3 on vertices in U, provided that the adequate number of times considered, we arrive at a tree T_m with only one vertex v_1 of degree $\Delta(T')$; whereas the degree of other vertices is 1 or 2. In addition, by repeating application of Lemma 3 on v_1, ($\Delta(T') - 5$)–times, we arrive at a tree T, such that $n_5(T) = 1$ and $n_i = 0$, for $i \geq 3$ and $i \neq 5$. On the other hand, by Lemma 2 we have $n_1(T) = 5$ and $n_2(T) = n - 6$. Therefore, $T \in T(1^{(5)}, (n-6)^{(2)}, 5^{(1)})$ and $D(T) \prec D(T')$ is followed by Lemma 3.

Table 1. Classes of Trees and their Multiplicative Version of Zagreb Indices.

Class	π_1	π_2
$T((n-2)^{(2)}, 2^{(1)})$	$2^{2(n-2)}$	$2^{2(n-2)}$
$T(1^{(3)}, (n-4)^{(2)}, 3^{(1)})$	$3^2 \times 2^{2(n-4)}$	$3^3 \times 2^{2(n-4)}$
$T(2^{(3)}, (n-6)^{(2)}, 4^{(1)})$	$3^4 \times 2^{2(n-6)}$	$3^6 \times 2^{2(n-6)}$
$T(3^{(3)}, (n-8)^{(2)}, 5^{(1)})$	$3^6 \times 2^{2(n-8)}$	$3^9 \times 2^{2(n-8)}$
$T(4^{(3)}, (n-10)^{(2)}, 6^{(1)})$	$3^8 \times 2^{2(n-10)}$	$3^{12} \times 2^{2(n-10)}$
$T(5^{(3)}, (n-12)^{(2)}, 7^{(1)})$	$3^{10} \times 2^{2(n-12)}$	$3^{15} \times 2^{2(n-12)}$
$T(1^{(4)}, (n-5)^{(2)}, 4^{(1)})$	$4^2 \times 2^{2(n-5)}$	$4^4 \times 2^{2(n-5)}$
$T(1^{(4)}, 1^{(3)}, (n-7)^{(2)}, 5^{(1)})$	$4^2 \times 3^2 \times 2^{2(n-7)}$	$4^4 \times 3^4 \times 2^{2(n-7)}$
$T(1^{(4)}, 2^{(3)}, (n-9)^{(2)}, 6^{(1)})$	$4^2 \times 3^4 \times 2^{2(n-9)}$	$4^4 \times 3^6 \times 2^{2(n-9)}$
$T(2^{(4)}, (n-8)^{(2)}, 6^{(1)})$	$4^4 \times 2^{2(n-8)}$	$4^8 \times 2^{2(n-8)}$
$T(1^{(5)}, (n-6)^{(2)}, 5^{(1)})$	$5^2 \times 2^{2(n-6)}$	$5^5 \times 2^{2(n-6)}$

Table 2. Classes of Trees and their General First Zagreb Indices.

Class	M_1^{α}
$T((n-2)^{(2)}, 2^{(1)})$	$(n-2)2^{\alpha} + 2$
$T(1^{(3)}, (n-4)^{(2)}, 3^{(1)})$	$3^{\alpha} + (n-4)2^{\alpha} + 3$
$T(2^{(3)}, (n-6)^{(2)}, 4^{(1)})$	$2 \times 3^{\alpha} + (n-6)2^{\alpha} + 4$
$T(3^{(3)}, (n-8)^{(2)}, 5^{(1)})$	$3 \times 3^{\alpha} + (n-8)2^{\alpha} + 5$
$T(4^{(3)}, (n-10)^{(2)}, 6^{(1)})$	$4 \times 3^{\alpha} + (n-10)2^{\alpha} + 6$
$T(5^{(3)}, (n-12)^{(2)}, 7^{(1)})$	$5 \times 3^{\alpha} + (n-12)2^{\alpha} + 7$
$T(1^{(4)}, (n-5)^{(2)}, 4^{(1)})$	$4^{\alpha} + (n-5)2^{\alpha} + 4$
$T(1^{(4)}, 1^{(3)}, (n-7)^{(2)}, 5^{(1)})$	$4^{\alpha} + 3^{\alpha} + (n-7)2^{\alpha} + 5$
$T(1^{(4)}, 2^{(3)}, (n-9)^{(2)}, 6^{(1)})$	$4^{\alpha} + 2 \times 3^{\alpha} + (n-9)2^{\alpha} + 6$
$T(2^{(4)}, (n-8)^{(2)}, 6^{(1)})$	$2 \times 4^{\alpha} + (n-8)2^{\alpha} + 6$
$T(1^{(5)}, (n-6)^{(2)}, 5^{(1)})$	$5^{\alpha} + (n-6)2^{\alpha} + 5$

4. MAIN THEOREMS

Based on Tables 1 and 2 and the transformations in Section 3, the main theorems are discussed below.

Remark 2. For $n \geq 12$, we assume that $T_1 := P_n$, $T_2 \in T\left(1^{(3)}, (n-4)^{(2)}, 3^{(1)}\right)$, $T_3 \in T\left(2^{(3)}, (n-6)^{(2)}, 4^{(1)}\right)$, $T_4 \in T\left(1^{(4)}, (n-5)^{(2)}, 4^{(1)}\right)$, $T_5 \in T\left(3^{(3)}, (n-8)^{(2)}, 5^{(1)}\right)$, $T_6 \in T\left(1^{(4)}, 1^{(3)}, (n-7)^{(2)}, 5^{(1)}\right)$, $T_7 \in T\left(4^{(3)}, (n-10)^{(2)}, 6^{(1)}\right)$, $T_8 \in T\left(1^{(5)}, (n-6)^{(2)}, 5^{(1)}\right)$, $T_9 \in T\left(1^{(4)}, 2^{(3)}, (n-9)^{(2)}, 6^{(1)}\right)$, $T_{10} \in T\left(2^{(4)}, (n-8)^{(2)}, 6^{(1)}\right)$ and $T_{11} \in T\left(5^{(3)}, (n-12)^{(2)}, 7^{(1)}\right)$.

Theorem 7. $\pi_1(T_1) > \pi_1(T_2) > \pi_1(T_3) > \pi_1(T_4) > \pi_1(T_5) > \pi_1(T_6) > \pi_1(T_7) > \pi_1(T_8) > \pi_1(T_9) > \pi_1(T_{10}) > \pi_1(T_{11})$.

Proof. Make use of Table 1.

Theorem 8. If n $\geq$ 12 and $T \in \tau(n)\backslash\{T_1, T_2, \dots, T_8\}$, then $\pi_1(T_1) > \pi_1(T_2) > \pi_1(T_3) > \pi_1(T_4) > \pi_1(T_5) > \pi_1(T_6) > \pi_1(T_7) > \pi_1(T_8) > \pi_1(T)$.

Proof. Theorem 7 shows that $\pi_1(T_1) > \pi_1(T_2) > \pi_1(T_3) > \pi_1(T_4) > \pi_1(T_5) > \pi_1(T_6) > \pi_1(T_7) > \pi_1(T_8)$. If $T \in \{T_9, T_{10}, T_{11}\}$, then the result follows from Theorem 7. If $\Delta(T) = 3$ and $n_3(T) \geq 6$, then $\pi_1(T_{11}) > \pi_1(T)$, by Theorems 3 and 1(I), and thus Theorem 7 implies $\pi_1(T_8) > \pi_1(T)$. Assume that $\Delta(T) = 4$. If $n_4(T) = 1$ and $n_3(T) \geq 3$, then by Theorems 4 and 1(I) we drive that $\pi_1(T_9) > \pi_1(T)$. Therefore, the result is an immediate consequence of Theorem 7. If $n_4(T) \geq 2$, then by Theorems 5 and 1(I) the $\pi_1(T_{10}) > \pi_1(T)$ will be yielded. If $\Delta(T) \geq 5$, then by Theorems 6 and 1(I) the $\pi_1(T_8) > \pi_1(T)$ can be obtained and again Theorem 7 gives the result. Ultimately, otherwise, $T \in \{T_1, T_2, \dots, T_8\}$.

Theorem 9. $\pi_2(T_1) < \pi_2(T_2) < \pi_2(T_3) < \pi_2(T_4) < \pi_2(T_5) < \pi_2(T_6) < \pi_2(T_7) < \pi_2(T_9) < \pi_2(T_8) < \pi_2(T_{11}) < \pi_2(T_{10})$.

Proof. Apply Table 1.

Theorem 10. If $n \geq 12$ and $T \in \tau(n)\backslash\{T_1, T_2, \dots, T_7, T_9\}$, then $\pi_2(T_1) < \pi_2(T_2) < \pi_2(T_3) < \pi_2(T_4) < \pi_2(T_5) < \pi_2(T_6) < \pi_2(T_7) < \pi_2(T_9) < \pi_2(T)$.

Proof. We get $\pi_2(T_1) < \pi_2(T_2) < \pi_2(T_3) < \pi_2(T_4) < \pi_2(T_5) < \pi_2(T_6) < \pi_2(T_7) < \pi_2(T_9)$ from Theorem 9. If $T \in \{T_8, T_{10}, T_{11}\}$, then Theorem 9 implies $\pi_2(T_9) < \pi_2(T)$. If $\Delta(T) = 3$ and $n_3\ (T) \geq 6$, then by Theorems 3, 1(II) and 9, $\pi_2(T_9) < \pi_2(T)$. Assume that $\Delta(T) = 4$. If $n_4\ (T) = 1$ and $n_3\ (T) \geq 3$, then by using Theorems 4, 1(II) and 9, $\pi_2(T_9) < \pi_2(T)$. If $n_4(T) \geq 2$, then by Theorems 5 and 1(II) we have $\pi_2(T_{10}) < \pi_2(T)$. Hence, Theorem 9 yields the result. If $\Delta(T) \geq 5$, then by Theorems 6 and 1(II) we have $\pi_2(T_8) < \pi_2(T)$ and Theorem 9 implies $\pi_2(T_9) < \pi_2(T)$. Eventually, otherwise, $T \in \{T_1, T_2, \dots, T_7, T_9\}$.

Theorem11.

(I) If $\alpha < 0$ or $\alpha > 1$, then

$$M_1^\alpha(T_1) < M_1^\alpha(T_2) < M_1^\alpha(T_3) < min\{M_1^\alpha(T_4), M_1^\alpha(T_5), M_1^\alpha(T_6), M_1^\alpha(T_7), M_1^\alpha(T_8), M_1^\alpha(T_9), M_1^\alpha(T_{10}), M_1^\alpha(T_{11})\}.$$

(II) If $0 < \alpha < 1$, then

$$M_1^\alpha(T_1) > M_1^\alpha(T_2) > M_1^\alpha(T_3) > max\{M_1^\alpha(T_4), M_1^\alpha(T_5), M_1^\alpha(T_6), M_1^\alpha(T_7), M_1^\alpha(T_8), M_1^\alpha(T_9), M_1^\alpha(T_{10}), M_1^\alpha(T_{11})\}.$$

(III) If $\alpha = 2$, then

$$M_1^\alpha(T_1) < M_1^\alpha(T_2) < M_1^\alpha(T_3) < M_1^\alpha(T_4) = M_1^\alpha(T_5) < M_1^\alpha(T_6) = M_1^\alpha(T_7) < M_1^\alpha(T_9) = M_1^\alpha(T_{11}) < M_1^\alpha(T_8) = M_1^\alpha(T_{10}).$$

(IV) If $\alpha = \frac{1}{2}$, then

$$M_1^\alpha(T_1) > M_1^\alpha(T_2) > M_1^\alpha(T_3) > M_1^\alpha(T_4) > M_1^\alpha(T_5) > M_1^\alpha(T_6) > M_1^\alpha(T_7) > M_1^\alpha(T_8) > M_1^\alpha(T_9) > M_1^\alpha(T_{11}) > M_1^\alpha(T_{10}).$$

Proof. (I) The proof of $M_1^\alpha(T_1) < M_1^\alpha(T_2)$ would suffice and other cases can be proved in a similar manner. For this purpose, the following equation is applied:

$$M_1^\alpha(T_1) - M_1^\alpha(T_2) = (2 \times 2^\alpha) - (3^\alpha + 1). \quad (1)$$

Let X = (2,2) and Y = (3,1), thenX $\prec$ Y. By Lemma 2 (I), the $(2 \times 2^\alpha) < (3^\alpha + 1)$ is yielded. Now, Equation (1) shows that $M_1^\alpha(T_1) < M_1^\alpha(T_2)$.

(II) Here, $M_1^\alpha(T_1) > M_1^\alpha(T_2)$ is proved. Other cases can be proved in a similar manner. It is easy to check that:

$$M_1^\alpha(T_1) - M_1^\alpha(T_2) = (2 \times 2^\alpha) - (3^\alpha + 1). \quad (2)$$

Let X = (2,2) and Y = (3,1), then $X \prec Y$. Thus, by Lemma 2(II) we have $(2 \times 2^{\alpha}) > (3^{\alpha} + 1)$. Therefore, Equation (2) implies $M_1^{\alpha}(T_1) > M_1^{\alpha}(T_2)$. To prove (III) and (IV), it is enough to apply Table 2.

Theorem 12.

I. If $\alpha < 0$ or $\alpha > 1$ and $T \in \tau(n)\backslash\{T_1, T_2, T_3\}$, then $M_1^{\alpha}(T_1) < M_1^{\alpha}(T_2) < M_1^{\alpha}(T_3) < M_1^{\alpha}(T)$.

II. If $0 < \alpha < 1$ and $T \in \tau(n) \setminus \{T_1, T_2, T_3\}$, then $M_1^{\alpha}(T_1) > M_1^{\alpha}(T_2) > M_1^{\alpha}(T_3) > M_1^{\alpha}(T)$.

III. If $\alpha = 2$ and $T \in \tau(n)\backslash\{T_1, T_2, \dots, T_7, T_9\}$, then $M_1^{\alpha}(T_1) < M_1^{\alpha}(T_2) < (T_3) < M_1^{\alpha}(T_4) = M_1^{\alpha}(T_5) < M_1^{\alpha}(T_6) = M_1^{\alpha}(T_7) < M_1^{\alpha}(T_9) = M_1^{\alpha}(T_{11}) < M_1^{\alpha}(T)$.

IV. If $\alpha = \frac{1}{2}$ and $T \in \tau(n) \setminus\{T_1, T_2, \dots, T_8\}$, then $M_1^{\alpha}(T_1) > M_1^{\alpha}(T_2) > M_1^{\alpha}(T_3) > M_1^{\alpha}(T_4) > M_1^{\alpha}(T_5) > M_1^{\alpha}(T_6) > M_1^{\alpha}(T_7) > M_1^{\alpha}(T_8) > M_1^{\alpha}(T)$.

Proof. (I) Theorem 11(I) shows that $M_1^{\alpha}(T_1) < M_1^{\alpha}(T_2) < M_1^{\alpha}(T_3)$. UsingTheorem 11(I), it suffices to prove that there exists $T_i \in \{T_4, T_5, \dots, T_{11}\}$ such that $M_1^{\alpha}(T_i) < M_1^{\alpha}(T)$. If $\Delta(T) = 3$ and $n_3(T) \geq 6$, then by Theorems 3 and 2(I), the $M_1^{\alpha}(T_{11}) < M_1^{\alpha}(T)$ is yielded. Assume that $\Delta(T) = 4$. If $n_4(T) = 1$ and $n_3(T) \geq 3$. Then by Theorems 4 and 2(I) we obtain $M_1^{\alpha}(T_9) < M_1^{\alpha}(T)$. If $n_4(T) \geq 2$, Theorems 5 and 2(I) imply that $M_1^{\alpha}(T_{10}) < M_1^{\alpha}(T)$. If $\Delta(T) \geq 5$, then Theorems 6 and 2(I) yields $M_1^{\alpha}(T_8) < M_1^{\alpha}(T)$. Finally, otherwise, $T \in \{T_4, T_5, \dots, T_{11}\}$ and thefore $M_1^{\alpha}(T_3) < M_1^{\alpha}(T)$ follows from Theorem 11(I).

(II) This case can be proved by the same procedure as mentioned in the proof (I). Instead of using Theorems 11(I) and 2(I) in the proof of (I), here we apply Theorems 11(II) and 2(II), respectively.

(III) Theorem 11 (III) yields $M_1^{\alpha}(T_1) < M_1^{\alpha}(T_2) < (T_3) < M_1^{\alpha}(T_4) = M_1^{\alpha}(T_5) < M_1^{\alpha}(T_6) = M_1^{\alpha}(T_7) < M_1^{\alpha}(T_9) = M_1^{\alpha}(T_{11})$. It will thus be sufficient to prove that there exists a $T_i \in \{T_8, T_{10}, T_{11}\}$, with $M_1^{\alpha}(T_i) < M_1^{\alpha}(T)$. If $\Delta(T) = 3$ and $n_3(T) \geq 6$, then by Theorems 3 and 2(I) we have $M_1^{\alpha}(T_{11}) < M_1^{\alpha}(T)$. Assume that $\Delta(T) = 4$. If $n_4(T) = 1$ and $n_3(T) \geq 3$. then Theorems 4 and 2(I) give $M_1^{\alpha}(T_9) < M_1^{\alpha}(T)$. If $n_4(T) \geq 2$, then by Theorems 5 and 2(I) we have $M_1^{\alpha}(T_{10}) < M_1^{\alpha}(T)$. If $\Delta(T) \geq 5$, then Theorems 6 and 2(I) yield $M_1^{\alpha}(T_8) < M_1^{\alpha}(T)$. Eventually, otherwise, $T \in \{T_8, T_{10}, T_{11}\}$ and again Theorem 11(III) gives the result.

(IV) This case can be proved by a similar argument as in the proof of (III). Instead of using Theoresms 11(III) and 2(I) in the proof of (III), here we apply Theorems 11(IV) and 2(II), respectively.

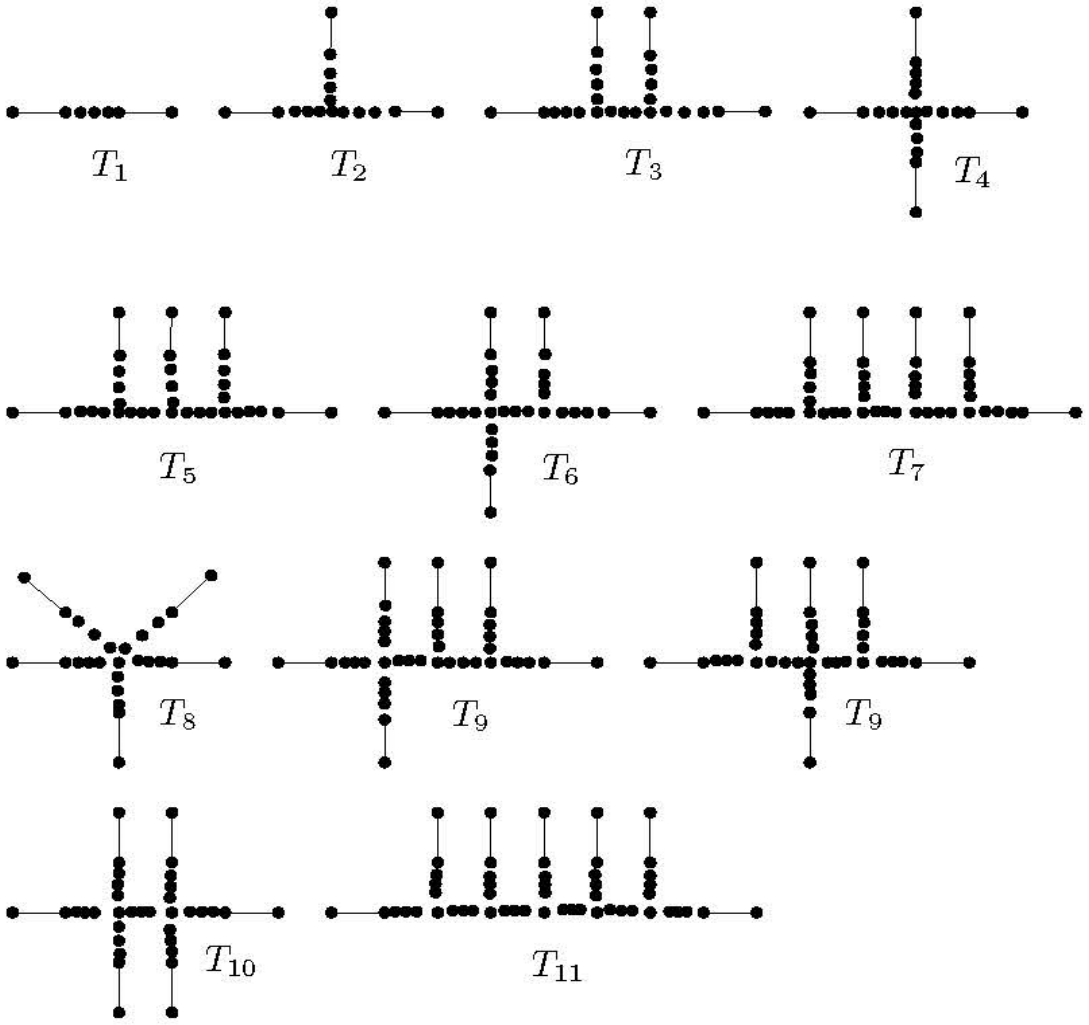

Figure 3. The Trees in Remark 2.

REFERENCES

1. A. T. Balaban, I. Motoc, D. Bonchev and O. Mekenyan, Topological indices for structure activity correlations, *Topics Curr. Chem*.**114** (1983) 21–55.
2. C. Bey, An upper bound on the sum of squares of degrees in a hypergraph, *Discrete Math*. **269** (2003) 259–263.
3. K. C. Das, Sharp bounds for the sum of the squares of the degrees of a graph, *Kragujevac J. Math.* **25** (2003) 31–49.
4. K. C. Das, A. Yurttas, M. Togan, A. S. Cevik and I. N. Cangu, The multiplicative Zagreb indices of graph operations, *J. Inequal. Appl.* **90** (2013) 1–14.
5. D. de Caen, An upper bound on the sum of squares of degrees in a graph, *Discrete Math*. **185** (1998) 245–248.

6. J. Devillers and A. T. Balaban, *Topological Indices and Related Descriptors in QSAR and QSPR*, Gordon and Breach Science Publishers (1999).
7. M. Eliasi, A simple approach to orther the multiplicative Zagreb indices of connectedgraphs, *Trans. Comb.* **1** (2012) 17–24.
8. M. Eliasi, A. Iranmanesh and I. Gutman, Multiplicative versions of first Zagreb index, *MATCH Commun. Math. Comput. Chem.* **68** (2012) 217–230.
9. M. Eliasi and D. Vukicević, Comparing the multiplicative Zagreb indices, *MATCH Commun. Math. Comput. Chem.* **69** (2013) 765–773.
10. M. Eliasi and A. Ghalavand, Ordering of trees by multiplicative second Zagreb index, *Trans. Comb*. **5** (1) (2016) 49–55.
11. I. Gutman, Multiplicative Zagreb indices of trees, *Bull. Int. Math. Virt. Inst*. **1** (2011) 13–19.
12. I. Gutman and K. C. Das, The first Zagreb index 30 years after, *MATCH Commun. Math. Comput. Chem*. **50** (2004) 83–92.
13. I. Gutman, Graphs with smallest sum of squares of vertex degree, *Kragujevac J. Math*. **25** (2003) 51–54.
14. I. Gutman and N. Trinajstić, Graph theory and molecular orbital.Total φ-electron energy of alternant hydrocarbons, *Chem. Phys. Lett*. **17** (1972) 535–538.
15. M. Karelson, *Molecular Descriptors in QSAR/QSPR*, Wiley, New York (2000).
16. X. Li and J. Zheng, A unified approach to the extremal trees for different indices, *MATCH Commun. Math. Comput. Chem*. **54** (2005) 195–208.
17. X. Li and H. Zhao, Trees with the first three smallest and largest generalized topological indices, *MATCH Commun. Math. Comput. Chem*. **50** (2004) 57–62.
18. M. Liu and B. Liu, Some properties of the first general Zagreb index, *Australas. J. Combin.* **47** (2010) 285–294.
19. J. Liu and Q. Zhang, Sharp upper bounds for multiplicative Zagreb indices, *MATCH Commun. Math. Comput. Chem*. **68** (2012) 231–240.
20. S. Nikolić, G. Kovacević, A. Miličević and N. Trinajstić, The Zagreb indices 30 years after, *Croat. Chem. Acta* **76** (2003) 113–124.
21. T. Rseti and I. Gutman, Relation between ordinary and multiplicative Zagreb indices, *Bull. Int. Math. Virt. Inst*. **2** (2012) 133–140.
22. R. Todeschini and V. Consonni, *Handbook of Molecular Descriptors*, Wiley–VCH (2000).
23. R. Todeschini and V. Consonni, New local vertex invariants and molecular descriptors based on functions of the vertex degrees, *MATCH Commun. Math. Comput. Chem*. **64** (2010) 359–372.
24. K. Xu and H. Hua, A unified approach to extremal multiplicative Zagreb indices for trees, unicyclic and bicyclic raphs, *MATCH Commun. Math. Comput. Chem*. **68** (2012) 241–256.

Iranian J. Math. Chem. 8 (4) December (2017) 403 − 411

Iranian Journal of Mathematical Chemistry

Journal homepage: ijmc.kashanu.ac.ir

The Uniqueness Theorem for Inverse Nodal Problems with a Chemical Potential

SEYFOLLAH MOSAZADEH •

Department of Pure Mathematics, Faculty of Mathematical Sciences, University of Kashan, Kashan 87317−53153, I R Iran

ARTICLE INFO

Article History:

Received 3 February 2016
Accepted 16 April 2016
Published online 5 November 2016
Academic Editor: Ali Reza Ashrafi

Keywords:

Boundary Value Problem
Inverse Nodal Problem
Eigenvalues
Nodal Points

ABSTRACT

In this paper, an inverse nodal problem for a second-order differential equation having a chemical potential on a finite interval is investigated. First, we estimate the nodal points and nodal lengths of differential operator. Then, we show that the potential can be uniquely determined by a dense set of nodes of the eigenfunctions.

1 INTRODUCTION

There are many problems in mathematics, chemistry, physics and some engineering sciences which are connected to the second-order differential equations. For example, in the process of the formation of *methyliodide* (CH_3I) by the biological and photochemical production mechanisms in a biogeochemical module, the following equation appears:

$$\frac{dc}{dt} = P - S + F_{air-Sea} + \frac{\partial}{\partial z}(A_v \frac{dc}{dz}), \qquad (1)$$

which describes the evolution of methyl iodide concentration (c [mmolm^{-3}]) over time under production (P), degradation (S), air–sea exchange (F), as well as turbulent vertical diffusion (A_v–diffusion coefficient) (see [26]). Using the separation of variables technique we can transform the equation (1) to the following second-order differential equation:

• Corresponding Author (Email address: s.mosazadeh@kashanu.ac.ir)
DOI: 10.22052/ijmc.2016.39228

$$y'' + \left(\lambda - \frac{A}{x^2} + q(x) \right) y = 0, \tag{2}$$

where λ is the spectral parameter, A is a real number, the potential $q(x)$ is real-valued. Equation (2) has a singularity at the endpoint $x = 0$. For other examples, in quantum chemistry or quantum mechanics, we refer to the quantum modeling of the *hydrogen atom*, or the *Hellman equation* to finding an approximation for the simplified description of complex systems, which can be transformed to (2) (see also [3, 4, 6, 13, 15, 17, 24]).

Inverse problems associated with the equation (2) with $A=0$ have various versions. The first version was studied by Borg and Levinson, and it is shown that the potential $q(x)$ can be uniquely determined from the given boundary condition and one possible reduced spectrum [5, 18]. For the second version, using two spectra λ_n and λ'_n, Marchenko uniquely determined the potential $q(x)$ and the corresponding boundary conditions [20]. Finally, Gelfand and Levitan proved that $q(x)$ uniquely determined by the spectral function [12].

Some inverse problems having singularities or turning points, and/or discontinuity conditions were studied by the above methods in many works (see [1, 2, 8-11, 16, 19, 23, 27]). Note that, in [22], we considered a second-order differential equation of Sturm-Liouville type having two turning points and singularities in a finite interval. Then, its asymptotic form of the solutions was studied, and obtained the infinite representation of the solutions of differential equation which plays an important role in investigating the corresponding inverse problem.

In later years, in some interesting works but without singularity, inverse problems were investigated using a new spectral data which are so-called *nodal points*, and their corresponding inverse problems are so-called *inverse nodal problems*. Mclaughlin seems to have been the first to consider this method for the one-dimensional Schrödinger equations [21]. For other works, see also [7, 14, 25].

In this work, we consider the inverse nodal problem associated with the singular differential equation (2) and the Dirichlet boundary condition

$$y(0) = 0 = y(1), \tag{3}$$

on the interval (0,1). We also assume that

$$q(x) \in x^{2-2k_0} \in L^1(0,1), \tag{4}$$

where k_0 is a member of $\{2,3,4,\ldots\}$. The problem (2)-(3) has infinitely many nontrivial solutions. The values of λ for which there exist nontrivial solutions are so-called *eigenvalues*, and their corresponding nontrivial solutions $y(x,\lambda)$ are so-called *eigenfunctions*. All the eigenvalues are real and the set of the eigenvalues is countably infinite, and also the eigenvalues can be arranged in increasing order as follows

$$\lambda_1 < \lambda_2 < \lambda_3 < \ldots,$$

such that $\lambda_n \to \infty$ as $n \to \infty$. In the present paper, first, we obtain the asymptotic formula for the eigenvalues, the nodes of the eigenfunctions and the nodal lengths (Section 2). Then,

we prove that the set of the nodal points of the boundary value problem (2)−(3) is dense in the interval (0,1) and the potential $q(x)$ can be uniquely determined from this new kind of spectral data (see Section 3).

2 ASYMPTOTIC FORMULA FOR NODAL POINTS

We consider the boundary value problem $L=L(q(x))$ defined by (2)-(3). Assume that in (2),

$$A = \nu^2 - \frac{1}{4},\ \nu = k_0 - \frac{1}{2},\quad k_0 \in \{\ 2,3,4,...\}. \tag{5}$$

From [11], we know that the equation (2) has two solutions $y_1(x,\lambda)$ and $y_2(x,\lambda)$, which are linearly independent with respect to x, and also have the following asymptotic forms as $\lambda \to \infty$:

$$y_1(x,\lambda) = \lambda^{(k_0-1)/2}\{\ (-1)^{k_0-1}e^{i\sqrt{\lambda}x}[1]_0 + e^{-i\sqrt{\lambda}x}[1]_0\ \}, \tag{6}$$

$$y_2(x,\lambda) = \frac{1}{4}i\lambda^{-k_0/2}\{\ -e^{i\sqrt{\lambda}x}[1]_0 + (-1)^{k_0-1}e^{-i\sqrt{\lambda}x}[1]_0\ \}, \tag{7}$$

where $[1]_0 = 1 + O((\sqrt{\lambda}x)^{-1})$. Therefore, the solution $y(x,\lambda)$ of the equation (2) under the condition $y(0)=0$ can be written as a linear combination of y_1 and y_2. Also, since the boundary value problem L is self-adjoint and y_1, y_2 are entire in λ, thus all of the eigenvalues of L are real and simple. In the case when k_0 is odd, it follows from (3), (7) that $y(x,\lambda)= y_2(x,\lambda)$ and the asymptotic form of the eigenvalues as follows

$$\sqrt{\lambda_n(q)} = n\pi + O\left(\frac{1}{n}\right). \tag{8}$$

Similarly, in the case when k_0 is even, we derive from (3), (6) that $y(x,\lambda)= y_1(x,\lambda)$ and also the eigenvalues of L may be calculated as (8).

For the boundary value problem L an analog of Sturm's oscillation theorem is true. More precisely, the eigenfunctions $y_n(x)= y(x,\lambda_n)$ has exactly $n-1$ (simple) zeros inside the interval (0,1), namely:

$$0 < x_n^{(1)} < x_n^{(2)} < ... < x_n^{(n-1)} < 1.$$

The set

$$X_L := \{\ x_n^{(j)}\},\quad n \geq 1,\quad j = \overline{1, n-1}, \tag{9}$$

is called the set of nodal points of the problem L. Also, let

$$I_n^{(j)} := [x_n^{(j)}, x_n^{(j+1)}]$$

be the j^{th} nodal domain of the n^{th} eigenfunction y_n, and let

$$\ell_n^{(j)} := \left|I_n^{(j)}\right| = x_n^{(j+1)} - x_n^{(j)}$$

be the associated *nodal length*. Inverse nodal problems consist in recovering the potential $q(x)$ from the given set X_L of nodal points or from a certain its part.

Now, in the following theorem, we develop asymptotic expressions for nodal points $x_n^{(j)}$ and the nodal lengths $\ell_n^{(j)}$ ($n=1,2,3,\ldots$, $j=1,2\ldots,n-1$) at which y_n, the eigenfunction corresponding to the eigenvalue λ_n of the problem L, vanishes.

Theorem 1. We consider the equation (2) under Dirichlet boundary condition (3). Let $q(x)$ satisfies (4), then the nodal points of the problem L defined by (2)-(3) are

$$\begin{cases} x_n^{(j)} = \dfrac{j}{n} + O\left(\dfrac{1}{n}\right), \\ n = 1,2,3,\ldots, \quad j = 1,2,3,\ldots,n-1, \end{cases} \tag{10}$$

and the nodal lengths are

$$\ell_n^{(j)} = \frac{1}{n} + O\left(\frac{1}{n}\right).$$

Proof. Suppose $v=k_0-1/2$ and k_0 is odd. Then, by (7)-(8) and solving $y_2(x,\lambda_n)=0$, we approximate the nodal points of the form (10). Similarly, in the case when k_0 is even, using (6), (8) and from $y_1(x,\lambda_n) = 0$ we arrive at (10). Moreover,

$$\begin{aligned} \ell_n^{(j)} &= x_n^{(j+1)} - x_n^{(j)} \\ &= \left(\frac{j+1}{n} + O\left(\frac{1}{n}\right)\right) - \left(\frac{j}{n} + O\left(\frac{1}{n}\right)\right) \\ &= \frac{1}{n} + O\left(\frac{1}{n}\right). \end{aligned}$$

□

Theorem 1, specially the relation (10), provide the sufficient conditions for the uniqueness theorem in the next section.

3 THE UNIQUENESS THEOREM

In this section, we show that the set of the nodal points $x_n^{(j)}$ of the form (10) is dense in (0,1). Then, we prove a uniqueness theorem for the solution of the inverse nodal problem associated with the boundary value problem L.

First, we consider the equation

$$w''(x,\lambda) + \lambda\, w(x,\lambda) = 0, \quad 0 \le x \le 1, \tag{11}$$

with the boundary conditions

$$w(0,\lambda) = 0 = w(1,\lambda). \tag{12}$$

It is easily shown that the solution of the problem (11)-(12) is $w(x,\lambda) = \sin(\sqrt{\lambda}x)$. Furthermore, the exact eigenvalues of the problem L_0 defined by (11)-(12) are

$$\xi_n = n^2\pi^2, \tag{13}$$

and their corresponding eigenfunctions are

$$w_n(x) = w(x,\xi_n) = \sin(n\pi x). \tag{14}$$

Since for each $n \in \{2,3,4,\ldots\}$ there exist $k \in \{0,1,2,\ldots\}$ and $m \in \{1,2,\ldots,2^k\}$ such that $n=2^{k+1}-m+1$, so according to (13)-(14), the set

$$\left\{ (2^{k+1}-m+1)^2\pi^2 \mid k = 0,1,2,..., \ m = 1,2,...,2^k \right\},$$

consists of all eigenvalues of (11)-(12) except $\xi_1=\pi^2$. Moreover, the eigenfunction corresponding to the eigenvalue $\xi_n=(2^{k+1}-m+1)\pi^2$ is

$$w(x,\xi_n) = \sin((2^{k+1}-m+1)\pi x),$$

so that $m/(2^{k+1}-m+1)$ is a zero of the eigenfunction $w_n(x)$. Therefore, the set of the nodal points of L_0 is

$$\begin{aligned} X_{L_0} &:= \left\{ \xi_n^j \right\}_{n\geq j,\, j=\overline{1,n-1}} \\ &= \left\{ \frac{m}{2^{k+1}-m+1} \mid k = 0,1,2,..., \ m = 1,2,...,2^k \right\} \cup \{0\}. \end{aligned} \tag{15}$$

Lemma 1. The set X_{L_0}, defined by (15), is dense in [0,1].

Proof. For each fixed $k \in \{0,1,2,\ldots\}$, we have

$$= \left\{ \frac{m}{2^{k+1}-m+1} \mid m = 1,2,...,2^k \right\} = \left\{ \frac{1}{2^{k+1}}, \frac{2}{2^{k+1}-1}, \frac{3}{2^{k+1}-2}, ..., \frac{2^k}{2^k+1} \right\}.$$

Moreover,

$$\frac{1}{2^{k+1}} - 0 = \frac{1}{2^{k+1}}, \qquad 1 - \frac{2^k}{2^k+1} = \frac{1}{2^k+1}, \tag{16}$$

and for $m=1,2,\ldots,2^k-1$,

$$\begin{aligned} \bar{\ell}_{m,k} &:= \frac{m+1}{2^{k+1}-(m+1)+1} - \frac{m}{2^{k+1}-m+1} \\ &= \frac{2^{k+1}+1}{(2^{k+1}-m)-(2^{k+1}-m+1)}. \end{aligned}$$

Hence, there exists a sufficiently large number $\bar{k}$ such that for each $k > \bar{k}$ we have

$$\bar{\ell}_{m,k} < \frac{1}{k+1}. \tag{17}$$

Now, let $\bar{x}_{m,k} := m/(2^{k+1}-m+1)$. Then, for each $x \in [0,1]$, there exists m $\in \{1,2,\ldots, 2^k-1\}$ such that

$$x \in [0, \bar{x}_{1,k}] \ \vee \ x \in [\bar{x}_{m,k}, \bar{x}_{m+1,k}] \ \vee \ x \in [\bar{x}_{2^k,k}, 1]. \tag{18}$$

On the other hand, the right sides of equations (16) and (17) tend to zero as $k \to \infty$. This together with the equation (18) completes the proof. □

Theorem 2. The set of the nodal points of the boundary value problem L, X_L, is dense in the interval (0,1).

Proof. It follows from (15) that the nodal points $\xi_n^{(j)}$ of L_0 have the form

$$\xi_n^{(j)} = \frac{j}{n}, \qquad n \geq 2, \quad j - 1,2,3,\ldots,n-1.$$

Thus, using (10) we obtain

$$x_n^{(j)} = \xi_n^{(j)} + O\left(\frac{1}{n}\right). \tag{19}$$

By (19) and Lemma 1, we conclude that X_L is dense in (0,1). □

Now, we prove the main result of this section.

Theorem 3. Consider the boundary value problems defined by

$$y'' + \left(\lambda - \frac{A}{x^2} + q_i(x)\right) y = 0, \qquad i = 1,2, \quad x \in (0,1), \tag{20}$$

and Dirichlet condition

$$y(0) = 0 = y(1). \tag{21}$$

Let q_1, q_2, satisfy the condition (4) and $x_n^{(j)}(q_1) = x_n^{(j)}(q_2)$. Then $q_1 = q_2$ (a.e.).

Proof. First, we consider the case when k_0 is odd, in (5). Let x be an arbitrary, fixed number in the interval [0,1]. Since the set of the nodal points X_L, defined in (9), is dense in the interval (0,1) by Theorem 2, it follows that there exists a subsequence $\{n_k\}$, $k=1,2,3,\ldots$, such that

$$\lim_{k \to \infty} x_{n_k}^{(j)} = x. \tag{22}$$

Let $\tilde{y}_i(x) = y_2(x, \lambda_{n_k}(q_i))$ be the solution of (20)-(21) with the potential $q_i(x)$. Then, using (20) we derive

$$\frac{d}{dx}(\tilde{y}_2\tilde{y}_1'-\tilde{y}_1\tilde{y}_2')(x)=\left\{\ q_1(x)-q_2(x)+\lambda_{n_k}(q_1)-\lambda_{n_k}(q_2)\ \right\}\tilde{y}_1(x)\tilde{y}_2(x)\,. \tag{23}$$

Integrating (23) from 0 to $x(j,n_k)=x_{n_k}^{(j)}:=x_{n_k}^{(j)}(q_1)=x_{n_k}^{(j)}(q_2)$, we get

$$(\tilde{y}_2\tilde{y}_1'-\tilde{y}_1\tilde{y}_2')(x)\,|_0^{x(j,n_k)}=\int_0^{x(j,n_k)}\left\{\ q_1(t)-q_2(t)+\lambda_{n_k}(q_1)-\lambda_{n_k}(q_2)\ \right\}\tilde{y}_1(t)\tilde{y}_2(t)dt\,. \tag{24}$$

Since $\tilde{y}_1(x(j,n_k))=\tilde{y}_2(x(j,n_k))=0$, the left side of (24) is equal to zero for each $k\in\{1,2,3,\ldots\}$. Thus,

$$\int_0^{x(j,n_k)}\left\{\ q_1(t)-q_2(t)+\lambda_{n_k}(q_1)-\lambda_{n_k}(q_2)\ \right\}\tilde{y}_1(t)\tilde{y}_2(t)dt=0\,,$$

for $k=1,2,3,\ldots$. We are done if we can show

$$\int_0^x(q_1(t)-q_2(t))dt=0\,.$$

For this goal, by (8) we have

$$\lambda_{n_k}(q_1)-\lambda_{n_k}(q_2)\to 0\quad\text{as}\ k\to\infty\,.$$

Hence, together with (22) and (24) these results imply

$$\lim_{k\to\infty}n_k^2\pi^2\int_0^x(q_1(t)-q_2(t))\tilde{y}_1(t)\tilde{y}_2(t)dt=0\,. \tag{25}$$

Moreover, it follows from (7) that there exists a constant *C* such that for sufficiently large *k*, we have

$$\left|\tilde{y}_1(x)\tilde{y}_2(x)-(n_k\pi)^{-2}\sin^2(n_k\pi x)\right|<C(n_k\pi)^{-3}.$$

So,

$$n_k^2\pi^2\tilde{y}_1(x)\tilde{y}_2(x)\approx\sin^2(n_k\pi x)\,,\quad k\to\infty\,. \tag{26}$$

Therefore, by (25)–(26) we get

$$\int_0^x(q_1(t)-q_2(t))dt=0\,. \tag{27}$$

Finally, since x was chosen arbitrary in the interval [0,1], together with (27) this yields $q_1=q_2$ (a.e.). In the case when k_0 is even, Theorem 3 can be proved similarly, by (6) and the same way as above. □

Theorem 3 shown that the solution of the inverse nodal problem associated with (2)−(3), the potential function *q(x)*, can be uniquely determined by a dense set of nodes of the eigenfunctions.

ACKNOWLEDGMENT This research is partially supported by the University of Kashan under grant number 464151/1.

REFERENCES

1. R. Kh. Amirov, On system of Dirac differential equations with discontinuity conditions inside an interval, *Ukrainian Math. J.* **57** (2005) 712–727.
2. R. Amirov and N. Topsakal, On inverse problem for singular Sturm-Liouville operator with discontinuity conditions, *Bull. Iranian Math. Soc.* **40** (2014) 585–607.
3. W. O. Amrein, A. M. Hinz and D. B. Pearson, *Sturm–Liouville Theory: Past and Present*, Birkhäuser Verlag, Basel, 2005.
4. R. P. Bell, *The Tunnel Effect in Chemistry*, Springer-Science, University Press, Cambridge, 1980.
5. G. Borg, Eine umkehrung der Sturm–Liouvillesehen eigenwertaufgabe, *Acta Math.* **78** (1945) 1–96.
6. J. P. Boyd, Sturm-Liouville eigenvalue problems with an interior pole, *J. Math. Physics* **22** (1981) 1575–1590.
7. Y. H. Cheng, C. K. Law and J. Tsay, Remarks on a new inverse nodal problem, *J. Math. Anal. Appl.* **248** (2000) 145–155.
8. W. Eberhard, G. Freiling and K. Wilcken-Stoeber, Indefinite eigenvalue problems with several singular points and turning points, *Math. Nachr.* **229** (2001) 51–71.
9. G. Freiling and V. Yurko, On constructing differential equation with singularities from incomplete spectral information, *Inv. Prob.* **14** (1998) 1131–1150.
10. G. Freiling and V. Yurko, On the determination of differential equations with singularities and turning points, *Results Math.* **41** (2002) 275–290.
11. G. Freiling and V. Yurko, Inverse problems for differential operators with singular boundary conditions, *Math. Nachr.* **278** (2005) 1561–1578.
12. I. M. Gelfand and B. M. Levitan, On the determination of a differential equation from its spectral function, *Amer. Math. Soc. Trans.* **1** (1951) 253–304.
13. D. M. Haaland and R. T. Meyer, Reaction of exited iodine atoms with methyl iodide rate constant determinations, *Int. J. Chem. Kinetics* **6** (1974) 297–308.
14. O. Hald and J. R. McLaughlin, Solutions of inverse nodal problems, *Inv. Prob.* **5** (1989) 307–347.
15. H. Hellmann, A new approximation method in the problem of many electrons, *J. Chem. Phys.* **3** (1935) p. 61.
16. A. Jodayree Akbarfam and A. B. Mingarelli, The canonical product of the solution of the Sturm-Liouville equation in one turning point case, *Canad. Appl. Math. Quart*. **8** (2000) 305–320.

17. K. Jörgens, Spectral theory of second-order ordinary differential operators, *Lecture Notes: Series no.2, Matematisk Institut*, Aarhus Universitet, 1962/63.
18. N. Levinson, The inverse Sturm–Liouville problem, *Mat. Tidsskr. B.* (1949) 25–30.
19. H. R. Marasi and A. Jodeyree Akbarfam, On the canonical solution of indefinite problem with *m* turning points of even order, *J. Math. Anal. Appl.* **332** (2007) 1071–1086.
20. V. A. Marchenko, Concerning the theory of a differential operator of the second order, *Dokl. Akad. Nauk. SSSR (N.S.)* **72** (1950) 457–460.
21. J. R. McLaughlin, Inverse spectral theory using nodal points as data—a uniqueness result, *J. Diff. Eqs.* **73** (1988) 354–362.
22. S. Mosazadeh, Infinite product representation of solution of indefinite Sturm-Liouville Problem, *Iranian J. Math. Chem.* **4** (2013) 27–40.
23. S. Mosazadeh, The stability of the solution of an inverse spectral problem with a singularity, *Bull. Iranian Math. Soc*. **41** (2015) 1061–1070.
24. J. K. Shaw, A. P. Baronavski, H. D. Ladouceur and W. O. Amrein, Applications of the Walker method in Spectral Theory and Computational Methods of Sturm-Liouville problems, *Lecture Notes in Pure and Appl. Math.* **191** (1997) 377–395.
25. C. T. Shieh and V. A. Yurko, Inverse nodal and inverse spectral problems for discontinuous boundary value problems, *J. Math. Anal. Appl.* **347** (2008) 266–272.
26. I. Stemmler, M. Rothe, I. Hense and H. Hepach, Numerical modeling of methyl iodide in the eastern tropical Atlantic, *Biogeosciences* **10** (2013) 4211–422.
27. V. Yurko, Recovering singular differential operators on noncompact star-type graphs from Weyl functions, *Tamkang J. Math.* **42** (2011) 223–236.

Iranian J. Math. Chem. 8 (4) December (2017) 413 − 423

Iranian Journal of Mathematical Chemistry

Journal homepage: ijmc.kashanu.ac.ir

Numerical Modeling for Nonlinear Biochemical Reaction Networks

Z. A. ZAFAR[•,1, 2], K. REHAN[3], M. MUSHTAQ[2] AND M. RAFIQ[2,4]

[1]Faculty of Information and Technology, University of Central Punjab, Lahore, Pakistan
[2]Department of Mathematics, University of Engineering and Technology, Lahore, Pakistan
[3]Department of Mathematics, University of Engineering and Technology, KSK Campus, Pakistan
[4]Faculty of Engineering, University of Central Punjab, Lahore, Pakistan

ARTICLE INFO

Article History:

Received 26 January 2016
Accepted 4 March 2016
Published online 7 September 2017
Academic Editor: Ivan Gutman

Keywords:

Michaelis–Menten model
NSFD method
RK4 method

ABSTRACT

Nowadays, numerical models have great importance in every field of science, especially for solving the nonlinear differential equations, partial differential equations, biochemical reactions, etc. The total time evolution of the reactant concentrations in the basic enzyme-substrate reaction is simulated by the Runge-Kutta of order four (RK4) and by Non-standard finite difference (NSFD) method. ANSFD model has been constructed for the biochemical reaction problem and numerical experiments are performed for different values of discretization parameter 'h'. The results are compared with the well–known numerical scheme, i.e. RK4. Unlike RK4 which fails for large time steps, the developed scheme NSFD gives results that converge to true steady states for any time step used.

1. INTRODUCTION AND PRELIMINARIES

In this paper, we consider the well-known Michaelis-Menten biochemical reaction model [1], i.e., the single enzyme substrate reaction scheme

$$E + A \rightleftharpoons Y \longrightarrow E + X, \tag{1}$$

where E is the enzyme, A the substrate, Y the intermediate complex and X the product. The time evolution of scheme (1) can be determined from the solution of the system of coupled nonlinear ODE [2].

• Corresponding Author: (Email address: zainzafar2016@hotmail.com)
DOI: 10.22052/ijmc.2017.47506.1170

$$\frac{dA}{dE} = -k_1 EA + k_{-1} Y\,, \tag{2}$$

$$\frac{dE}{dt} = -k_1 EA + (k_{-1} + k_2)Y, \tag{3}$$

$$\frac{dY}{dt} = k_1 EA - (k_{-1} + k_2)Y, \tag{4}$$

$$\frac{dX}{dt} = k_2 Y, \tag{5}$$

subject to the initial conditions

$$A(0) = A_0, E(0) = E_0, Y(0) = 0, X(0) = 0 \tag{6}$$

where the parameters k_1, k_{-1} and k_2 are positive rate constants for each reaction. Systems (2) – (5) can be reduced to only two equations for A and Y and in dimensionless form of concentrations of substrate x, and intermediate complex between enzyme and substrate$y$, are given by [2].

$$\frac{dx}{dt} = -x + (\beta - \alpha)y + xy \tag{7}$$

$$\frac{dy}{dt} = \frac{1}{\sigma}(x - \beta y - xy) \tag{8}$$

subject to the initial conditions

$$x(0) = 1, y(0) = 0 \tag{9}$$

where α,β and σ are dimensionless parameters.

The time evolution of the reaction can be determined from the traditional purely numerical methods like the classical fourth order Runge-Kutta method (RK4), but we are interested in this work to solve the system of coupled nonlinear ODEs (7) and (8) by using NSFD. To do so, we proceed as follows:

1.1 EQUILIBRIUM POINT

To calculate equilibrium point, equate (7) and (8) equal to zero i.e,

$$-x + (\beta - \alpha)y + xy = 0 \tag{10}$$

$$\frac{1}{\sigma}(x - \beta y - xy) = 0 \tag{11}$$

we obtain $(x^*, y^*) = (0,0)$,that is the equilibrium point.

2. RK4 METHOD

In this section, we solve the systems (7) and (8) by RK4 Scheme as follows:

$$
\begin{aligned}
k_1 &= h(-x_n + (\beta-\alpha)y_n + x_n y_n) \\
m_1 &= \frac{h}{\sigma}(x_n - \beta y_n - x_n y_n) \\
k_2 &= h[-(x_n + \frac{k_1}{2}) + (\beta-\alpha)(y_n + \frac{m_1}{2}) + (x_n + \frac{k_1}{2})(y_n + \frac{m_1}{2})] \\
m_2 &= \frac{h}{\sigma}[(x_n + \frac{k_1}{2}) - \beta(y_n + \frac{m_1}{2}) - (x_n + \frac{k_1}{2})(y_n + \frac{m_1}{2})] \\
k_3 &= h[-(x_n + \frac{k_2}{2}) + (\beta-\alpha)(y_n + \frac{m_2}{2}) + (x_n + \frac{k_2}{2})(y_n + \frac{m_2}{2})] \\
m_3 &= \frac{h}{\sigma}[(x_n + \frac{k_2}{2}) - \beta(y_n + \frac{m_2}{2}) - (x_n + \frac{k_2}{2})(y_n + \frac{m_2}{2})] \\
k_4 &= h[-(x_n + k_3) + (\beta-\alpha)(y_n + m_3) + (x_n + k_3)(y_n + m_3)] \\
m_4 &= \frac{h}{\sigma}[(x_n + k_3) - \beta(y_n + m_3) - (x_n + k_3)(y_n + m_3)]
\end{aligned}
$$

$$x_{n+1} = x_n + \frac{1}{6}[k_1 + 2k_2 + 2k_3 + k_4] \tag{12}$$

$$y_{n+1} = y_n + \frac{1}{6}[m_1 + 2m_2 + 2m_3 + m_4] \tag{13}$$

2.1 NUMERICAL EXPERIMENTS

Numerical experiments are performed using values of parameters given in Table 2.1.

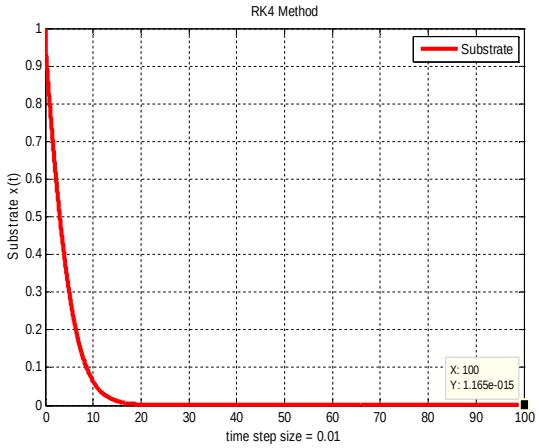

Figure 2.1. Concentration of Substrate.

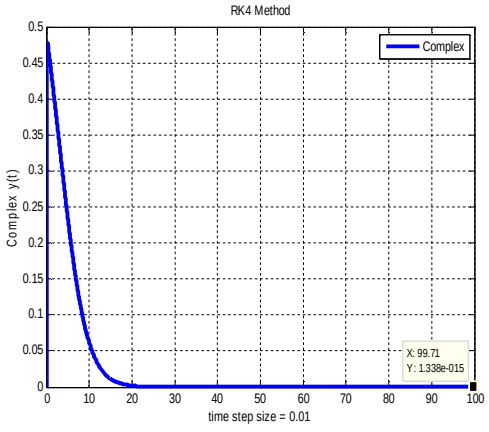

Figure 2.2. Concentration of Intermediate Complex between Enzyme and Substrate.

Table 2.1. The Parameters α, β and σ.

Parameters	Value
α	0.375
β	1
σ	0.1

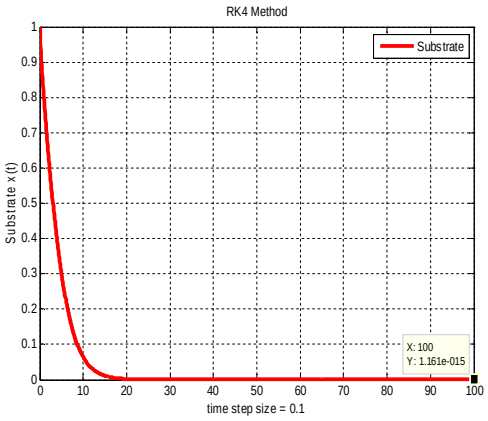

Figure 2.3. Concentration of Substrate.

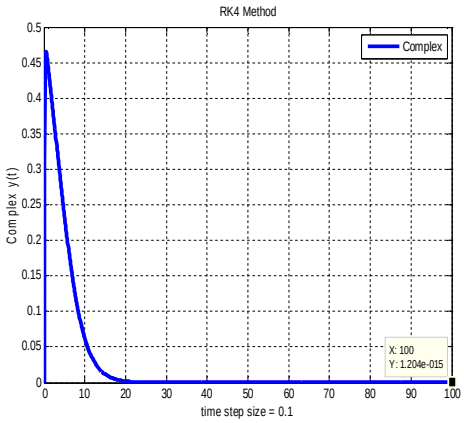

Figure 2.4. Concentration of Intermediate Complex between Enzyme and Substrate.

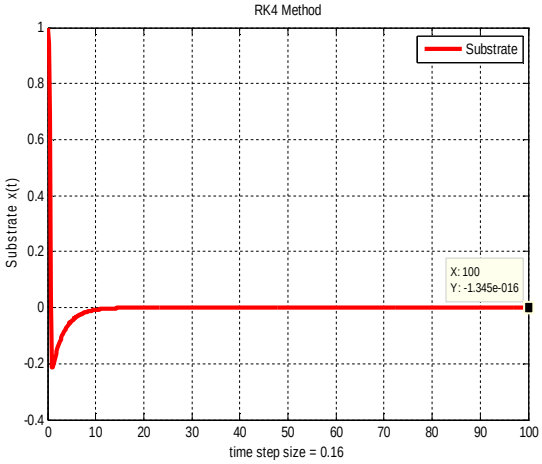

Figure 2.5. Concentration of Substrate.

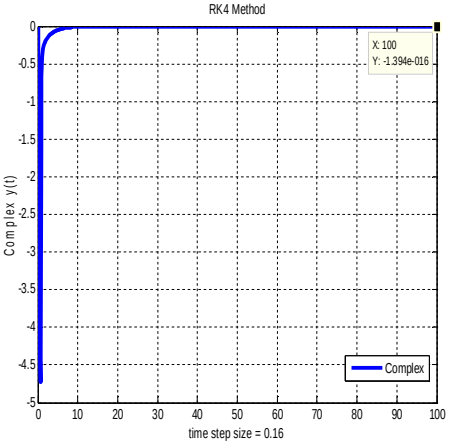

Figure 2.6. Concentation of Intermediate Complex between Enzyme and Substrate.

3. NONSTANDARD FINITE DIFFERENCE METHOD

In this section we shall construct Non-Standard Finite Difference Scheme for the equations (7) and (8). First order time derivatives are described by using forward difference approximation [4, 5]. $\dot{f}(t)$ can be approximated as

$$\frac{df(t)}{dt} = \lim_{l \to 0} \frac{f(t+l) - f(t)}{l} + O(l)$$

x^n and y^n are the approximations of $x(nl)$ and $y(nl)$, for $n = 0,1,2, \ldots,$ and where 'l' is step size of time. For satisfying biological nature of the continuous time model, it should be non–negative. The numerical method which has been developed to solve the system must hold Conservation law proposed by Mickens [6, 7]. To construct the NSFD scheme for system (7)−(8) we note the following statements

(i) The linear and nonlinear terms on the right hand side of Equation (7) are in the form $-x \approx -x^{n+1}$, $(\beta - \alpha)y \approx (\beta - \alpha)y^n$, $xy \approx x^n y^n$

(ii) The linear and nonlinear terms on the right hand side of Equation (8) are in the form $x \approx x^n$, $-\beta y \approx -\beta y^{n+1}$, $-xy \approx -x^n y^{n+1}$

So,

$$\frac{x^{n+1} - x^n}{h} = -x^{n+1} + (\beta - \alpha)y^n + x^n y^n \tag{14}$$

$$\frac{y^{n+1} - y^n}{h} = \frac{1}{\sigma}\{x^n - \beta y^{n+1} - x^n y^{n+1}\} \tag{15}$$

Eq. (14) implies that

$$x^{n+1} = \frac{x^n + h\{(\beta - \alpha)y^n + x^n y^n\}}{1 + h} \tag{16}$$

and Eq. (15) implies that

$$y^{n+1} = \frac{y^n + \frac{h}{\sigma}x^n}{1 + \frac{h\beta}{\sigma} + \frac{h}{\sigma}x^n}.$$

3.1 CONVERGENCE ANALYSIS

The stability and convergence of the proposed NSFD scheme about equilibrium point (0,0) are discussed here. Let

$$F = \frac{x + h\{(\beta - \alpha)y + xy\}}{1 + h},$$

$$G = \frac{y + \frac{h}{\sigma}x}{1 + \frac{h\beta}{\sigma} + \frac{h}{\sigma}x},$$

and the Jacobian matrix is

$$J(F^*)=\begin{bmatrix}\frac{\partial F}{\partial x} & \frac{\partial F}{\partial y}\\ \frac{\partial G}{\partial x} & \frac{\partial G}{\partial y}\end{bmatrix}$$

where as

$$\frac{\partial F}{\partial x}=\frac{1+hy}{1+h},\quad \frac{\partial F}{\partial y}=\frac{h\{(\beta-\alpha)+x\}}{1+h},$$

$$\frac{\partial G}{\partial x}=\frac{(1+\frac{h\beta}{\sigma}+\frac{h}{\sigma}x)\frac{h}{\sigma}}{(1+\frac{h\beta}{\sigma}+\frac{h}{\sigma}x)^2},\quad \frac{\partial G}{\partial y}=\frac{1}{1+\frac{h\beta}{\sigma}+\frac{h}{\sigma}x}$$

At $(x^*,y^*)=(0,0)$ we have

$$\frac{\partial F}{\partial x}=\frac{1}{1+h},\quad \frac{\partial F}{\partial y}=\frac{h(\beta-\alpha)}{1+h},\quad \frac{\partial G}{\partial x}=\frac{\frac{h}{\sigma}}{(1+\frac{h\beta}{\sigma})},\quad \frac{\partial G}{\partial y}=\frac{1}{1+\frac{h\beta}{\sigma}}.$$

Define,

$$J=\begin{bmatrix}\frac{1}{1+h} & \frac{h(\beta-\alpha)}{1+h}\\ \frac{\frac{h}{\sigma}}{(1+\frac{h\beta}{\sigma})} & \frac{1}{1+\frac{h\beta}{\sigma}}\end{bmatrix}.$$

Lemma [11]: For the quadratic equation $\mu^2-\mu A+B=0$, both roots satisfy $|\mu_i|<1; i=1,2$ if and only if the following conditions are satisfied:

(i) $1+B>A$

(ii) $1+A+B>0$

(iii) $B<1$

Let us define$A=trace(J)$ and $B=\det(J)$, where

$$trace(J)=\frac{1}{1+h}+\frac{1}{1+\frac{h\beta}{\sigma}}=\frac{2+h+\frac{h\beta}{\sigma}}{(1+h)(1+\frac{h\beta}{\sigma})}$$

and

$$\det(J)=\left(\frac{1}{1+h}\times\frac{1}{1+\frac{h\beta}{\sigma}}\right)-\left(\frac{h(\beta-\alpha)}{1+h}\times\frac{\frac{h}{\sigma}}{1+\frac{h\beta}{\sigma}}\right)=\frac{1-(\beta-\alpha)\frac{h^2}{\sigma}}{(1+h)(1+\frac{h\beta}{\sigma})}$$

The first condition of the Lemma is $1+B>A$, so by using the values of A and B we have

$$1+\frac{1-(\beta-\alpha)\frac{h^2}{\sigma}}{(1+h)(1+\frac{h\beta}{\sigma})}>\frac{2+h+\frac{h\beta}{\sigma}}{(1+h)(1+\frac{h\beta}{\sigma})}\Rightarrow(1+h)(1+\frac{h\beta}{\sigma})+1-(\beta-\alpha)\frac{h^2}{\sigma}>2+h+\frac{h\beta}{\sigma}$$

which proves that $h^2>0$.

The second condition of the Lemma is $1+A+B>0$, so by using the values of A and B we get

$$2+2h+2\frac{h\beta}{\sigma}+\frac{h^2\alpha}{\sigma}>0.$$

The third condition of the Lemma is $1>B$, so by using the values of A and B we obtain

$$h\alpha<\sigma+\beta+2h\beta\Rightarrow 0<\sigma+\beta+(2\beta-\alpha)h.$$

Since $h>0$ and all conditions of the theorem are true, the *System is Stable* for all values of h and converges to steady state.

3.2 NUMERICAL EXPERIMENTS

Numerical experiments are performed using values of parameters given in Table 2.1.

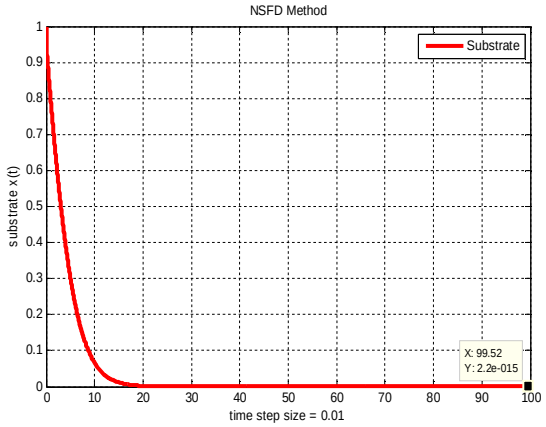

Figure 3.1. Concentration of Substrate.

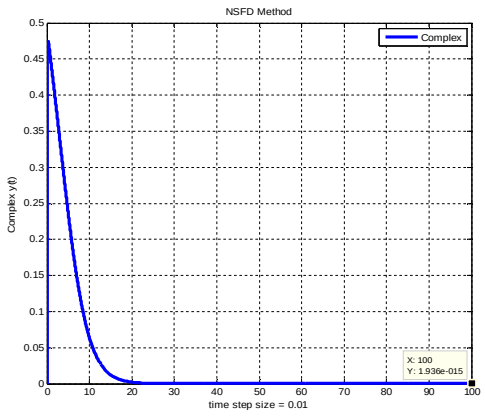

Figure 3.2. Concentration of Intermediate Complex between Enzyme and Substrate.

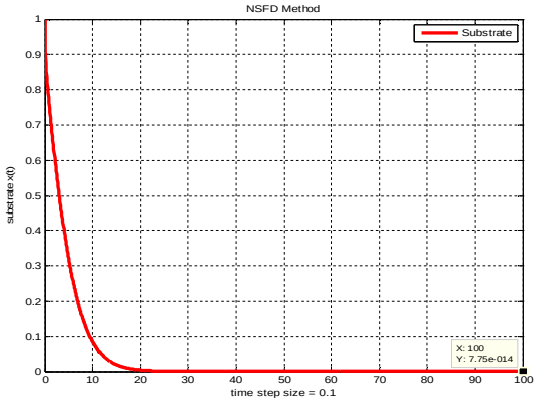

Figure 3.3. Concentration of Substrate.

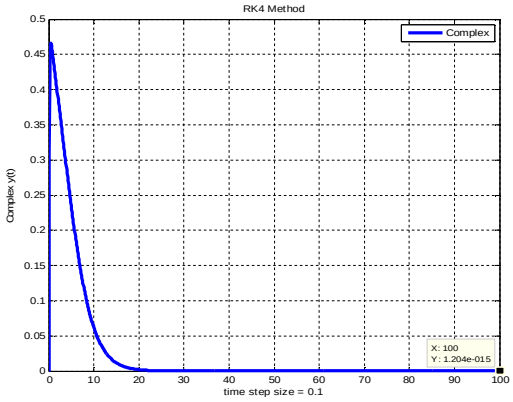

Figure 3.4. Concentration of Intermediate Complex between Enzyme and Substrate.

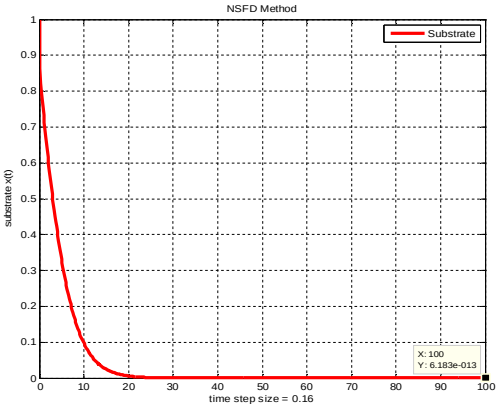

Figure 3.5. Concentration of Substrate.

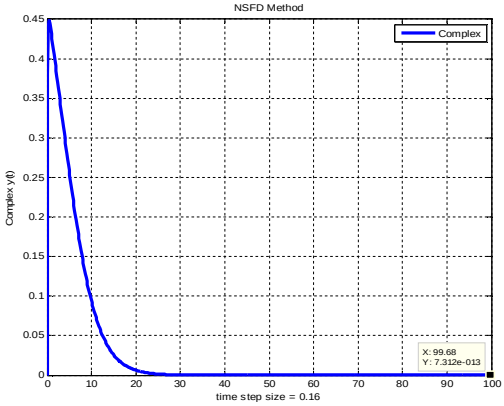

Figure 3.6. Concentration of Intermediate Complex between Enzyme and Substrate.

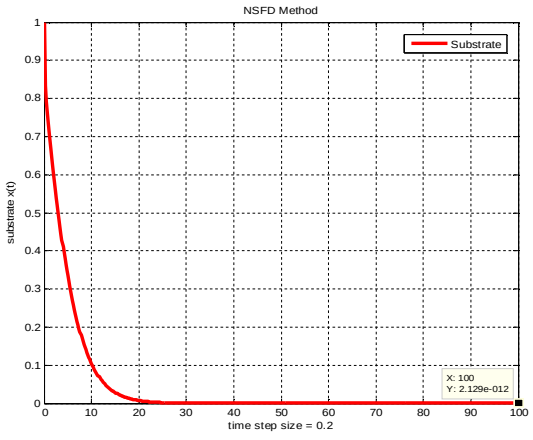

Figure 3.7. Concentration of Substrate.

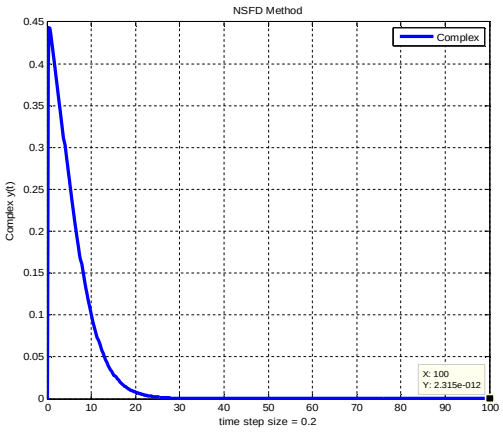

Figure 3.8. Concentration of Intermediate Complex between Enzyme and Substrate.

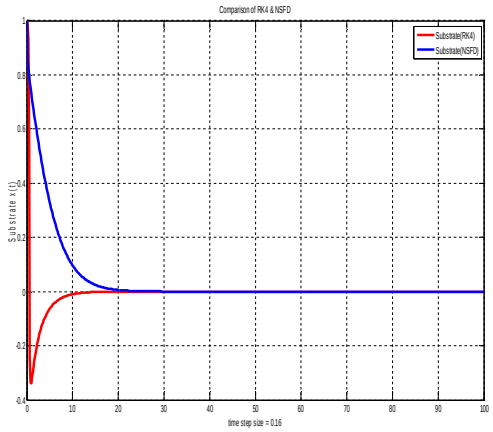

Figure 3.9. Comparison between NSFD and RK4.

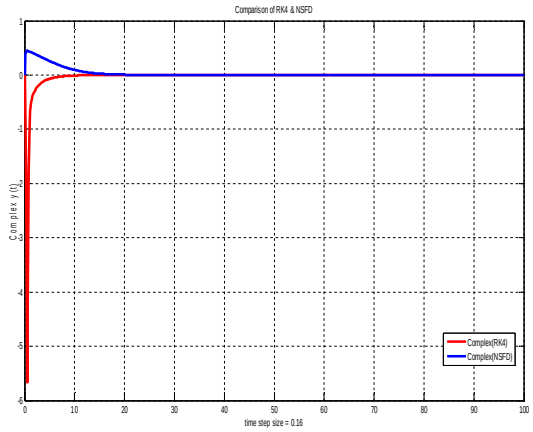

Figure 3.10. Comparison between NSFD and RK4.

4. RESULTS AND DISCUSSION

The Numerical modelling of well–known Michaelis–Menten non–linear reaction system has been analysed in this paper. The model has one equilibrium points. An unconditionally convergent non–standard finite difference numerical model has been constructed and numerical experiments are performed for different values of discretization parameter 'h'. Results are compared with well-known numerical method i.e. Runge–Kutta method of order four (RK4). Table 4.1 shows the effect of different time step, h for both numerical schemes.

Table 4.1. The Effect of Different Time Step.

h	RK4	Numerical Model
.01	Convergence	Convergence
0.1	Convergence	Convergence
0.16	Divergence(method failed)	Convergence
0.2	Divergence	Convergence
2	Divergence	Convergence
10	Divergence	Convergence
100	Divergence	Convergence

Table 4.1 shows that the RK-4 method converge for small values of parameter h and it diverges for the large values but our NSFD model will remain convergent even for a very

large value of discretization parameter i.e. $h = 1000$. It isto be noted that the authors of [11] solved this problem by multistage homotopy perturbation method and homotopy perturbation method. In both cases they statedthat the step size h should be very small otherwise the methods will diverge, but in our case, the step size is irrelevant.

5. CONCLUSION

Figures 3.9 and 3.10 show the comparison of NSFD scheme with Runge-Kutta method of order 4. It can be observed that when step size has been increased up to 0.16, the RK–4 scheme gives negative values of both concentrations, while the proposed NSFD scheme preserves positivity and convergence of the solution for these values of step size. Unlike RK-4 which fails for large time steps, the developed NSFD scheme gives results that converged to true steady states for any time step used. The proposed scheme is easy to implement and numerically stable.

REFERENCES

1. S. Schnell andC. Mendoza, Closed form solution for time dependent enzyme kinetics, *J Theor Biol*.**187** (1997) 207–212.
2. A. K. Sen, An application of the Adomian decomposition method to the transient behavior of a model biochemical reaction, *J Math Anal Appl*. **131** (1988) 232–245.
3. P. Pongsumpun, Mathematical model of Dengue disease with incubation period of virus, *World Acad. Sci. Eng. Technol.* **44** (2008) 328–332.
4. M. Rafiq, M.O.Ahmed, S. Ahmed, R. Siddique and A. Pervaiz, Some finite Difference Methods for One Dimensional Burgers Equation for Irrotational Incompressible Flow Problem, *Pak. J. Engg. & Appl. Sci.* **9** (2011) 13–16.
5. Z. Zafar, M. O. Ahmad, A. Pervaiz and M. Rafiq, Fourth Order Compact Method for One Dimensional Inhomogeneous Telegraph Equation with $O(h^4, k^3)$, *Pak. J. Engg. & Appl. Sci*. **14** (2014) 96–101.
6. R. E. Mickens, Numerical Integration of population models satisfying conservation laws: NSFD METHODS, *Biological Dynamics* **1** (2007) 427–436.
7. R. E. Mickens, Dynamical consistency: a fundamental principle for constructing Non–standard finite difference schemes for differential equations, *J. Differ. Equ. Appl.* **11** (2005) 645–653.

8. A. A. M. Arafa, S. Z. Rida and H. Mohamed, An application of the homotopy analysis method to the transient behavior of a biochemical reaction model, *Inf. Sci. Lett*. **3** (2014) 29–33.
9. S. O. Edeki, E. A. Owoloko, A. S. Osheku, A. A. Opanuga, H. I. Okagbue and G. O. Akinlabi, Numerical solutions of nonlinear biochemical model using a hybrid numerical – analytical technique, *Int. J. Math. Anal.* **9** (2015) 403–416.
10. F. Brauer and C. Castillo Chavez, *Mathematical Models in Population Biology and Epidemology*, Springer–Verlag, *2012*.
11. I. Hashim, M. S. H. Chowdhury and S. Mawa, On multistage homotopy perturbation method applied to non–linear biochemical reaction model, *Chaos Soltion & Fractals* **36** (2008) 823–827.
12. Z. Zafar, K. Rehan and M. Mushtaq, Fractional-order scheme for bovine babesiosis disease and tick populations, *Adv. Difference Equ.* (2017) 2017:86.

Iranian J. Math. Chem. 8 (4) December (2017) 425 − 437

Iranian Journal of Mathematical Chemistry

Journal homepage: ijmc.kashanu.ac.ir

Numerical Solution of Gas Solution in a Fluid: Fractional Derivative Model

SHAHROKH ESMAEILI•

Department of Applied Mathematics, University of Kurdistan, P.O. Box 416, Sanandaj, Iran

ARTICLE INFO

Article History:

Received 23 May 2016
Accepted 12 June 2016
Published online 8 September 2017
Academic Editor: Ali Reza Ashrafi

Keywords:

Fractional derivatives
Gas solution
Müntz polynomials
Gaussian quadrature
Collocation method

ABSTRACT

A computational technique for solution of mathematical model of gas solution in a fluid is presented. This model describes the change of mass of the gas volume due to diffusion through the contact surface. An appropriate representation of the solution based on the Müntz polynomials reduces its numerical treatment to the solution of a linear system of algebraic equations. Numerical examples are given and discussed to illustrate the effectiveness of the proposed approach.

1. INTRODUCTION

A number of examples in nature can illustrate the capability of liquids to dissolve gases; in fact, human life would not be feasible if blood cannot dissolve oxygen, nor marine life is likely to happen if oxygen did not dissolve in water. The solubility anticipation of oxygen gas in the liquid is important as it can be used in aquaculture and biological issues such as oxygen uptake in lungs and its dissolution in the blood. The prediction of CO_2 gas solubility in water can be used for growing plants and in the production of carbonated drinks [24]. Such interesting natural phenomena are described by differential equations.

This paper is concerned with providing good quality algorithm for the numerical solution of the three–term fractional differential equations of the form

$$p'(t) + F(t)D^{1/2}p(t) + G(t)p(t) = H(t), \qquad (1.1)$$

combined with the suitable initial condition $p(0) = p_0$. This equation describes the change of mass of the gas volume due to diffusion through the contact surface [2]. Here, $D^{1/2}p(t)$

• Corresponding Author: (Email address: (sh.esmaeili@uok.ac.ir)
DOI: 10.22052/ijmc.2017.54560.1203

denotes the fractional derivative $D_*^{1/2}p(t)$ in the Caputo version [7] and the Riemann–Liouville fractional derivative ${}^{RL}_{0}D_t^{1/2}p(t)$, defined by

$$D_*^{1/2}p(t) = \frac{1}{\sqrt{\pi}}\int_0^t \frac{p'(s)}{\sqrt{t-s}}ds, \tag{1.2}$$

$${}^{RL}_{0}D_t^{\frac{1}{2}}p(t) = \frac{1}{\sqrt{\pi}}\frac{d}{dt}\int_0^t \frac{p(s)}{\sqrt{t-s}}ds, \tag{1.3}$$

respectively [9,23]. It is well-known that the fractional derivative of Riemann–Liouville and Caputo type are closely linked by the following relationship:

$$D_*^{1/2}p(t) = {}^{RL}_{0}D_t^{1/2}[p(t)-p(0)]. \tag{1.4}$$

Fractional calculus, including the operators of fractional order integration and differentiation, is known to provide an excellent setting for capturing in a model framework concerned with real–world problems in a variety of disciplines from physics, chemistry, biology and engineering [1, 4, 17, 23]. In order to approximate fractional derivatives, a number of methods have been proposed [4, 6, 11]. Since few of the fractional differential equations can be solved explicitly, it is necessary to employ numerical techniques to find the approximate solution. Especially, numerical schemes for the multi–term fractional differential equations have been developed in the past ten to fifteen years and have been studied in numerous papers [4, 9, 10, 22].

As a fractional derivative is a non–local operator, it is very natural to consider a global method like the spectral method for its numerical solution. Spectral collocation methods are efficient and highly accurate techniques for numerical solution of differential equations [13, 25]. The basic idea of the spectral collocation method is to assume that the unknown solution$p(t)$can be approximated by a linear combination of some basis functions, called the trial functions, such as orthogonal polynomials.

Whereas the classical orthogonal polynomials work well for numerical solution of conventional differential equations, their application for the fractional differential equations implies at least two difficulties in connection with the collocation method. First, according to Theorems 4.1 in [16], the solutions of the problem (1.1) can contain some fractional–power terms with which the classical orthogonal polynomials cannot match. In this case, the rate of convergence of the numerical approximations is not reasonable when the classical polynomial bases are used. Second, to apply a collocation method, it is required that the derivatives of any trial function can be expressed in terms of the same trial bases. However, the fractional derivatives of a classical polynomial are not polynomials. Therefore, roughly speaking, a good approximation for the fractional derivatives via the classical orthogonal polynomials is not hoped to be obtained.

In the present article, the Müntz–Legendre polynomials are used, which are a family of generalized orthogonal polynomials. These polynomials were introduced and investigated in [5, 18]. A fractional derivative of a Müntz–Legendre polynomial is again a

Müntz–Legendre polynomial. This is a crucial feature of these bases for using them in the collocation method for the numerical solution of the fractional differential equations.

The structure of the paper is as follows. In the next section, the derivation of mathematical model of gas solution in a fluid is briefly recalled. Then, to construct a numerical algorithm, this equation as a three–term fractional differential equation is reformulated. In Section 3, the Müntz–Legendre polynomials and related topics are introduced. A description of the proposed numerical scheme is provided in Section 4. Some details concerning the practical implementation are discussed in Section 5. Finally, the numerical results to demonstrate the efficiency of the proposed method are given in Section 6.

2. PROBLEM STATEMENT

The mathematical model of the process of solution of a compressible gas volume in a fluid, when there are no convection currents, is described by the system [2, 23]

$$\frac{d}{d\tau}\left(V_0 f\left(\frac{\tau}{\theta}\right) P(0,\tau)\frac{M}{RT}\right) = SK\left.\frac{\partial C}{\partial x}\right|_{x=0}, \qquad 0 < \tau < \theta, \tag{2.1}$$

$$-\sqrt{K}\left.\frac{\partial C}{\partial x}\right|_{x=0} = {}^{RL}_{0}D_{\tau}^{1/2}[C(0,\tau) - C(x,0)], \tag{2.2}$$

$$P(0,\tau) = \kappa C(0,\tau), \qquad P(x,0) = \kappa C(x,0), \tag{2.3}$$

where V_0 is the initial gas volume, θ is the time of the gas compression to zero volume, f is a function describing a change of the gas volume, such that $f(0) = 1$ and $f(1) = 0$, M is the molecular weight of the gas, R is the molar gas constant, K is the gas diffusion coefficient in the fluid, S is the contact surface between the gas and the fluid, κ is the Henry's constant, $C(x,\tau)$ is the gas concentration, and $P(x,\tau)$ is the unknown gas pressure (Figure 1).

The gas pressure near the contact surface $P(0,\tau)$ is to be found. The x–axis goes down from the contact surface, for which $x = 0$. The gas temperature T is assumed to be constant, which implies the gas compression is slow enough. If necessary, a weak nonisothermality can be accounted by making a correction to the function $f(\tau/\theta)$. The depth of the fluid is taken infinite [2, 23].

The change of the gas volume mass due to diffusion through the contact surface is described by (2.1). The mass change depends on the change of the gas concentration near the contact surface, which is given by (2.2). Taking into account the condition (2.3), makes the consideration of mass transfer process for $x > 0$ unnecessary.

The problem (2.1)–(2.3) for determining the dimensionless gas pressure

$$p(\tau) = \frac{P(0,\tau)}{P(x,0)} = \frac{C(0,\tau)}{C(x,0)},$$

near the constant surface can be written as [23]

$$p'(t) + F(t)D_*^{1/2}p(t) + G(t)p(t) = 0, \qquad p(0) = 1, \tag{2.4}$$

where

$$t = \frac{\tau}{\theta} \in (0,1], \quad F(t) = \frac{\lambda}{f(t)}, \quad G(t) = \frac{f'(t)}{f(t)}, \quad \lambda = \frac{RTS\sqrt{K\theta}}{\kappa M V_0}.$$

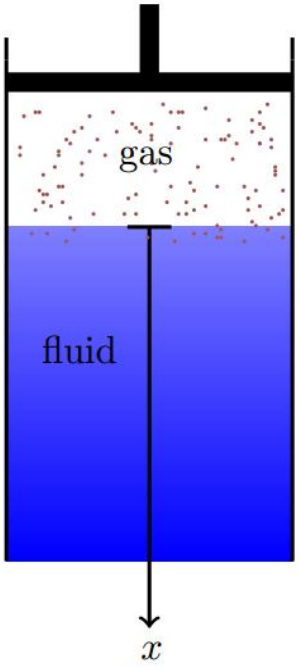

Figure 1. Solution of a gas in a fluid [23].

3. MÜNTZ–LEGENDRE POLYNOMIALS

Let the complex numbers from the set $\Lambda_n = \{\lambda_0, \dots, \lambda_n\}$ satisfy the condition $\Re(\lambda_k) > -\frac{1}{2}$ and $\lambda_k \neq \lambda_j$, $k \neq j$. Then, for every $n = 0,1,2, \dots$, the Müntz–Legendre polynomials on the interval $[0,1]$ are defined by [5, 18]

$$L_n(\Lambda_n; x) = \sum_{k=0}^{n} c_{nk} x^{\lambda_k}, \qquad c_{nk} = \frac{\prod_{\nu=0}^{n-1}(\lambda_k + \bar{\lambda}_\nu + 1)}{\prod_{\nu=0,\nu\neq k}^{n}(\lambda_k - \lambda_\nu)}. \tag{3.1}$$

For the Müntz–Legendre polynomials (3.1), the orthogonality relation

$$\int_0^1 L_n(\Lambda_n; x)\bar{L}_m(\Lambda_m; x)\, dx = \frac{\delta_{nm}}{\lambda_n + \bar{\lambda}_m + 1},$$

holds for every $m, n = 0,1,2, \dots$ [5].

In this paper, the case when the powers of the Müntz basis elements build an arithmetic progression is considered [12, 20]. In other words, we assume that $\lambda_k = k/2$. In this case, the Müntz–Legendre polynomials on the interval $[0,1]$ are represented by the formula

$$L_n(t) = \sum_{k=0}^{n} c_{nk} t^{k/2}, \qquad c_{nk} = \frac{(-1)^{n-k}}{k!\,(n-k)!} \prod_{\nu=0}^{n-1} (k+\nu+2). \tag{3.2}$$

The functions $L_k(t)$, $k = 0,1,\dots,n$ form an orthogonal basis for $\mathbb{M}_n$, where

$$\mathbb{M}_n = \operatorname{span}\{1, t^{1/2}, t, t^{3/2}, \dots, t^{n/2}\}.$$

The denseness of $\mathbb{M}_n$ in $C[0,1]$, the set of continuous functions on the interval $[0,1]$, in the uniform norm is characterized by $\sum_{k=1}^{\infty} 1/k = \infty$ [5].

4. MÜNTZ–LEGENDRE COLLOCATION METHOD

In this section, the collocation method based on Müntz–Legendre polynomials is applied for solving an initial value problem of the form

$$p'(t) + F(t) D_*^{1/2} p(t) + G(t) p(t) = H(t), \tag{4.1}$$

$$p(0) = p_0. \tag{4.2}$$

Under certain conditions on the functions F, G and H, the initial value problem (4.1)–(4.2) possesses unique solution p in an appropriate space of functions [9, 16]. As a generally applicable method to determine the exact solution of initial value problem (4.1)–(4.2) is not readily accessible, some numerically computed approximate solutions are inevitable. Numerical evaluation of this solution is the aim of this section. At first, the solution p is approximated by $p_n \in \mathbb{M}_n$ as the finite sum

$$p_n(t) = \sum_{k=0}^{n} a_k L_k(t), \tag{4.3}$$

where a_k are unknown coefficients. It is worthwhile to note that if $p_n \in \mathbb{M}_n$, then $D_*^{1/2} p_n$ belongs to $\mathbb{M}_n$, too. This key property is crucial for application of the collocation method to the initial value problem (4.1)–(4.2).

The unknown coefficients a_k in approximation (4.3) are obtained from the initial condition

$$p_n(0) = p_0, \tag{4.4}$$

and the fact that $p_n(t)$ should satisfy the fractional differential equation in some suitably chosen collocation points ξ_j, $j = 1,2,\dots,n$. More precisely, the relation holds as follows:

$$p'(\xi_j) + F(\xi_j) D_*^{1/2} p(\xi_j) + G(\xi_j) p(\xi_j) = H(\xi_j). \tag{4.5}$$

Substituting (4.3) into (4.4), the equation

$$\sum_{k=0}^{n} a_k g_{k0} = p_0, \tag{4.6}$$

with $g_{k0} = L_k(0)$ is obtained. In its turn, equation (4.5) can be presented in form of n algebraic equations

$$\sum_{k=0}^{n} a_k g_{kj} = H(\xi_j), \quad j = 1,2,\dots,n, \tag{4.7}$$

where

$$g_{kj} = L_k'(\xi_j) + F(\xi_j) D_*^{1/2} L_k(\xi_j) + G(\xi_j) L_k(\xi_j).$$

Note that $L_k'(\xi_j)$ and $D_*^{1/2} L_k(\xi_j)$ in (4.7) can be computed by using the subsequent stable methods (5.3) and (5.8), respectively. The equations (4.6) and (4.7) are nothing else but a linear system of $n + 1$ equations for the $n + 1$ unknown coefficients a_k that can be solved by one of the known methods. Substituting the coefficients a_k into (4.3) leads to an approximated solution of the fractional initial value problem (4.1)–(4.2).

It should be noted that, the error analysis of the collocation method based on nonclassical polynomials is very complicated and is beyond the scope of this paper.

5. IMPLEMENTATION ISSUES

In this section, some details to provide additional insight on this new method are presented.

5.1. NUMERICAL EVALUATION OF $L_n(t)$ AND $D^{1/2}L_n(t)$

A direct evaluation of Müntz–Legendre polynomials in the form (3.1) can be problematic in finite arithmetic, especially when n is a large number and x is close to 1. These problems have been addressed by Milovanović in [18]. He stated that the coefficients c_{nk} become very large when n increases, but their sums are always equal to 1.

Here, a stable method for evaluating the Müntz–Legendre polynomials defined by (3.2) is presented. The proposed technique is based on a three–term recurrence relation induced from the following theorem.

Proposition 5.1. ([12]) Let $L_n(t)$ be Müntz–Legendre polynomial defined by (3.2) and $t \in [0,1]$. Then

$$L_n(t) = P_n^{(0,1)}(2\sqrt{t} - 1), \tag{5.1}$$

holds true, where $P_n^{(0,1)}$ is a Jacobi polynomial.

Hence, in view of [21, (18.9.2)], the Müntz–Legendre polynomials $L_n(t)$ can be evaluated by means of the three–term recursion

$$b_{1n}L_{n+1}(t) = b_{2n}(t)L_n(t) - b_{3n}L_{n-1}(t), \quad n \geq 1, \tag{5.2}$$

where $L_0(t) \equiv 1$, $L_1(t) = 3\sqrt{t} - 2$, and

$$b_{1n} = 2(n+1)(n+2)(2n+1),$$
$$b_{2n}(t) = 2(n+1)\left[(2n+1)(2n+3)\left(2\sqrt{t}-1\right) - 1\right],$$
$$b_{3n} = 2n(n+1)(2n+3).$$

Another result of Proposition 5.1 is a formula for evaluating $L_n'(t)$. More precisely, by means of [21, (18.9.15)] the first derivative of $L_n(t)$ is given by

$$L_n'(t) = \frac{n+2}{2\sqrt{t}} P_{n-1}^{(1,2)}\left(2\sqrt{t}-1\right). \tag{5.3}$$

Proposition 5.2. ([12]) Let $L_n(t)$ be Müntz–Legendre polynomial defined by (3.2) and $t \in [0,1]$. Then

$$D_*^{1/2}L_n(t) = \frac{n+2}{\sqrt{\pi}} \int_0^1 (1-x^2)^{-1/2} P_{n-1}^{(1,2)}\left(2x\sqrt{t}-1\right)dx, \tag{5.4}$$

holds true.

5.2. GAUSS–TYPE QUADRATURE RULES

An n–point quadrature rule for the weight function w is called a formula of the type

$$\int_a^b w(x)f(x)dx = \sum_{k=1}^{n} w_k f(x_k) + R_n[f], \tag{5.5}$$

where the sum on the right–hand side of the equation provides an approximation to the integral and R_n is the error. The numbers x_k, $k = 1, \dots, n$ are called *nodes* and w_k are called *weights* of the quadrature rule. Among all quadrature rules of the form (5.5) those of the Gaussian type have the best performance. More precisely, if nodes x_k and weights w_k are chosen in the way that quadrature rule (5.5) becomes exact for polynomials of degree at most $2n-1$, then this quadrature rule is called a Gauss–type quadrature rule. It can be proved that the nodes x_k in a Gaussian quadrature are the roots of the orthogonal polynomial $\pi(t;w)$ associated with the weight function and the weights w_k can be obtained from the following system of linear equations:

$$\sum_{k=1}^{n} w_k x_k^j = \int_a^b x^j w(x)dx, \quad j = 0,1,\dots,2n-1. \tag{5.6}$$

As n increases, finding roots of $\pi(t;w)$ and solving the linear system (5.6) become an ill–conditioned and time consuming problem. Alternatively, the Golub–Welsch

algorithm to determine the nodes and the weights of a Gaussian quadrature can be used [15].

The construction of the Gaussian quadrature (5.5) for an arbitrary$n \geq 1$ can be realized very easy by MATHEMATICA package `OrthogonalPolynomials`[8,19]. Alternatively, for this purpose, there is also Gautschi's package `OPQ` written in MATLAB [14]. These packages provide many other calculations with orthogonal polynomials and different quadrature rules, and they are downloadable from Web Sites: `www.mi.sanu.ac.rs/~gvm/` and `www.cs.purdue.edu/archives/`, respectively.

To calculate the integral on the right–hand side of (5.4), N–point Gaussian quadrature rule

$$\int_0^1 (1-x^2)^{-1/2} f(x)dx = \sum_{k=1}^{N} w_k f(x_k), \quad f \in \mathbb{P}_{2N-1}, \tag{5.7}$$

is used. The weight function $w(x) = (1-x^2)^{-1/2}$ is a nonclassical one and no explicit formulae are known for x_k and w_k. However, the Chebyshev and Golub–Welsch algorithms to calculate the nodes and weights in (5.7) can be used [14, 15]. The quadrature rule (5.7) with $N = \lceil n/2 \rceil$ becomes exact for computing the integral in (5.4). The nodes and weights in the generalized Gaussian quadrature rule (5.7) are reported in Table 1.

Table 1: Nodes and weights in 10–point Gaussian quadrature rule (5.7).

Nodes x_k	Weights w_k
0.013428248384359	0.034319541263749
0.165229282898357	0.077205134746572
0.165088161001579	0.114617582317493
0.292182309608721	0.145264568917587
0.438817309663802	0.169221867374936
0.591551320859218	0.187274168806872
0.736030889552124	0.200396120129594
0.858545000002092	0.209464924712622
0.947393707327565	0.215148632394853
0.994059476652251	0.217883786130620

After obtaining the nodes x_k and weights w_k, the fractional derivative $D_*^{1/2} L_n(t)$ can be computed by using the formula

$$D_*^{1/2} L_n(t) = \frac{n+2}{\sqrt{\pi}} \sum_{k=1}^{\lceil n/2 \rceil} w_k \, P_{n-1}^{(1,2)}\left(2x_k\sqrt{t} - 1\right). \tag{5.8}$$

This section ends with a brief discussion of collocation points. Grid points for orthogonal collocation method should lie approximately in a minimal–energy configuration associated with inverse linear repulsion between points. Hence, a proper choice of collocation points is crucial for the accuracy of the numerical solution and for its computational stability [13, 25]. In the proposed case, a particularly convenient choice for the collocation points ξ_j is $\xi_j = t_j^2$, $j = 1, \dots, n$ where t_j are Chebyshev points associated with the interval $[0,1]$, i.e.,

$$t_j = \frac{1}{2}\left(1 - \cos\frac{\pi j}{n}\right), \quad j = 0,1, \dots, n .$$

6. NUMERICAL EXPERIMENTS

In this section, some numerical studies are presented to illustrate and test the behavior of the approach described in the Section 4. As is common, there is no comparison to other known methods. The main reason for this is that the numerical solution for this problem comes only in [23] and has a slow convergence. The following numerical experiments were implemented through MATHEMATICA and MATLAB.

Example 1. As the first experiment, given $\lambda = 8/(3\sqrt{\pi})$ and the change of gas volume $f(t) = 1 - \sqrt{t}$, then the initial value problem (2.4) has the analytical solution

$$p(t) = 1 + \sqrt{t} - \frac{1}{3}t + \left(\frac{32}{27\pi} - \frac{1}{3}\right)t\sqrt{t} .$$

The analytical and numerical solutions of this problem are plotted in Figure 2. Furthermore, to explore the dependence of errors on the discretization parameter n, the error in the ∞–norm is used. As it is seen, the presented method provides accurate results even with a few number of nodes.

Example 2. Consider the initial value problem (2.4) with $f(t) = 1 - t$. In this case, it is hard to find a closed form solution of (2.4). However, thanks to the work of Babenko [3, (7.25)], if the compression is slow ($\lambda \gg 1$), the following asymptotic representation for $p(t)$ is obtained:

$$p(t) = 1 + \frac{2\sqrt{t}}{\sqrt{\pi}}\frac{1}{\lambda} + \left(\frac{3}{2}t - 1\right)\frac{1}{\lambda^2} + \mathcal{O}\left(\frac{1}{\sqrt{t}\lambda^3}\right), \quad t > 0 . \tag{6.1}$$

Moreover, in the case of rapid compression ($\lambda \ll 1$), a similar expression in powers of λ can be obtained [3, (7.26)] as follows:

$$p(t) = \frac{1}{1-t} + \frac{2}{\sqrt{\pi}}\left(\frac{\sqrt{t}}{1-t} - \frac{\sin^{-1}\sqrt{t}}{(1-t)^{3/2}}\right)\lambda + \mathcal{O}\left(\frac{\lambda^2}{(1-t)^2}\right), \quad t < 1 . \tag{6.2}$$

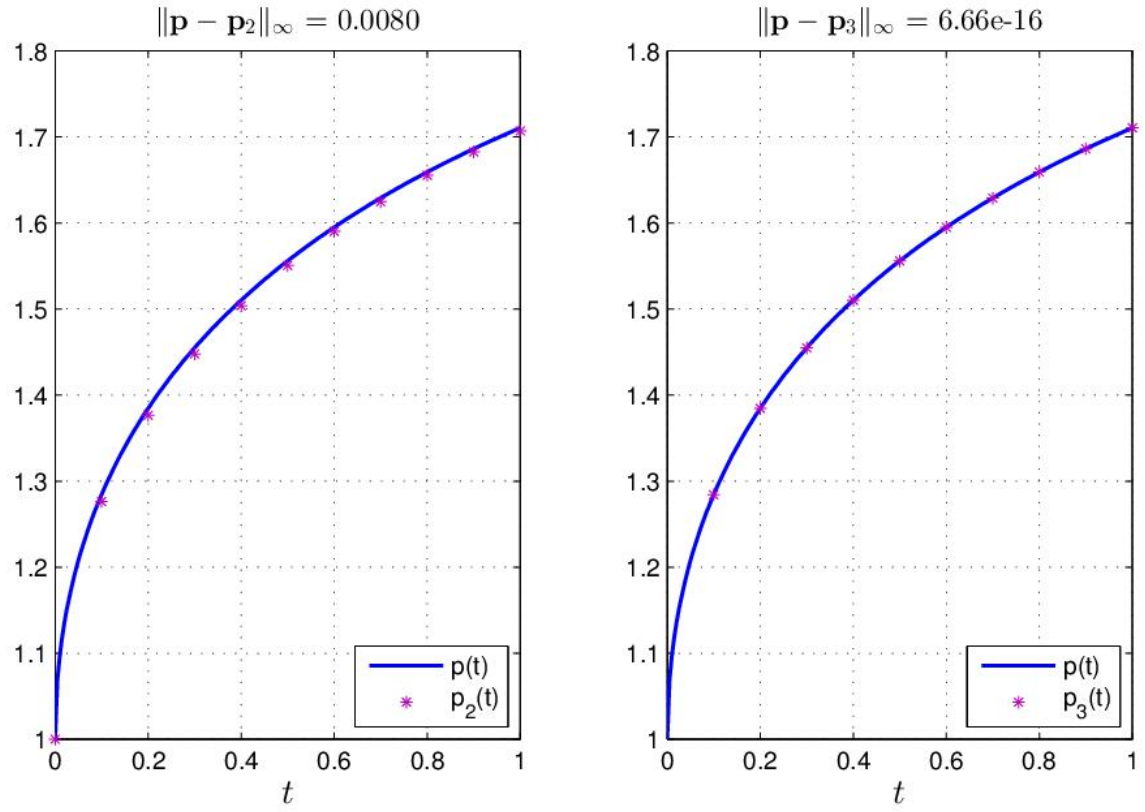

Figure 2: Analytical and numerical solutions of problem (2.4) (Example 1).

In Figure 3, the numerical and asymptotic solutions of problem (2.4) are illustrated. These results indicate that the approximate solutions of the present method are in agreement with asymptotic solutions. It can be shown that the maximum pressure, p_{max}, occurs at $t = 1$. On the other hand, from (6.1), the following asymptotic expression is obtained

$$p(t) \approx 1 + \frac{2}{\sqrt{\pi}}\frac{1}{\lambda} + \frac{1}{2}\frac{1}{\lambda^2} + \mathcal{O}(1)\frac{1}{\lambda^3}, \quad \lambda \to \infty . \tag{6.3}$$

The numerical solutions for various values of n are reported in Table 2. As tabulated, the asymptotic expression (6.3) as a reference "exact" solution is used. It can be seen that the presented method provides accurate results and indicate an exponential decay.

Table 2: Numerical solutions at $t = 1$ and related errors with $\lambda = 5$ (Example 2).

n	5	10	15	20	25	30
$p_n(1)$	1.2457842	1.2456764	1.2456758	1.2456758	1.2456758	1.2456758
Error	1.08(–04)	5.93(–07)	2.19(–09)	5.89(–12)	1.24(–14)	2.22(–16)

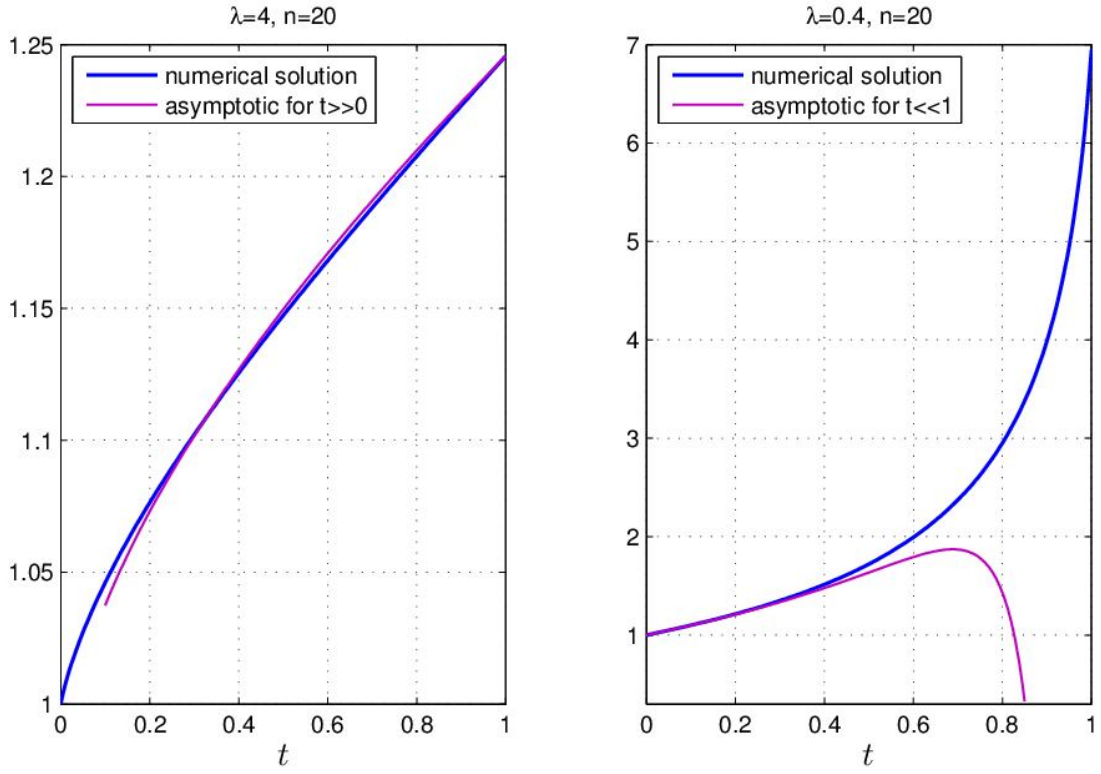

Figure 3. Numerical and asymptotic solutions of problem (2.4): slow compression (left) and rapid compression (right) (Example 2).

7. CONCLUSION

In this paper, a computational technique based on the Müntz polynomials for solution of mathematical model of gas solution in a fluid is presented. The exact solution of this problem can contain some fractional–power terms with which the Müntz polynomials can match. An appropriate representation of the solution based on the Müntz polynomials reduces its numerical treatment to the solution of a linear system of algebraic equations. The numerical results obtained by the new method indicated the effectiveness of the proposed approach.

REFERENCES

1. A. Ansari and M. Ahmadi Darani, On the generalized mass transfer with a chemical reaction: Fractional derivative model, *Iranian J. Math. Chem.* **7** (2016) 77–88
2. Y. I. Babenko, *Heat and Mass Transfer: The Method of Calculation for the Heat and Diffusion Flows (in Russian)*, Khimiya, Leningrad, 1986.

3. Y. I. Babenko, *The Method of Fractional Differentiation in Applied Problems of Heat and Mass Transfer Theory (in Russian)*, NPO Professional Publ, St Petersburg, 2009.
4. D. Baleanu, K. Diethelm, E. Scalas and J.J. Trujillo, *Fractional Calculus: Models and Numerical Methods* 2nd ed., World Scientific, Singapore, 2016.
5. P. Borwein, T. Erdélyi and J. Zhang, Müntz systems and orthogonal Müntz–Legendre polynomials, *Trans. Amer. Math. Soc.***342** (1994) 523–542.
6. D. W. Brzeziński, Accuracy problems of numerical calculation of fractional order derivatives and integrals applying the Riemann–Liouville/Caputo formulas, *Appl. Math. Nonlinear Sci.* **1** (2016) 23–44.
7. M. Caputo, Linear models of dissipation whose *Q* is almost frequency independent – II, *Geophys. J. Roy. Astron. Soc.* **13** (1967) 529–539.
8. A. S. Cvetković, G. V. Milovanović, The Mathematica package orthogonal polynomials, *Facta. Univ. Ser. Math. Inform.* **19** (2004) 17–36.
9. K. Diethelm, *The Analysis of Fractional Differential Equations*, Springer, Berlin, 2010.
10. K. Diethelm and Y. Luchko, Numerical solution of linear multi–term initial value problems of fractional order, *J. Comput. Anal. Appl.* **6** (2004) 243–263.
11. S. Esmaeili and G. V. Milovanović, Nonstandard Gauss–Lobatto quadrature approximation to fractional derivatives, *Fract. Calc. Appl. Anal.* **17** (2014) 1075–1099.
12. S. Esmaeili, M. Shamsi and Y. Luchko, Numerical solution of fractional differential equations with a collocation method based on Müntz polynomials, *Comput. Math. Appl.* **62** (2011) 918–929.
13. B. A. Finlayson, *The Method of Weighted Residuals and Variational Principles, with Application in Fluid Mechanics, Heat and Mass Transfer*, Academic Press, New York, 1972.
14. W. Gautschi, *Orthogonal Polynomials in* MATLAB*: Exercises and Solutions*, SIAM, Philadelphia, 2016.
15. G. H. Golub and J. H. Welsch, Calculation of Gauss quadrature rules, *Math. Comp*. **23** (1969) 221–230.
16. Y. Luchko and R. Gorenflo, An operational method for solving fractional differential equations with the Caputo derivatives, *Acta Math. Vietnam.* **24** (1999) 207–233.
17. F. Mainardi, *Fractional Calculus and Waves in Linear Viscoelasticity: An Introduction to Mathematical Models*, Imperial College Press, London, 2010.
18. G. V. Milovanović, Müntz orthogonal polynomials and their numerical evaluation, in: W. Gautschi, G. H. Golub and G. Opfer (Eds.), *Applications and Computation of Orthogonal Polynomials*, Birkhäuser, Basel **131** (1999) 179–194.
19. G. V. Milovanović and A. S. Cvetković, Special classes of orthogonal polynomials and corresponding quadratures of Gaussian type, *Math. Balkanica*. **26** (2012) 169–184.

20. P. Mokhtary, F. Ghoreishi and H. M. Srivastava, The Müntz–Legendre Tau method for fractional differential equations, *Appl. Math. Model.* **40** (2016) 671–684.
21. F. W. J. Olver, D. W. Lozier, R. F. Boisvert and C. W. Clark, *NIST Handbook of Mathematical Functions*, Cambridge University Press, Cambridge, 2010.
22. A. Pedas and E. Tamme, Spline collocation methods for linear multi–term fractional differential equations, *J. Comput. Appl. Math.* **236** (2011) 167–176.
23. I. Podlubny, *Fractional Differential Equations*, Academic Press, San Diego, CA, 1999.
24. J. M. Prausnitz, R. N. Lichtenthaler and E. Gomes de Azevedo, *Molecular Thermodynamics of Fluid–Phase Equilibria, 3th ed.*, Prentice Hall, Englewood Cliffs, 1999.
25. L. N. Trefethen, *Approximation Theory and Approximation Practice*, SIAM, Philadelphia, PA, 2013.

ABSTRACTS
IN
PERSIAN

Borderenergetic Graphs Of Order 12

BORIS FURTULA AND IVAN GUTMAN

Faculty of Science,University of Kragujevac, P.O.Box 60,34000 Kragujevac, Serbia

گراف های فعال مرزی از مرتبهٔ 12

ادیتور رابط : علیرضا اشرفی

چکیده

گراف G از مرتبهٔ n را فعال مرزی گویند هرگاه انرژی‌اش برابر با (2n-2) باشد و G از گراف کامل K_n متمایز باشد. چنین گرافی برای اولین‌بار درسال 2001 کشف شد اما مطالعهٔ منظم آن درسال 2015 آغاز شد. تاکنون تعداد گراف‌های فعال مرزی از مرتبه $n\leq 11$ تعیین شده است. درحال حاضر مشخص می‌کنیم که دقیقا 572 عدد گراف فعال مرزی همبند از مرتبهٔ 12 وجوددارد.

لغات کلیدی: انرژی گراف، گراف فعال مرزی، طیف (گراف)

A Numerical Study of Fractional Order Reverse Osmosis Desalination Model using Legendre Wavelet Approximation

OMAR BELHAMITI[1] AND BELKACEM ABSAR[2]

[1]Laboratory of Pure and Applied Mathematics, Abdelhamid Ibn Badis University, Mostaganem 27000, Algeria
[2]Laboratory of Science and Technology of the Environment and Promotion, University of Mostaganem, Mostaganem 27000, Algeria

مطالعهٔ عددی از مرتبهٔ کسری مدل نمک‌زدایی اسمز معکوس با استفاده از تقریب موجک لژاندر

ادیتور رابط : علیرضا اشرفی

چکیده

هدف از این مطالعه، گسترش یک دستاورد جدید در مدلسازی و شبیه‌سازی سیستم نمک‌زدایی اسمز معکوس با استفاده از معادلات دیفرانسیل کسری است. با استفاده از ترکیب مدل موجک لژاندر با تکنیک جداسازی و شبه- خطی سازی، صحت و کاربرد مدل خود را نشان می‌دهیم. به منظور نشان‌دادن کارایی تکنیک دیفرانسیل کسری و پررنگ کردن کاربرد گسترده و بازدهی این مدل، مثالهایی ارائه شده است. مشتق کسری در مفهوم کاپوتو توصیف شده است.

لغات کلیدی: سیستم نمک زدایی اسمز معکوس، روش موجک لژاندر، تکنیک DQL، مشتق کسری کاپوتو

Solving Time-fractional Chemical Engineering Equations by Modified Variational Iteration Method as Fixed Point Iteration Method

AMAD HAGHBIN[1] AND HOSSEIN JAFARI[2]

[1]Department of Mathematics, Gorgan branch, Islamic Azad University, Gorgan, Iran
[2]Department of Mathematics, University of Mazandaran, P. O. Box 47416−95447, Babolsar, Iran

حل معادلات کسری-زمانی مهندسی شیمی با روش تکرار تغییرات اصلاح شده به عنوان روش تکرار نقطه ثابت

ادیتور رابط : علیرضا اشرفی

چکیده

در اینجا روش تکرار تغییرات برای یافتن جواب تقریبی مسائل کسری مهندسی شیمی توسعه داده شده است. چون هنوز ضرایب لاگرانژ در روش تکرار تغییرات بطور صریح مشخص نشده است، در این مقاله روش تکرار تغییرات به کمک روش تکرار نقطه ثابت بهبود یافته و سپس برای حل مسائل کسری-زمانی مهندسی شیمی بکار رفته است. جواب‌های تقریبی بدست آمده در مقایسه با نتایج عددی مقالات دیگر، کارایی، موثر بودن و دقت روش را نشان می دهند.

لغات کلیدی: معادلات دیفرانسیل کسری، روش تکرار تغییرات، قضیه نقطه ثابت، راکتور شیمیایی

The Ratio and Product of the Multiplicative Zagreb Indices

RAMIN KAZEMI

Department of Statistics, Faculty of Science, Imam Khomeini International University, Qazvin, Iran

نسبت و ضرب شاخص‌های زاگرب ضربی

ادیتور رابط : سندی کلاوزر

چکیده

شاخص زاگرب ضربی اول $\prod_1(G)$ برابر حاصل ضرب توان دوم درجه‌ها و شاخص زاگرب ضربی دوم $\prod_2(G)$ برابر حاصل ضرب درجهٔ زوج رئوس مجاور گراف مولکولی G است. همچنین، شاخص زاگرب جمعی-ضربی $\prod_3(G)$ برابر ضربِ مجموع درجهٔ زوج رئوس مجاور G است. در این مقاله، یک نسخهٔ جدید از شاخص زاگرب جمعی-ضربی معرفی و گشتاورهای نسبت و ضرب همهٔ شاخص‌ها در یک گراف مولکولی به طور تصادفی انتخاب شده با ساختار درختی از مرتبهٔ n مطالعه می‌شود. همچنین، یک زبَرمارتینگل بر اساس نابرابری زبَرمارتینگلی دوب معرفی می‌شود.

لغات کلیدی: گراف مولکولی با ساختار درختی، شاخص زاگرب ضربی، گشتاور، نابرابری زبَرمارتینگلی دوب.

Extremal Trees with Respect to Some Versions of Zagreb Indices Via Majorization

MEHDI ELIASI AND ALI GHALAVAND

Department of Mathematics, Khansar faculty of Mathematics and Computer Science, Khansar, Iran

درختهای اکسترمال نسبت به برخی نسخه‌های شاخص‌های زاگرب به وسیلهٔ ماجریزیشن

ادیتور رابط : ایوان گوتمن

چکیده

موضوع این مقاله، بکارگیری روشهای ماجریزیشن در شناسایی رده‌هایی از درختان با مقادیر اکسترمال (مینیمال یا ماکسیمال) برخی از شاخص‌های توپولوژیکی از میان همهٔ درختان از مرتبهٔ $n \geq 2$ است.

لغات کلیدی: ماجریزیشن، شاخص اول زاگرب تعمیم‌یافته، شاخص زاگرب ضربی

The Uniqueness Theorem for Inverse Nodal Problems with a Chemical Potential

SEYFOLLAH MOSAZADEH

Department of Pure Mathematics, Faculty of Mathematical Sciences, University of Kashan, Kashan 87317−53153, I. R. Iran

قضیهٔ یکتایی برای مسائل گره‌ای عکس دارای پتانسیل شیمیایی

ادیتور رابط : علیرضا اشرفی

چکیده

در این مقاله، مسألهٔ گره‌ای عکس برای یک معادلهٔ مرتبهٔ دوم دارای پتانسیل شیمیایی روی یک بازهٔ متناهی بررسی می‌شود. ابتدا تقریبی برای نقاط گره‌ای و طولهای گره‌ای عملگر دیفرانسیل به‌دست می‌آوریم، سپس نشان می‌دهیم که می‌توان تابع پتانسیل را به‌وسیلهٔ مجموعه‌ای چگال از نقاط گره‌ای به‌طور یکتا تعیین کرد.

لغات کلیدی: مسألهٔ مقدار مرزی، مسألهٔ گره‌ای عکس، مقادیر ویژه، نقاط گره‌ای.

Numerical Modeling for Nonlinear Biochemical Reaction Networks

Z. A. ZAFAR[1,2], K. REHAN[3], M. MUSHTAQ[2] AND M. RAFIQ[2,4]

[1]Faculty of Information and Technology, University of Central Punjab, Lahore, Pakistan
[2]Department of Mathematics, University of Engineering and Technology, Lahore, Pakistan
[3]Department of Mathematics, University of Engineering and Technology, KSK Campus, Pakistan
[4]Faculty of Engineering, University of Central Punjab, Lahore, Pakistan

مدلسازی عددی برای شبکه‌های واکنش بیوشیمیایی غیرخطی

ادیتور رابط : علیرضا اشرفی

چکیده

امروزه، مدلهای عددی در هر شاخه از علم اهمیت فراوانی دارند بخصوص برای حل معادلات دیفرانسیل غیرخطی، معادلات دیفرانسیل جزئی، واکنش‌های بیوشیمیایی و غیره. کل زمان تکامل غلظت‌های واکنش‌دهنده بر پایهٔ واکنش لایه- آنزیم، توسط رانگ- کوتا از مرتبهٔ 4 (RK4) و روش تفاضل متناهی غیراستاندارد (NSFD) شبیه‌سازی شده است. مدل ANSFD برای مسألهٔ واکنش بیوشیمیایی ساخته شده و آزمایش‌های عددی برای مقادیر مختلف پارامتر گسسته‌سازی "h"، انجام شده است. نتایج به دست آمده، با طرح عددی معروف یعنی RK4 مقایسه شده‌اند. برخلاف RK4 که برای مراحل بلندمدت شکست می‌خورد، طرح پیشرفتهٔ NSFD نتایجی ارائه داد که به حالات پایدار واقعی برای هر گام زمانی استفاده شده، همگرا می‌شوند.

لغات کلیدی: مدل میکائلیس- منتن ، روش NSFD، روش RK4

Numerical Solution of Gas Solution in a Fluid: Fractional Derivative Model

SHAHROKH ESMAEILI

Department of Applied Mathematics, University of Kurdistan, Sanandaj, Iran

حل عددی مسألهٔ محلول گاز در یک سیال: مدل مشتق کسری

ادیتور رابط : علیرضا اشرفی

چکیده

یک روش محاسباتی برای حل مدل ریاضی محلول گاز در یک سیال ارائه می‌شود. این مدل، تغییر جرم حجمی گاز انتشاریافته بر اثر تماس با سطح سیال را توصیف می‌کند. یک نمایش مناسب از جواب بر پایهٔ چندجمله‌ایهای مونتس، حل عددی مسأله را به حل یک دستگاه خطی از معادله‌های جبری تبدیل می‌کند. چند مثال عددی نیز برای تأیید دقت و کارایی این روش ارائه شده است.

لغات کلیدی: مشتق‌های کسری، محلول گاز، چندجمله‌ایهای مونتس، چهارگوشهٔ گاوسی، روش هم‌مکانی

این نشریه طبق مجوز شماره 89/3/11/104372 مورخه 89/11/27 دارای اعتبار **علمی -پژوهشی** از وزارت علوم ، تحقیقات و فناوری می باشد. همچنین این مجله در پایگاه اطلاعاتی ISC (Islamic World Science Citation Center) وابسته به وزارت علوم ، تحقیقات و فناوری نمایه می شود.

IRANIAN JOURNAL OF

MATHEMATICAL CHEMISTRY

CONTENTS

December 2017

ISSN

2228-6489 (Print Version)

2008-9015 (Online Version)